T490

NOVEL MELT TRANSURETHANE PROCESS
FOR CYCLOALIPHATIC POLYURETHANES AND THEIR
SELF-ORGANIZATION FOR NANO-MATERIALS

THESIS SUBMITTED TO

COCHIN UNIVERSITY OF SCIENCE AND TECHNOLOGY

FOR THE DEGREE
OF
DOCTOR OF PHILOSOPHY
IN CHEMISTRY

UNDER THE FACULTY OF TECHNOLOGY

By
DEEPA PUTHANPARAMBIL

CHEMICAL SCIENCES & TECHNOLOGY DIVISION
NATIONAL INSTITUTE FOR INTERDISCIPLINARY
SCIENCE AND TECHNOLOGY (CSIR)
(Formerly: Regional Research Laboratory)
THIRUVANANTHAPURAM-695 019
KERALA, INDIA

FEBRUARY 2008

DECLARATION

I hereby declare that the matter embodied in the thesis entitled **"NOVEL MELT TRANSURETHANE PROCESS FOR CYCLOALIPHATIC POLYURETHANES AND THEIR SELF-ORGANIZATION FOR NANO-MATERIALS"** are the results of the investigations carried out by me at the Chemical Sciences and Technology Division, National Institute for Interdisciplinary Science and Technology (CSIR), Thiruvananthapuram, under the supervision of Dr. M. Jayakannan and the same has not been submitted elsewhere for any other degree.

Deepa Puthanparambil

Thiruvananthapuram
February 2008

i

राष्ट्रीय अंतर्विषयी विज्ञान तथा प्रौद्योगिकी संस्थान

(वैज्ञानिक एंव प्रौद्योगिकी अनुसंधान परिषद्)

(पहले क्षेत्रीय अनुसंधान प्रयोगशाला)

NATIONAL INSTITUTE FOR INTERDISCIPLINARY SCIENCE AND TECHNOLOGY

(Council of Scientific & Industrial Research)

(formerly Regional Research laboratory)

इन्डस्ट्रियल इस्टेट डाक घर, तिरुवनन्तपुरम 695 019, भारत

Industrial Estate P.O., Thiruvananthapuram 695 019, India

CERTIFICATE

This is to certify that the work embodied in the thesis entitled **"NOVEL MELT TRANSURETHANE PROCESS FOR CYCLOALIPHATIC POLYURETHANES AND THEIR SELF-ORGANIZATION FOR NANO-MATERIALS"** has been carried out by **Ms. Deepa Puthanparambil** (Reg. No.2787) under my supervision at the Chemical Sciences and Technology Division of National Institute for Interdisciplinary Science and Technology (Formerly: *Regional Research Laboratory*), Thiruvananthapuram and the same has not been submitted elsewhere for any other degree.

Trivandrum

Dr. M. Jayakannan

(Research Supervisor)

Acknowledgements

Synopsis

Polyurethanes have attained a wide interest because of their unique reversible thermal behaviour with feasibility to fabricate elastomeric engineering thermoplastic materials. The hydrogen bonding in the urethane linkages in the chain behaves as 'virtual cross-linked' hard segments and are surrounded by the soft long chain networks to provide the reversible elastomeric behaviour. Generally, polyurethanes are prepared by reacting diisocyanates with di- or poly-functional hydroxyl compounds, however, the diisocyanates are highly hazardous and its continuous exposure causes un-curable respiratory diseases. The research work pertaining to this thesis was performed to develop a non-isocyanate green chemical process for polyurethanes and also self-organize the resultant novel polymers into nano-materials. The thesis was focused on the following three major aspects:

(i) Design and development of *novel melt transurethane* process for polyurethanes under non-isocyanate and solvent free melt condition.

(ii) Solvent induced self-organization of the novel cycloaliphatic polyurethanes prepared by the melt transurethane process into micro-porous templates and nano-sized polymeric hexagons and spheres.

(iii) Novel polyurethane-oligophenylenevinylene random block copolymer nano-materials and their photoluminescence properties.

The thesis work has been divided into four chapters. First chapter gives a brief introduction on polyurethanes in general, their applications and different methodologies involved in their synthesis. It also gives a brief account on the different self-organization approaches known in the polymer literature for the formation of different morphologies such as honeycomb, pores and spheres.

The second chapter describes the design and development of *novel melt transurethane* process for polyurethanes under non-isocyanate and solvent free melt condition.

Melt Transurethane Process

iv
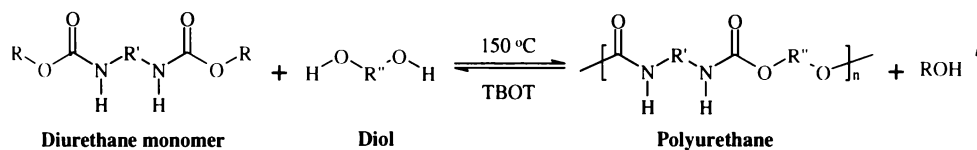
In this process a di-urethane monomer was polycondensed with equimolar amounts of diol in presence of Ti-catalyst under melt condition to produce polyurethanes followed by the removal of low boiling alcohol from equilibrium. The diurethane monomers were synthesized from commercially available diamines and dimethyl carbonate in presence of a base as a catalyst. The new transurethane process was investigated for A + B, A-A + B and A-A + B-B (A-urethane and B-hydroxyl) type condensation reactions and also monomers bearing primary and secondary urethane or hydroxyl functionalities. The transurethane process was confirmed by ^{1}H and ^{13}C-NMR and molecular weight of the polymers were determined by solution viscosity and gel permeation chromatography. The number average degree of polymerization, (n = 25-50) indicated that the transurethane occurred up to 95-98 % reaction conversion in the polycondensation. The mechanistic aspects of the melt transurethane process and role of the catalyst were investigated using model reactions, ^{1}H-NMR and MALDI-TOF Mass spectroscopy. The model reaction products were subjected to NMR and HR-MS analysis to investigate the role of the catalyst in the transurethane process. The polymer samples were further subjected for end group analysis using MALDI-TOF mass spectrometry to understand the mechanistic aspects in detail. Thermal properties of the polyurethanes were analyzed by differential scanning calorimetry and thermogravimetric analysis. Almost all the polyurethanes were stable up to 280 °C and thermal properties particularly T_g of the polyurethanes can be easily fine-tuned from -30 to 120 °C by using appropriate diols in the melt transurethane process.

The third chapter expends the structural diversity of the newly synthesized cycloaliphatic polyurethanes to produce myriad morphologies such as micro-pores and polymeric hexagons and spheres based on the simple solvent induced self-organization strategy.
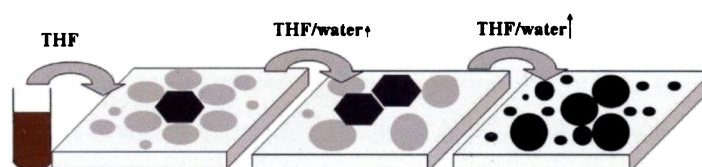
The hydrogen bonding of the polyurethanes are very unique to their chemical structure and they undergo selective phase separation process in solution to produce

various morphologies. Fully cycloaliphatic polyurethanes undergo selective segregation in solvent like chloroform and tetrahydrofuran (THF) to produce micro-porous templates. The increase of water content in the polymer solution (THF+ water) enhances the phase separation process and the micro pores coalesce to isolate the encapsulated polymer matrix into polymeric hexagons or densely packed solid spheres. The morphologies of the films produced by the above self-organization process were investigated by scanning electron microscopy (SEM) and transmission electron microscopy (TEM). Various experimental techniques such as concentration dependent FT-IR and ^{1}H-NMR, thermal property (T_g), and theoretical AM1 model calculations were employed as tools to trace the factors which control the morphology of polyurethanes. These studies have proved that morphology evolution of polyurethanes is highly dependent on the hydrogen bonding ability and chemical structure of the polymer backbone.

The fourth chapter describes the synthesis and self-organization of novel luminescent polyurethane- oligo(phenylenevinylene) random block copolymers.
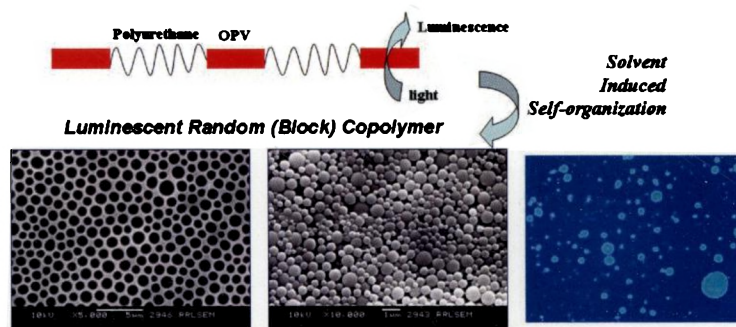
Oligophenylenevinylene (OPV) unit with di-hydroxyl functionality was specially designed and copolymerized with polyurethane segments under the non-isocyanate and solvent-free melt transurethane polymerization process to obtain polyurethane-oligo phenylenevinylene random block copolymers. The amount of OPV content in the random copolymers was varied from 0 to 50 %. The structure of the polymers as well as the percentage incorporation of OPV in the polymers was determined by ^{1}H-NMR spectroscopy. Their molecular weights were determined by GPC and thermal anlaysis were done by DSC and TGA. These copolymers were subjected to solvent induced self-organization in THF or THF + water solvent combinations. The morphological studies were done by various analytical techniques such as SEM, TEM and fluorescence microscopy. The polymers showed the

formation of micro-pores or vesicles in films obtained from THF whereas the increase in the water content in the solvent combination produced micro to nano meter sized spheres. It was also found that the spheres produced from the copolymers with lesser OPV content were monodisperse and smaller in size. However, the increase in the OPV content increased the size of the spheres. The fluorescence microscopy analysis of the samples confirmed the formation of luminescent nano-spheres. The photophysical studies revealed that the increase in the OPV content in the polymer backbone enhances the π-stacking in the polymer chain. The copolymer with higher OPV content showed larger luminescence quenching due to strong π-aggregation. Time resolved fluorescent decay measurements were also performed to understand the decay-process of the random copolymers.

The last chapter summarizes the outcome of the research work carried out in this Ph.D. thesis.

Contents

Chapter-1

Introduction to Polyurethanes

1.1. General Introduction to Polyurethanes

The history of mankind is a tale of continuing quest where he tries to replace old materials with newer improved materials which can meet his basic needs more efficiently. Beginning of the twentieth century saw a spectacular boom in the field of polymer science where industries and academicians alike investigated for materials which could replace natural rubber. The progress of this substitution process developed a new platform to drive science and technology into new directions of advanced high performance structures. As polymers emerged as duplicates to natural rubber and fibers, research was focused on using polymers as replacements for metals. Resistance to corrosion and ease of fabrication and low energy consumption in their production are advantages of polymers over metals. A polymer would be more acceptable to the community at large if it is capable of sustaining high loads and stresses over long time periods as well as over broad temperature ranges. Good environmental stability, fatigue and impact resistance are also necessary requirements for a polymer. In the middle of the twentieth century, when plastics were in the fore front, there existed a wide gap between the elastic ranges of metals and plastics on one hand and conventional rubbers on the other. There was a need for polymers that could combine the melt processability of plastics, the resilience and elasticity of rubber and stiffness and load bearing capability between plastics and rubber. In the search for elastomeric fibers a concept emerged from the early works of Shivers, J. C. and coworkers (DuPont) that a block copolymer with an alternating hard and soft segment would make a good elastomeric material.[1-2] This led to the development of melt processable materials called engineering thermoplastic elastomers. These materials consist of blocks of hard crystallisable or glassy segments to avail a network structure within the polymer backbone alternating with blocks of soft amorphous segments with sufficient lengths and low T_g to confer entropy driven elasticity. Polyurethanes, polyurea, polyamides and polyesteramides belong to the category of engineering thermoplastic elastomers. Needless to say that styrenic block copolymers, polyolefin blends and elastomeric alloys also come under this category. These polymers share a number of desirable characteristics of both rubber and engineering plastics. They are suitable for use under high loading, are creep resistant, have good elasticity, flexibility and have a broad service temperature range without significant property change and are solvent and chemical resistant. They are also superior in the

sense that they can be processed like thermoplastics into materials with variety and complex shapes.[3] Scheme-1.1 represents a pie diagram showing the various types of elastomeric materials in application.
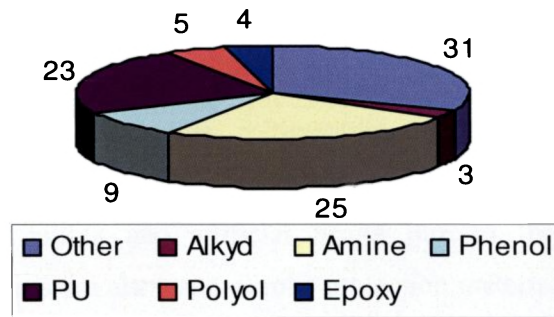
Scheme-1.1: Pie diagram showing various types of elastomeric materials in application

Among the thermoplastic elastomers, thermoplastic polyurethane elastomers bear the recognition of being the first homogeneous, thermoplastically processable elastomers. They combine the mechanical properties of vulcanised rubber such as softness, flexibility and elasticity and have the processability of simple thermoplastic polymers. Thermoplastic polyurethanes bridge the gap between rubber and plastics as it shows a number of physical properties ranging from a hard rubber to a soft engineering thermoplastic. This is possible mainly because the crosslinks in such polymers are physical and reversible and differ from the usual chemical crosslinks observed in rubber. Advantages of thermoplastic elastomers over conventional elastomers lies in the fact that additional chemical crosslinking reactions are not needed and hence fabrication of objects can be easily achieved by using conventional equipments. They can be melted and processed repeatedly by techniques such as reaction injection moulding, blow and compression moulding and melt extrusion. In the recent years thermoplastic polyurethanes are found to have a large share in the thermoplastic elastomeric family.[4-7]

Thermoplastic polyurethane elastomers find application as coatings, binder resins, fibers, flexible and rigid foams and high performance elastomeric products. Polyurethane industry runs far and wide due to their regular applications in construction engineering, in automotive and consumer goods industries, etc., in the

form of rigid and flexible foamed plastics, protective coatings, lacquers and adhesives and also in less down to earth applications like the landing pad of the lunar module. They are used as solid elastomeric products for furnishing automobile fascia, footwear and skateboard wheels. When used in the form of flexible foams, they find applications as upholstered furniture, auto parts, mattresses, and carpet underlay. Rigid foamed products include commercial roofing, residential sheathing, and insulation for water heaters, tanks, pipes, refrigerators and freezers. Polyurethanes also find application as blood-contacting biomaterials such as catheters, vascular grafts, general purpose tubing and artificial hearts due to their good blood compatibility. Polyurethanes are also used as relic protection materials. e.g., honored to be the eight wonder in the world, the terracotta figures of Qin Shihuang's tomb have been protected by polyurethanes. [5, 8-12]

1.2. Thermoplastic Behavior of Polyurethanes

Polyurethanes have attained wide interest because of their unique reversible behavior with feasibility to fabricate rubber-like articles. This excellent reversibility of polyurethanes arises from the uniqueness of the urethane linkage when compared to the linkages in other thermoplastic elastomers such as polyamides and polyureas. All the three polymers contain hydrogen bonding entities and among them polyurea has a bifurcated hydrogen bonding unit which provides high melt stability but poor solubility.[13] Where as polyamide consists of an amide bond, a urethane linkage comprises of a half amide and a half ester bond and the oxygen of the ester bond provides more degrees of rotational freedom (scheme-1.2) which makes the urethane linkage exceptional.[14]
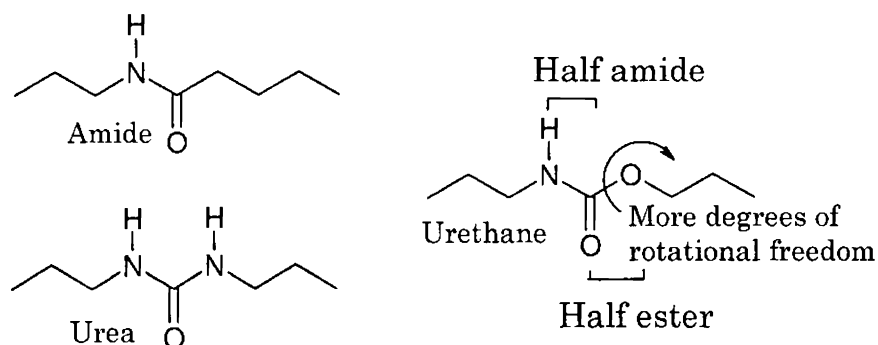
Scheme-1.2: Different types of linkages seen in thermoplastic elastomers

Polyurethanes can be termed as linear segmented block copolymers, consisting of a hard segment which comprises of the polar urethane linkage formed between the diisocyanate and the chain extender whereas the soft segment consists of the long flexible polyether or polyester chain.[4] At ambient conditions, the hard segment exhibits a glassy or semicrystalline state where as the soft segment remains viscous and rubbery. Hence the hard segment provides dimensional stability, thermo-reversibility, high glass transition temperature (T_g), hardness and chemical resistance to the polyurethanes by acting as virtual crosslinks as well as reinforcing fillers. The soft segment on the other hand provides necessary flexibility, extensibility and elasticity to the polymer.[15-16] The structure and properties of these segmented block copolymers depends largely on many factors such as the system viscosity, block length, hard segment mobility resulting in block incompatibility, hard segment interactions and the composition of the blocks.[9,17]Thermodynamic incompatibility between the hard and the soft domains combined with the crystallization of either or both segments within these structures result in microphase separation. The outcome of this microphase separation is a special morphology which is characterized by a cylindrically shaped hard domain with the height given by the hard segment length and a diameter/height ratio < 1; this results in the conformation of a single chain macromolecule as freely oriented hard segment domains embedded within the random coiled soft segments as shown in scheme-1.3.[18]

Scheme-1.3: Model for the morphology and chain conformation of a
segmented polyetherurethane (adapted from ref. 18)

Microphase separations results in phase separated morphologies within the polyurethane elastomers and this has been probed extensively by various research groups by suitable characterization methods such as infrared spectroscopy, transmission electron microscopy, WXRD and in situ modulus measurements.[16,18-24] The degree of microphase separation was found to be lowest when the hard segments and the soft segments were short and polar in nature. With the increase in the length of the hard segment, the volume fraction of the hard segment dispersed in the soft segment decreases which enhances the phase separation.[25-26] Efforts have also been made to determine the effect of chain length and distribution of hard segments on the physical properties of elastomers.[27-28] Wang et al. have coupled the use of dynamic mechanical analysis along with dynamic IR spectral measurements to measure the viscoelastic behavior of polyurethane during its creep recovery study. They suggested that large displacements during the studies on the polymer resulted in permanent damage which were attributed to the irreversible alteration of the microscopic network structure of the polyurethane elastomer.[29] Ferguson et al. have also utilized polyurethanes for the preparation of wet spun filaments which showed spherulitic growth (spherulites are partly oriented aggregated crystallites containing amorphous region) and birefringence based on the soft segment composition.[30] ^{2}H NMR is also a valuable tool in detecting the spatial variations during molecular mobility within microphases as well as to determine the degree of phase separation in polyurethane blocks.[31] Even though the morphology of segmented polyurethanes are effected by many factors such as chemical composition, sequence length of hard segment and hydrogen bonding, it is generally accepted that hydrogen bonding between functional groups is very closely related to phase separation.[32] Recently, Sheth, et al. have obtained segmented copolyurethanes without the aid of chain extenders by the reaction between 1,4-phenylene diisocyanate and poly(tetramethylene oxide) and the polymer was subjected to time dependent morphology development. Films of the copolymers were cast from solution and on heat treatment the semi-crystalline microphase morphology was erased and with time the hard domain first developed into short rods which grew longer and eventually evolved as well defined percolated structures (scheme-1.4). These structures were attributed to the symmetry of the monodisperse hard segment domain as well as hydrogen bonding between these domains.[33]They further extended their works to synthesize poly(urethane urea)

copolymers containing various extends of branching in the hard segment and they concluded that branching reduced the ability of the hard segments to pack effectively resulting in the absence of a well-structured hydrogen bonded network.[34]
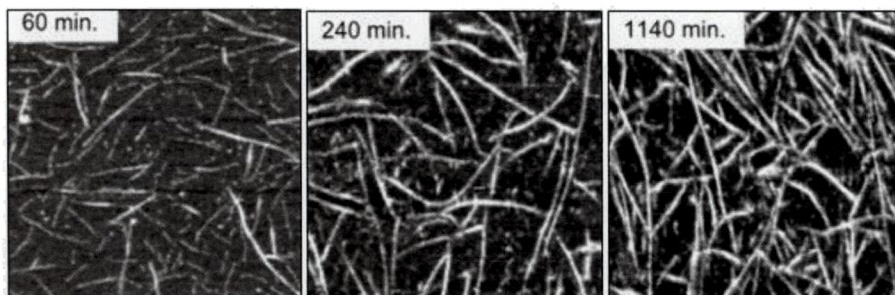
Scheme-1.4: Ambient temperature tapping-mode AFM phase images of polyurethanes captured at various times following heat treatment (adapted from ref. 33)

1.3. Mechanical and Thermal Properties of Polyurethanes

Mechanical and thermal properties of these thermoplastic elastomers have been studied thoroughly by many investigators. Rutkowska et al. utilized simple stress-strain measurements and swelling in different solvents to establish the size and extent of reaction of various bonds in the polyurethanes.[35] Illinger et al. and Seefried et al. utilized the dynamic mechanical relaxation spectra to understand the influence of chemical composition on the thermal transitions of polyurethane block copolymers.[36-37] The thermograms of these segmented block copolymers exhibited few key features such as specific heat capacity jumps at the glass transition temperature of the soft segment rich microphase associated with the micro-Brownian motion of the flexible segments within the polymer chains. An endothermic enthalpy relaxation at a higher temperature was associated with the melting of the hard segment rich microphase.[17,30,38-42]Modulus decreases below the glass transition temperature was attributed to be caused by the breakdown of the hydrogen bonds which were in agreement with the observations of Huh et al.[42] These transitions can be varied in intensity as well as temperature by varying the chemical composition of the polymers. Few types of polyurethane are known which were prepared without the aid of chain extenders.[43] MacKnight and coworkers have developed a series of homopolyurethanes (scheme-1.5) and studied the glass transition and melting of these polymers using DSC. In these polyurethanes the value of x varied from 2-10. They

found that among the different series of polyurethanes the one with largest amount of aromatic moiety, i.e. type A has the highest T_g value.[44]

Type-A

Type-B

Type-C
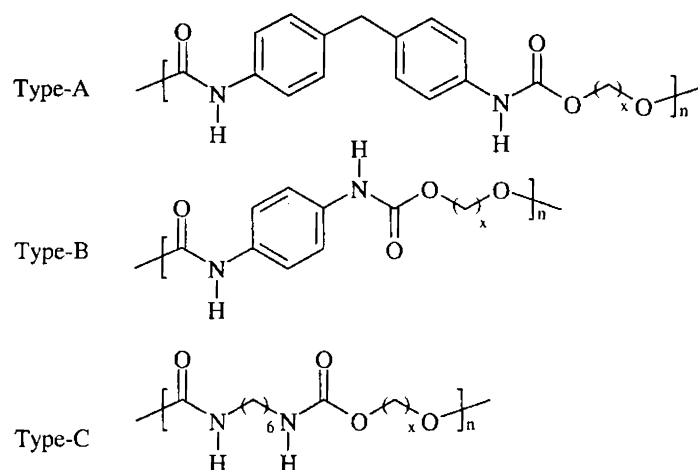
Scheme-1.5: Different types of homopolyurethanes with aromatic and aliphatic units

For example the T_g values of the three different types of homopolyurethanes (A, B and C) with x = 4 were found to be 109, 42 and 59 °C, respectively. Also the T_g values of the type-A series of polyurethanes were more sensitive to the number of methylene units in the diol part when compared to type-C series of polyurethanes. When the value of x was 10, the T_g values of the type-A and C polyurethanes were 72 and 55 °C, respectively.[44] The studies on these systems also suggested that polyurethanes synthesized from symmetrical isocyanates alone (type-A and C) showed crystalline nature and the T_m values were found to be 200 °C and 171 °C for type A and C polyurethanes, respectively with a value of x = 6.[44] McKiernan et al. reported the synthesis of a series of linear aliphatic polyurethanes derived from long chain diols and short chain di-isocyanates and they showed that hydrogen bonding was the key factor for controlling the crystallization processes in such polymers.[45] From the above discussions one clearly understands that segmented polyurethane blocks have always fascinated researchers. The focus of research on these copolymers were mostly on studying the microphase separation and how the phase separation was effected by varying various factors such as the structure of the monomers, the hard segment length and distribution of their molecular weights, etc. They have also tried to determine the morphology of these block copolymers and explained the emergence of various morphologies based on the microphase separation.

1.4. Synthesis of Polyurethanes

1937 was a remarkable year in the polyurethane (PU) chemistry, because Otto Bayer synthesized polyurethanes and it's like polyureas using the most common polyaddition reaction between di-isocyanates and diols[46] as shown in scheme-1.6.

OCN—R—NCO + HO—R'—OH ⟶
Diisocyanate   **Diol**   **Polyurethane**

R-N=C=O + R'-OH ⟶ R-N=C-O ⟶ R-N-C=O
Isocyanate   Alcohol   Urethane
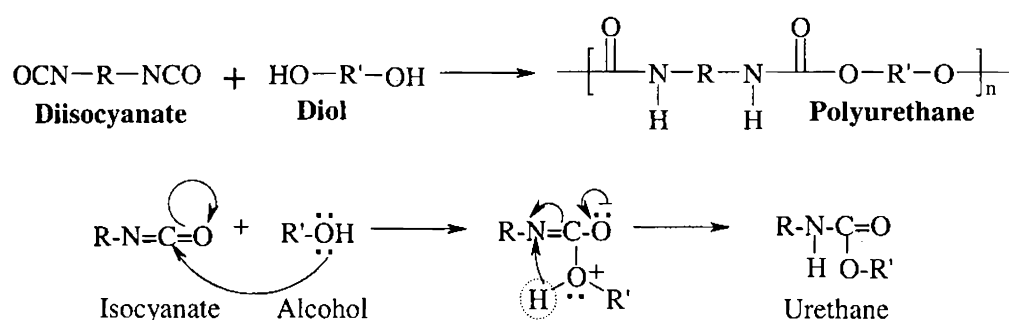
Scheme-1.6: Conventional synthesis of polyurethanes and mechanism of urethane formation

Typically polyurethanes are synthesized by the reaction of aromatic diisocyanate with di- or poly-functional hydroxyl compounds such as polyester, polyether, polycarbonate or hydrocarbon polymers and the resulting prepolymers are then reacted with chain extenders such as low molecular weight diols or diamines to yield polyurethanes of high molecular weights.[47-48] To this very end aromatic di-isocyanates have dominated the polyurethane industry and they have shown exceptional behavior when compared to their aliphatic counter parts. But when long term exposure, processing and external use is required they tend to show few drawbacks. (i) toxicity of the aromatic di-isocyanates which can cause many respiratory diseases[49-50] and (ii) exceptionally high reactivity of isocyanates which results in many side reactions such as formation of allophanates, biurets, uretidinone, and isocyanurates as shown in scheme-1.7 which are difficult to process.[51-53] In order to overcome these drawback many new polymerization methods were implemented for the synthesis of polyurethanes without the aid of isocyanates. These methods christened as 'non-isocyanate routes' for the synthesis of polyurethanes gained immense importance. A detailed description of the many non-isocyanate routes known in the literature is given in the introductory part of the second chapter; a few of them are mentioned here. The reaction of bis(chloroformates) with diamines via interfacial polycondensation,[54] reaction of dinitrile carbonate with diols or polyols,[55]

Curtius rearrangement of acyl azides to isocyanates and their in situ reaction with alcohols,[56-57] use of blocked isocyanate to generate urethane linkages are few of the examples.[58] Though these reactions are successful in forming urethane linkages, low molecular weight formation makes these processes less preferable over the conventional isocyanate-chemistry.
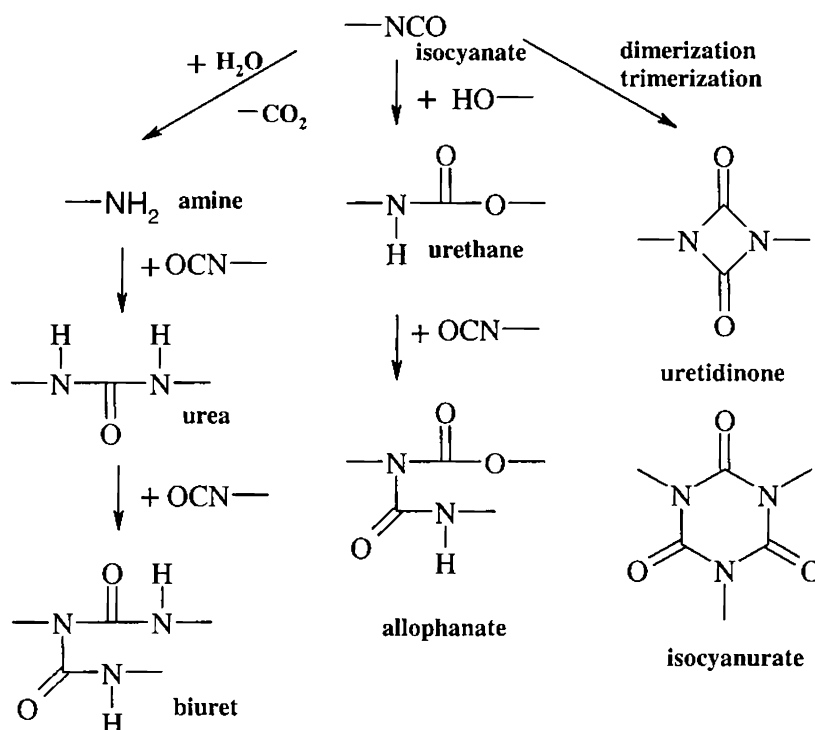
Scheme-1.7: Various side reactions during polyurethane synthesis

A third drawback about aromatic polyurethanes arises from their intense weatherability.[59-61] Aromatic urethane linkage containing polymers underwent discoloration and mechanical property loss with passage of time. This can be related to the ultra-violet initiated autooxidation of urethane linkages to quinoneimide structure as shown in scheme-1.8.[59] It was also shown that polyurethanes based on aromatic di-isocyanates and diols when exposed to light at room temperature degraded into primary aromatic amines and hydroperoxy groups and color formation was attributed to the oxidation of the amino group and radical reactions involving hydroperoxide.[60]
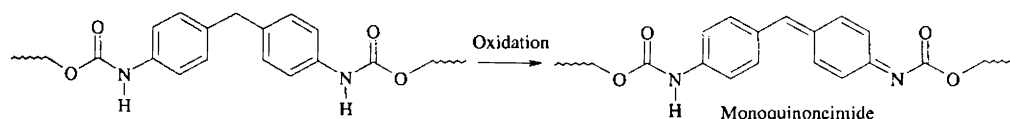
Scheme-1.8: Ultra-violet initiated autooxidation of aromatic urethane linkages

Another major concern for polyurethane industry is the thermal instability of aromatic urethane linkages which were found to decompose at 120 °C.[52, 62-65] Modification of the aromatic urethane linkage by replacing an aromatic alcohol with an aliphatic alcohol improved the thermal stability up to 200 °C.[66] It was also found that urethane linkages flanked by alkyl groups on either side had better thermal stability up to a temperature of 250 °C [62-63] but many properties such as reversibility of aromatic polyurethanes had to be sacrificed because of their high crystallizability.[67] Many attempts are reported to improve the thermal stability of the polyurethanes and some of them include the copolymers of urethane-urea, urethane-ester, urethane-ether and urethane-imides and among them urethane-urea copolymers retained the usual properties of a homopolyurethane.[68-73] But the incorporation of urea linkages results in the insolubility of the polymers and further characterization of these polymers become difficult.[13]Hence one of the major challenges involved in the synthesis of polyurethanes is the selection of monomers with structural backbone capable of retaining the better properties of both an aromatic as well as an aliphatic unit.

1.5. Cycloaliphatic Thermoplastics

In the early 1990's, a significant interest has been observed in cycloaliphatic systems which have replaced many aromatic thermoplastics. The introduction of cycloaliphatic structures produces intermediate physical properties between aromatic and linear aliphatic (scheme-1.9). T_g, hardness and flexibility for cycloaliphatic systems are lower than aromatic systems but higher than linear aliphatics.[74-75] The rigidity arising from the conformational restriction in the cyclic ring makes them relatively high heat (high T_g and T_m) compared to linear aliphatic systems.[76] Additionally, cycloaliphatic polymers have improved processability due to their reduced melt viscosity, stiffness, chemical tolerance and resistance to degradation under UV-light compared to their aromatic counterparts.[77]

| Aromatic | Cycloaliphatic | Linear aliphatic |

Rigid
Thermoreversible
Sensitive to UV light
Less biodegradable

Semirigid
Thermoreversible
Weatherable
Biodegradable

Flexible
Less reversible
Weatherable
Biodegradable
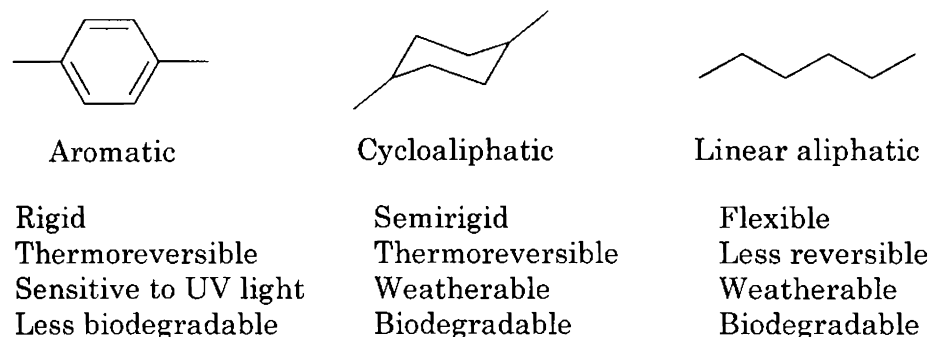
Scheme-1.9: Comparison of the properties of polymers prepared from different types
of structural units

Matuszak et al. made a comparative study about the thermal stability of biscarbamates and polyurethanes containing aromatic, aliphatic and cycloaliphatic units and they found that the thermal stability was found to be highest in the case of cycloaliphatics.[78] Recently, cycloaliphatic ring containing polymers such as polyesters, (scheme-1.10) polycarbonates, polyamides and their blends have attained more attention because of their excellent physical properties compared to their aromatic and linear-aliphatic polymers.
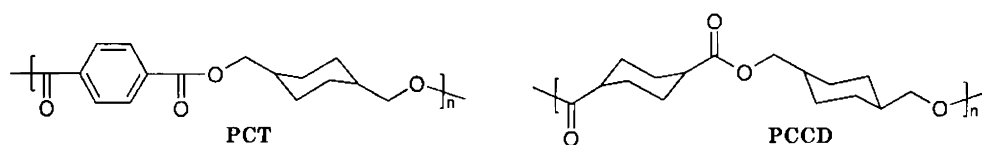
Scheme-1.10: Examples of few commercially available cycloaliphatic polyesters

Srinivasan et al. and Vanhaecht et al. reported the synthesis of a series of polyamides based on 1, 4-cyclohexane dicarboxylic acid and studied the influence of stereochemistry of cis-trans isomerization of cyclohexane rings on the thermal properties and crystallization processes.[79-80] In the area of polyurethanes also there are reports using cycloaliphatic derivatives as monomers for their synthesis. Cotter et al. reported the synthesis of polyurethanes and polyureas based on piperazine and bipiperidyl bis(carbamoyl chloride) derivatives, but the low reactivity of the monomers resulted in the formation of brittle low molecular weight polymers.[81-82] Nakamura et al. reported polyurethanes containing norbornene diols and the studies

mainly focused on the cross-linking behavior of the reactive norbornene moieties for curing applications (scheme-1.11).[83]
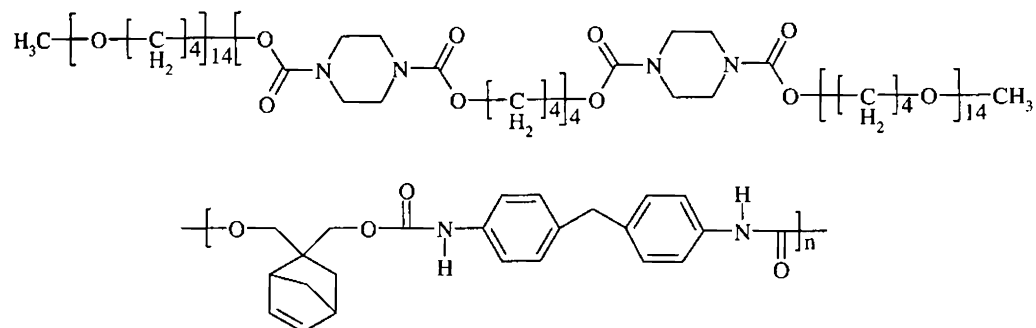
Scheme-1.11: Examples of polyurethanes based on piperazine derivative and norbornene diol

Bachmann et al. reported the synthesis of new polyurethanes/polyureas based on dianhydrohexitol (sugar based bi-cyclic ring, scheme-1.12) and the role of monomer stereochemistry on the resultant polymers were examined.[84] Since conformational restriction can bring about changes in the stability of isomers, the effect of the ratio of cis-trans isomers on the properties of cycloaliphatic polyurethanes were also analysed.[85-86]
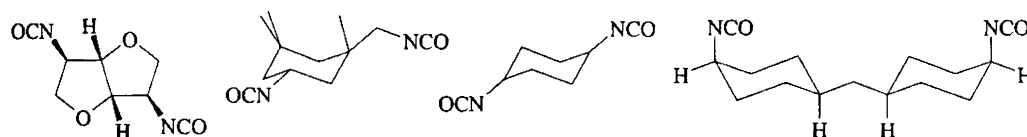
Scheme-1.12: Few examples of cycloaliphatic diisocyanates used for polyurethane synthesis

Cycloaliphatic-diisocyanates containing rings of isophorone, cyclohexyl, dicyclohexylmethane (scheme-1.12) and cyclohexyl-triisocyanate were explored for thermoset (or thermoplastic) adhesives, coatings and two dimensional medical applications.[87-95] The studies were mostly paying attention to analyze the polymerization conditions, thermal stability, chemical resistance and fatigue performance, etc. of the polyurethanes.

From all the above discussions it is clear that a new polymerization route devoid of isocyanates, resulting in the formation of thermally stable and soluble polyurethanes based on cycloaliphatic systems would be really attractive.

1.6. Solvent Induced Self-organization

The desire to emulate the elegance of nature has inspired many academicians to come up with the concept of "self-organization". Polymeric assembled materials or polymolecular assemblies with well-defined structure on sub-micrometer and nanometer scales have been a subject of intensive research due to their broad potential applications.[96-97]Solvent induced self-organization is one of the easiest techniques known in the literature for forming various morphologies. Initial works were pioneered by Widawski, et al. who were successful in generating polymeric membranes-'honey-combs' through the use of star-polymers and polymeric micelles containing polystyrene units from carbon disulphide under a flow of moist gas.[98] Later on many research groups developed such morphologies based on a variety of polymeric backbone structures as well as various experimental conditions.[99-102] Srinivasarao et al. and Karthaus et al. suggested that formation of hexagonally packed array of holes should be possible for many polymeric systems that are dissolved in a volatile solvent and exposed to an atmosphere containing moisture.[103-104]
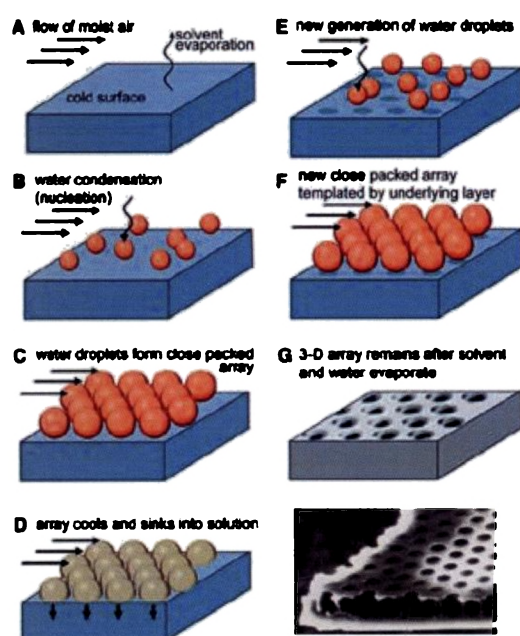
Scheme-1.13: Breath figure technique for the formation of honey-comb morphology and a cross section of such a morphology (adapted from ref. 98 & 103)

The mechanism for the formation of honey-comb morphology is depicted in scheme-1.13. Crucial point for the formation of regular honey-comb patterns was the prevention of coalescence of water droplets. Though few reports suggested that a special complex polymeric architecture was not required for the formation of regular honey-comb patterns, Bolognesi et al. opted that the presence of polar group along the polystyrene chain was required for such morphology developments. [103-105] Cui and coworkers demonstrated that the formation of honey-comb morphology was due to Marangoni-Benard convection which results in breath figure method of film fabrication.[106-108] In order to minimize the use of water and to have an easier way to prepare membranes with large surface area, novel methods for fabricating breath figure patterns were employed. The humid environment was mimicked by adding small amount of water to the water miscible solvent and breath figure patterns were generated under the dry environment. The pore size depended directly on the water content in the polymer solution and inversely on the rotating speed during spin casting.[109-110] Cheng et. al., have fabricated honey-comb patterned films from amphiphilic dendronized block copolymer as shown in scheme-1.14 by on-solid surface spreading method and on-water spreading method.[111]
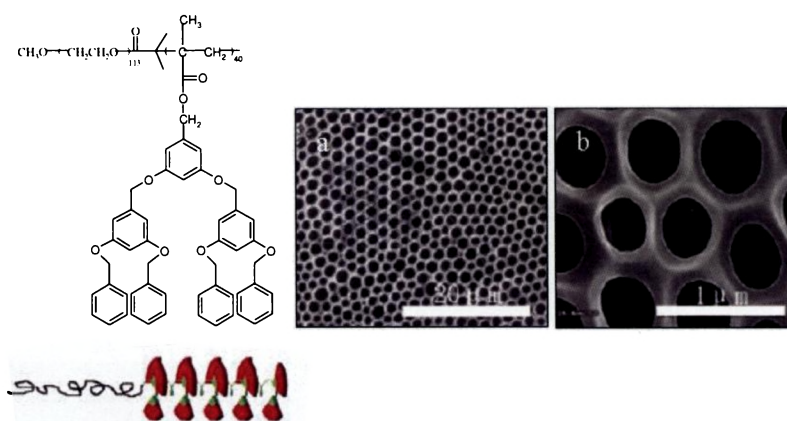
Scheme-1.14: Honey-comb patterned films from amphiphilic dendronised block copolymers by on solid surface spreading (a) and on-water spreading (b) (adapted from ref. 111)

Park et al. have investigated the effects of interfacial energy between water and solvent as well as polymer concentration on the formation of porous structures of polymer films prepared by spin coating of cellulose acetate butyrate in mixed solvent

of tetrahydrofuran and chloroform under humid conditions. They suggested that the degree of mixing between water droplets and polymer solution inside the film would decrease upon increasing the interfacial energy between the two, whereas a higher interfacial energy limits the nucleation of water droplets at the top of the film.[112] Three-dimensional honey-comb patterns have also been observed in methacrylic comb polymer bearing hydrogen bonded urethane and hydrophobic bulky anchoring groups. The authors proved that a unique molecular design involving manipulation of supramolecular architecture and hydrophilic/hydrophobic balance was a necessary condition for the formation of such ordered morphology and mere water droplet condensation as suggested by others was alone not a sufficient driving force.[113] Bormashenko et al. recently patterned annular structures of polystyrene from poor solvent like acetone and they suggested that the theory of viscous dewetting developed by de Gennes explained the formation of toroidal structures. The phenomenon of submicrometric self-assembling was the outcome of the capillary interaction between bubbles filled with solvent vapor formed under the evaporation of the solvent mixture. Here solvent plays a crucial role on surface patterning without any evidence for the influence of humidity on the self-organization process. [114]

Later on various morphologies such as ordered hexagonal structures, spheres, lamellae, cylinders and vesicles were designed through supramolecular self-assembly of synthetic rod-coil triblock and diblock copolymers (scheme-1.15).[115-120]These unique morphologies exhibited by the copolymers arises from the difference in the chain rigidity of the rod-like and coil-like blocks and this greatly affects the aspects of molecular packing and thermodynamic stability of the morphology of such materials.[116]
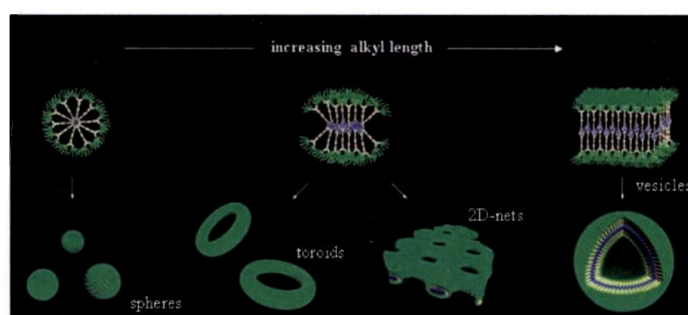
Scheme-1.15: Self-organization of amphiphiles resulting in various morphologies
(adapted from ref. 118)

Solvent induced self-organization is the easiest and economical physical method known for the synthesis of polymolecular assemblies such as honey-combs. Other methods developed for preparing micropatterned surfaces include photolithography, photochemical reaction, photodecomposition of self-assembled monolayers, selective etching, micro-contact printing and spray drying.[111,121] Various chemical methods are also known for the synthesis of polymeric particles with varied morphologies. Dispersion polymerization, seeded growth and two step swelling techniques, emulsion polymerization, suspension, electrospinning, precipitation and interfacial polymerization are few such examples.[121-125] Luhmann et al. have reported the formation of hexagonally shaped, rod like and spherical particles during the aqueous dispersion polymerization of tetrafluoroethylene using perfluorinated surfactants. The shape of the particles depends very much on the experimental conditions. They also suggest that spherical or cobblestone dispersion particles are thought to be formed by inter and intra-particular agglomeration of rod and/ or hexagonal PTFE dispersion particles.[126]Nagao et al. utilized a surfactant-free heterogeneous emulsion polymerization of polystyrene in acidic medium to produce micrometer sized monodispersed polymeric particles.[123] Solution induced phase separation have been reported for the synthesis of porous polylactide microspheres by emulsion-solvent evaporation method.[127] Magnetic poly(methyl methacrylate-divinylbenzene-glycidyl methacrylate) microspheres have been prepared by a modified suspension polymerization in presence of oleic acid-coated magnetite nanoparticles.[128] Wang et al. have synthesized polymer microspheres (scheme-1.16a) from divinylbenzene and methacrylic acid in a near-θ solvent via the precipitation polymerization technique.[129]
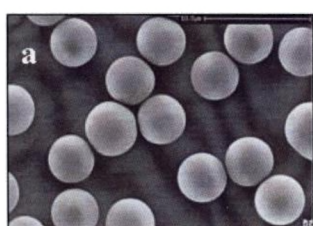
Methacrylic acid crosslinked with divinylbenzene in acetonitrile/toluene
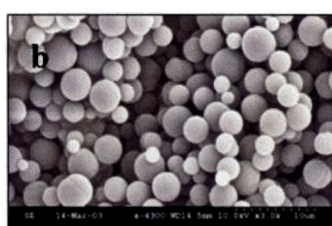
Poly(styrene-codivinyl benzene) particles in acetonitrile

Scheme-1.16: Microspheres obtained by precipitation polymerization (adapted from ref. 129 and 130)

A similar technique was adapted by Shim et al. for the formation of fully cross linked, stable poly(styrene-co-divinylbenzene) microspheres (scheme-1.16b).[130] Another approach which has gained greater significance is the use of templates to grow polymeric particles. Park et al. have used the technique of sacrificial templating of polymeric beads in order to generate macroporous membranes of organic polymers by filling the void spaces among the beads of the crystalline assembly with liquid precursor such as UV-curable polyurethanes, UV-curable polyacrylates, thermally curable epoxies, etc. via capillary action.[131] Yin et al. have demonstrated the use of replica molding to generate polyurethane templates which could be used for the fabrication of large colloidal crystals. These colloidal crystals have in turn been used as templates to generate macroporous materials known as inverse opals. [132] Batra et al. have used surface deposited polystyrene beads as two dimensional hexagonal arrayed templates for cross linked polyvinyl alcohol yielding laterally patterned ordered polymeric arrays of wells for the spatial localization of proteins.[133]Polycarbonate membrane templates have been used by Porrata et al. for the self-assembly of peptide nanotubes.[134]

1.7. Self-organization in Polyurethanes

Though styrene based polymers are known to show various morphologies, there are few reports in the literature for the self-organization of polyurethanes. The technique of electrospinning was used by Thandavamoorthy et al. for self-assembling polyurethane nanofibres into three-dimensional honey-comb meshes.[124] Chen et al. reported the synthesis of epoxy resin/ polyurethane hybrid network via a new technique, viz., frontal polymerization and the morphology of these hybrids consists of isotropic and well pronounced homogeneous networks of two-dimensional platelets.[135] Microporous polyurethane membranes as moisture responsive barriers in protective clothing were formulated by grafting polyethylene glycols on to polyurethanes, producing porous membranes with diverse, complex and irregular structures plausible for both liquid and particle penetration.[136] Jabbari et al. have utilized a two-step suspension polycondensation method for the synthesis of polyurethane microspheres with a porous morphology and the nature of the pores depended on the formation of carbondioxide and also the extent of cross linking reactions such as allophanate and biuret linkages.[121] Interfacial polycondensation was

utilized by Hong et al. and Frere et al. for the synthesis of polyurethane microcapsules possessing good mechanical properties and they show promise as sustained release systems.[125,137] When the above technique was combined with spontaneous emulsification, the process resulted in the formation of polyurethane nanocapsules.[138] Anionic polyurethane dispersions have been used for the synthesis of radiation curable polyurethane based microspheres.[139] Ramanathan et al. have reported the dispersion polycondensation of a polycondensable macromonomer with an amphiphilic block copolymer as steric stabilizer resulting in the formation of uniform polyurethane spheres.[140] Phadtare et al. have utilized the above strategy to prepare polyurethane spheres (core) which can be used to assemble gold nanoparticles (shell) and these structures were used for the immobilization of enzymes such as pepsin[141] (scheme-1.17) and endoglucanase.[142]
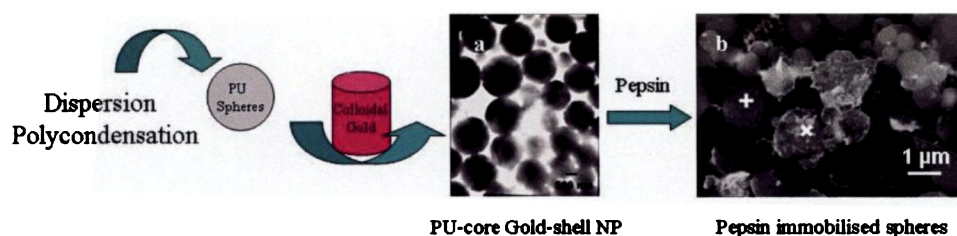
Scheme-1.17: Polyurethane spheres prepared by dispersion polycondensation getting converted into PU core-gold-shell nanoparticles whose TEM images are shown in (a) which are then used for the immobilization of pepsin enzyme whose SEM images are shown in (b). (adapted from ref. 141)

Similarly, core-shell type waterborne polyacrylate-polyurethane microspheres have been prepared by aqueous dispersion polycondensation. In these microspheres, polyurethane acts as the shell and acrylic polymer functions as the core and they were found to possess excellent storage stability, water resistance and coating properties.[143]

The properties of polyurethanes have been modified by the incorporation of π-conjugated oligomers such as oligo-phenylenevinylene (OPV) units into the polymeric backbone. These polymers were mainly synthesized to study their performance as opto-electronic devices, mechanochromic properties and as light emitting electrochemical cells, etc.[144-147] Kuo et al. synthesized polyurethanes with a hole transport oligo-p-phenylene-vinylene segment and an electron transport aromatic oxadiazole segment and the electro luminescent devices obtained from the polymers

showed improved performance such as higher current density and lower driving voltage thereby increasing the device efficiency. The crucial factor is the dipole moment alignment of the carbamate linkers which assists in the hole injection process towards the hole transport layer for better charge balanced conditions.[144-145] Crenshaw et al. synthesized mechanochromic, photoluminescent thermoplastic polyurethanes either by physical blending or by covalent incorporation of cyano-OPVs as built-in deformation sensors (scheme-1.18). These polymers would reversibly change their photoluminescent color as a function of applied strain. Photoluminescent studies suggested that the thermodynamic equilibrium of the physical blends lead to large-scale phase separation which greatly affects the polymer's mechanochromic response where as the covalently bound materials did not express any large-scale phase separation.[146]
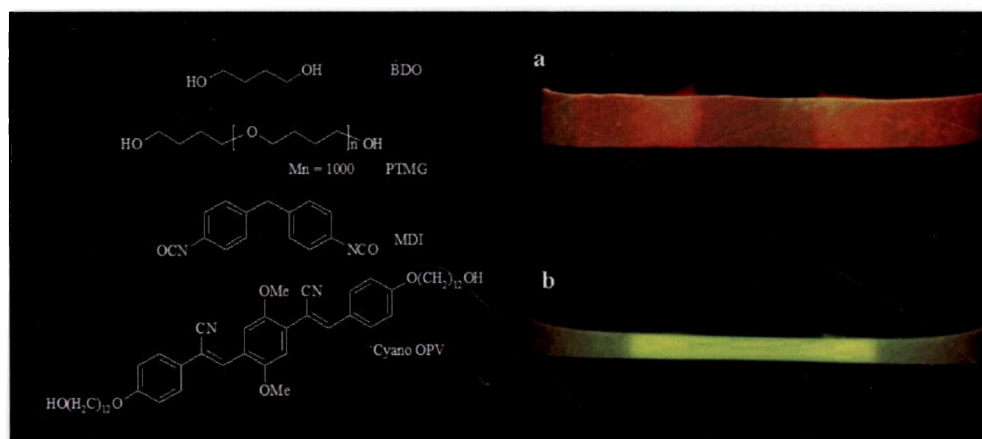
Scheme-1.18: Monomers used for the formation of TPU-cyano OPV blends and the pictures of mechanochromic films excited under UV light of wavelength 365 nm in the unstretched (a) and stretched (b) state. (adapted from ref. 146)

To improve the electroluminescent performance of poly (phenylene vinylene)s, Wang et al. have introduced polyurethane ionomers into electroluminesecnt device. They have synthesized a polymer blend comprising a hole transport poly (phenylene vinylene) and lithium ion conducting water borne polyurethane ionomer which acts as the polymer electrolyte mixture for use as light emitting electrochemical cell. The phase separated morphology of the hard and soft segments in the polyurethane chain provides ideal environment for ion conduction.[147]

1.8. Self-organization through Hydrogen-Bonding

Self-organization is a potent tool to build two and three dimensional functional materials through intermolecular interactions such as hydrogen bonding. These bonds are very versatile and directional in nature and they are well tuned to respond to any external conditions. Similar to the secondary and ternary structures in proteins, these supramolecular interactions play a key role in unprecedented control of the molecular structure and the intriguing function of the self-assembled molecules. Proper positioning of hydrogen bonding in materials produces new types of supramolecular arrangements with properties such as thermoplastic behavior and controlled molecular packing for special morphological architectures.[148-149]There are a number of reports known in the literature for the utilization of hydrogen bonding as tectons for the formation of self-assembled structures. Since a single hydrogen bond is only moderately strong, the incorporation of several hydrogen bonds with specific orientations results in fascinating supramolecular assemblages. Triple, quadruple and sextuple hydrogen bonded arrays are well known for quiet some time.[150-155] Jorgenson and coworkers have studied the association of linear arrays of three hydrogen bonding sites and depending upon the orientation of the donor and acceptor in these structures they calculated the association constants.[150] Different orientations possible for hydrogen bonded donor and acceptor groups for a typical triple hydrogen bonded system is shown in scheme-1.19.
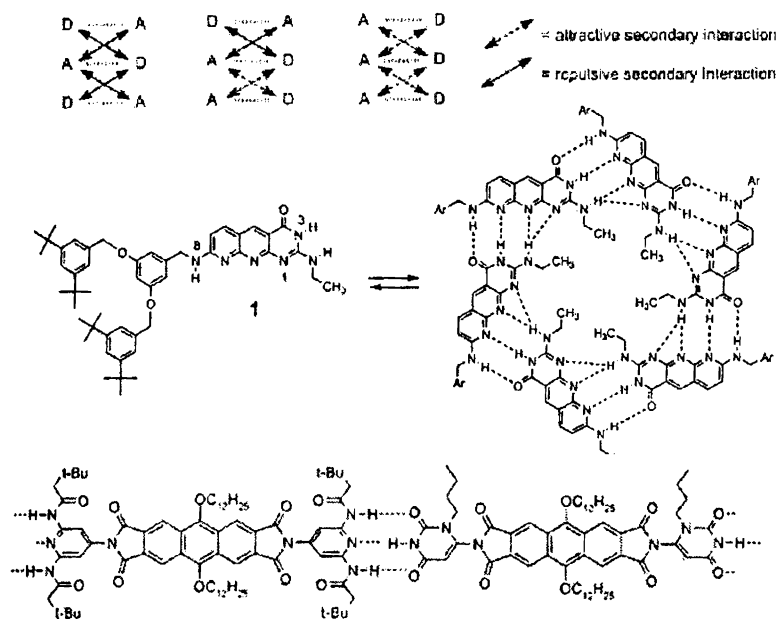
Scheme-1.19: Different types of orientation in a triple hydrogen bonded system and examples for few triple hydrogen bonded systems (adapted from ref. 150-152)

They suggested that diagonally opposed sites repel each other electrostatically when they are of the same kind where as disparate sites attract each other.[150]A triple hydrogen bonded donor '1' was allowed to self organize to form hexameric disk shaped aggregates with 18 hydrogen bonds as shown in scheme-1.19 by Kolotuchin, et al.[151] The pioneering works on triple hydrogen bonding units by Lehn group has resulted in supramolecular main chain polymers which showed lyotropic liquid crystallinity (scheme-1.19).[152-153]Another striking outcome of self-organization through highly specific hydrogen bonding interactions is the formation of low molecular weight organo gelators (LMOG) which preferentially grow in one-dimension resulting in the formation of fibers, strands or tapes.[156] Moniruzzaman, et al. have extended the ability of hydrogen bonding in simple carbamates containing alkyl side chains for the formation of thermoreversible gels. These carbamates were then used for blending with different polymeric systems such as polyethylene, polycarbonate etc. and the role of hydrogen bonding in effecting the physical properties of these polymers in blends were studied in detail. This group has also studied the morphology and crystallization of self assembling systems with single and double hydrogen bonding motifs.[156-159] It was observed that hydrogen bonding moieties at the chain ends of polymer can improve the mechanical and morphological properties of the parent polymers. Kautz et al. have functionalised hydroxyl-telechelic poly(ethylene butylenes) with lateral urethane and urea hydrogen bonded functionalities and end-to-end ureidopyrimidinone (UPy) hydrogen bonding functionalities. They found that those polymers with a lateral urea and end-to-end UPy based polymers gave rise to one dimensional aggregation of end groups into long fibers. The mechanical properties of these polymers were also enhanced due to the difficulty in chain pull-out from the fibrils.[160]

From the above discussions based on self-organization with relevance to hydrogen bonding especially in polyurethanes, studies are really inadequate. Morphology development in polyurethanes is mainly based on the microphase separation and only very few reports are known which could effectively incorporate the importance of hydrogen bonding. Also most of the research groups gave importance to self-organization of only small molecules which results in the formation of supramolecules that can mimic the properties of traditional macromolecules. Since hydrogen bonding is reversible, these self-assembled small

molecules are under thermodynamic equilibrium and their properties can be well adjusted by changing external stimuli and so they can be used as "smart materials". However, their relatively poor mechanical stability such as low strength and their phase transitions give them a low-added value with respect to the covalently bonded polymers.[161] Hence more intellectual input is required for self-organizing polymers such as polyurethanes which would be really promising for many applications.

1.9. Conclusion

In this introduction part, importance has been given to the elastomeric properties of polyurethanes. Emphasis has been laid to this property based on microphase separation and how this could be modified by modifying the segment lengths, as well as the structure of the segments. Implication was also made on the mechanical and thermal properties of these copolymers based on various analytical methods usually used for characterization of polymers. A brief overview of the challenges faced by the polyurethane chemistry was also done, pointing to the fact that though polyurethane industry is more than 75 years old, still a lot of questions remain unanswered, that too mostly in the synthesis of polyurethanes. A major challenge in this industry is the utilization of more environmental friendly "Green Chemistry Routes" for the synthesis of polyurethanes which are devoid of any isocyanates or harsh solvents.

The research work in this thesis was focused to develop non-isocyanate green chemical process for polyurethanes and also self-organize the resultant novel polymers into nano-materials. The thesis was focused on the following three major aspects:

    (i)   Design and development of *novel melt transurethane* process for polyurethanes under non-isocyanate and solvent free melt condition.

    (ii)   Solvent induced self-organization of the novel cycloaliphatic polyurethanes prepared by the melt transurethane process into micro-porous templates and nano-sized polymeric hexagons and spheres.

    (iii)   Novel polyurethane-oligophenylenevinylene random block copolymer nano-materials and their photoluminescence properties.

The second chapter of the thesis gives an elaborate discussion on the *"Novel Melt Transurethane Process"* for the synthesis of polyurethanes under non-isocyanate and solvent free melt condition. The polycondensation reaction was carried out between equimolar amounts of a di-urethane monomer and a diol in the presence of a catalyst under melt condition to produce polyurethanes followed by the removal of low boiling alcohol from equilibrium. The polymers synthesized through this green chemical route were found to be soluble (devoid of any cross links), thermally stable and free from any isocyanate entities. The polymerization reaction was confirmed by various analytical techniques with specific reference to the evaluation of the extent of

reaction which is the main watchful point for any successful polymerization reaction. The mechanistic aspects of the reaction were another point of consideration for the novel polymerization route which was successfully dealt with by performing various model reactions. Since this route was successful enough in synthesizing polyurethanes with novel structures, they were employed for the solvent induced self-organization which is an important area of research in the polymer world in the present scenario. Chapter three mesmerizes the reader with multitudes of morphologies depending upon the chemical backbone structure of the polyurethane as well as on the nature and amount of various solvents employed for the self-organization tactics. The rationale towards these morphologies-*"Hydrogen Bonding"* have been systematically probed by various techniques. These polyurethanes were then tagged with luminescent oligo(phenylene vinylene) units and the effects of these OPV blocks on the morphology of the polyurethanes were analyzed in chapter four. These blocks have resulted in the formation of novel *"Blue Luminescent Balls"* which could find various applications in optoelectronic devices as well as delivery vehicles.

1.10. References

1. Charch, W. H.; Shivers, J. C. *Text. Res. J.* **1959**, *29*, 536.

2. Frazer, A. H.; Shivers, J. C. US Patent 2929803, **1960**.

3. Tanner, D.; Gabara, V.; Scheefgen, J. R. *International Symposium on Polymers for Advanced Technologies* Lewin, M (Ed.) **1987**, pg. 384.

4. Frick, A.; Rochman, A. *Polym. Test.* **2004**, *23*, 413.

5. Odian, G. *Principles of Polymerization* Third Edition, John Wiley & Sons, Inc. New York, **2002**, pg. 136, 149.

6. Bachmann, F.; Reimer, J.; Ruppenstein, M.; Thiem, J. *Macromol. Chem. Phys.* **2001**, *202*, 3410.

7. Singer, S. M.; Allott, M. T. US Patent 5599874, **1997**.

8. Eisenbach, C. D.; Nefzger, H. *Hand Book of Polymer Synthesis: Part A* Kricheldorf, H. R. (Ed.) Marcel Dekker, Inc. New York 10016, **1992**, pg. 685.

9. Velankar, S.; Cooper, S. L. *Macromolecules* **1998**, *31*, 9181.

10. Krol, P.; Pitera, B.P. *Eur.Polym.J.* **2001**, *37*, 251.

11. Poussard, L.; Burel, F.; Couvercelle, J-P.; Merhi, Y. ; Tabrizian, M. ; Bunel, C. *Biomaterials* **2004**, *25*, 3473.

12. Wang, L-Q.; Liang, G-Z.; Dang, G-C.; Wang, F.; Fan, X-P.; Fu, W-B. *Chinese J. Chem.* **2005**, *23*, 1257.

13. Born, L.; Hespe, H. *Colloid Polym. Sci.* **1985**, *263*, 335.

14. Saotome, K.; Komoto, H. *J. Polym. Sci. Part A-1* **1967**, *5*, 119.

15. Huang, F-J.; Wang, T-L. *J. Poly. Sci. Part A Polym. Chem.* **2004**, *42*, 290.

16. Lunardon, G.; Sumida, Y.; Vogl, O. *Die Angewandte Makromolekulare Chemie*, **1980**, *87*, 1.

17. Li, Y. Kang, W.; Stoffer, J. O.; Chu, B. *Macromolecules* **1994**, *27*, 612.

18. Eisenbach, C. D.; Heinemann, T.; Ribbe, A.; Stadler, E. *Die Angewandte Makromolekulare Chemie* **1992**, *202*, 221.

19. Elwell, M. J. ; Ryan, A. J. ; Grunbauer, H. J. M.; Van Lieshout, H. C. *Macromolecules* **1996**, *29*, 2960.

20. Lee, H. S.; Wang, Y. K.; MacKnight, W. J.; Hsu, S. L. *Macromolecules* **1988**, *21*, 270.

21. Saiani, A.; Rochas, C.; Eeckhaut, G.; Daunch, W. A.; Leenslag, J-W.; Higgins, J. S. *Macromolecules* **2004**, *37*, 1411.

22. Seymour, R. W.; Estes, G. M.; Cooper, S. L.; *Polym. Prepr. Am. Chem. Soc. Div. Polym. Chem.* **1970**, *11*, 867.

23. Cooper, S. L.; Estes, G. M.; Seymour, R. W. *Macromolecules* **1971**, *4*, 452.

24. Tang, W.; MacKnight, W. J.; Hsu, S. L. *Macromolecules* **1995**, *28*, 4284.

25. Savelyev, Y. V. ; Akhranovich, E. R. Grekov, A. P. ; Privalko, E. G.; Korskanov, V. V.; Shtompel, V. I.; Privalko, V. P.; Pissis, P.; Kanapitsas, A. *Polymer* **1998**, *39*, 3425.

26. Yontz, D. J.; Hsu, S. L. *Macromolecules* **2000**, *33*, 8415.

27. Fu, B.; Feger, C.; MacKnight, W. J.; Schneider, N. S. *Polymer* **1985**, *26*, 889.

28. Qin, Z. Y.; Macosko, C. W.; Wellinghoff, S. T. *Macromolecules* **1985**, *18*, 553.

29. Wang, H.; Thompson, D. G.; Schoonover, J. R.; Aubuchon, S. R.; Palmer, R. A. *Macromolecules* **2001**, *34*, 7084.

30. Ferguson, J.; Patsavoudis, D. *Eur. Polym. J.* **1972**, *8*, 385.

31. Meltzer, A. D.; Spiess, H. W.; Eisenbach, C. D.; Hayen, H. *Macromolecules* **1992**, *25*, 993.

32. Ning, L.; De-Ning, W.; Sheng-Kang, Y. *Macromolecules* **1997**, *30*, 4405.

33. Sheth, J. P.; Klinedinst, D. B.; Pechar, T. W.; Wilkes, G. L.; Yilgor, E.; Yilgor, I. *Macromolecules* **2005**, *38*, 10074.

34. Sheth, J. P.; Wilkes, G. L.; Fornof, A. R.; Long, T. E.; Yilgor, I. *Macromolecules* **2005**, *38*, 5681.

35. Rutkowska, M.; Kwiatkowski, A. *J. Polym. Sci. Polym. Symp.* **1975**, *53*, 141.

36. Illinger, J. L.; Schneider, N. S.; Karasz, F. E. *Polym. Eng. Sci.* **1972**, *12*, 25.

37. Seefried, Jr. C. G.; Koleske, J. V.; Critchfield, F. E.; Pfaffenberger, C. R. *J. Polym. Sci. Polym. Phys. Ed.* **1980**, *18*, 817.

38. Koberstein, J. T. ; Russell, T. P. *Macromolecules* **1986**, *19*, 714.

39. Privalko, V. P.; Lipatov, Y. S.; Mirontsov, L. I.; Dashevskii, L. I. *Colloid Polym. Sci.* **1985**, *263*, 691.

40. Wilkes, G. L.; Emerson, J. A. *J. Appl. Phys.* **1976**, *47*, 4261.

41. Ferguson, J.; Hourston, D. J.; Meredith, R.; Patsavoudis, D. *Eur. Polym. J.* **1972**, *8*, 369.

42. Huh, D. S.; Cooper, S. L. *Polym. Eng. Sci.* **1971**, *11*, 369.

43. Clark, A. J.; Echenique, J.; Haddleton, D. M.; Straw, T. A.; Taylor, P. C. *J. Org. Chem.* **2001**, *66*, 8687.

44. MacKnight W. J.; Yang, M.; Kajiyama, T. *Anal. Calorimetry, Proc. Am. Chem. Soc. Symp.*, **1968**, p.99.

45. McKiernan, R. L.; Heintz, A. M.; Hsu, S. L.; Atkins, E. D. T.; Penelle, J.; Gido, S. P. *Macromolecules* **2002**, *35*, 6970.

46. Bayer, O. *Angew. Chem.* **1947**, *A59*, 257.

47. Yilgor, E.; Yilgor, I. *Polymer* **2001**, *42*, 7953.

48. Wu, Y.; Natansohn, A.; Rochon, P. *Macromolecules* **2004**, *37*, 6090.

49. Figovsky, O. *In Interface Phenomena in Polymer Coating. Encyclopedia of Surface and Colloid Science*, Marcel Dekker Inc.: New York, **2002**; p. 2653.

50. Kebir, N.; Morandi, G.; Campistron, I.; Laguerre, A.; Pilard, J-F. *Polymer* **2005**, *46*, 6844.

51. Blencowe, A.; Clarke, A.; Drew, M. G. B.; Hayes, W.; Slark, A.; Woodward, P. *React. Funct. Polym.* **2006**, *66*, 1284.

52. Lu, Q-W.; Hoye, T. R.; Macosko, C. W. *J. Polym. Sci., Part A: Polym. Chem.* **2002**, *40*, 2310.

53. Caraculacu, A.A.; Coseri, S. *Prog. Polym. Sci.* **2001**, *26*, 799.

54. Hoff, G. P.; Wicker, D. B. *In Perlon U. Polyurethanes* at I. G. Farben, Boringen, Augsburg, P. B. Report 1122, Sept. 12, **1945**.

55. Dieter, J. A.; Frisch, K. C.; Wolgemuth, L. G. *J. Paint Technol.* **1975**, *47*, 65.

56. Kumar, A.; Ramakrishnan, S. *J. Polym. Sci., Part A: Polym. Chem.* **1996**, *34*, 839.

57. (a) Okaniwa, M.; Takeuchi, K.; Asai, M.; Ueda, M. *Macromolecules* **2002**, *35*, 6224. (b) Okaniwa, M.; Takeuchi, K.; Asai, M.; Ueda, M. *Macromolecules* **2002**, *35*, 6232.

58. Wicks. Jr, Z. M. *Prog. Org. Coat.* **1975**, *3*, 73.

59. Schollenberger, C. S. Stewart, F. D. J. *Elastoplast.* **1972**, *4*, 294.

60. Schultze, H. *Makromol. Chem.* **1973**, *172*, 57.

61. Frisch, K. C.; Klempner, D. *Comprehensive Polymer Science*, Eastmond, G. C.; Ledwith, A.; Russo, S.; Sigwalt, P.(Ed.) Volume 5, Chapter 24, pg.413.

62. Spindler, R.; Frechet, J. M. J. *Macromolecules* **1993**, *26*, 4809.

63. Rokicki, G.; Piotrowska, A. *Polymer* **2002**, *43*, 2927.

64. Steinlein, C.; Hernandez, L.; Eisenbach, C. D. *Macromol. Chem. Phys.* **1996**, *197*, 3365.

65. Javni, I.; Petrovic, Z. S.; Guo, A.; Fuller, R. *J. Appl. Polym. Sci.* **2000**, *77*, 1723.

66. Saunders, H. H.; Frisch, K. C. *Polyurethanes, Chemistry and Technology, High Polymers*, VolXVI/1, Interscience New York, **1962**; p.103.

67. Kojio, K.; Fukumaru, T.; Furukawa, M. *Macromolecules* **2004**, *37*, 3287.

68. (a) Ning, L.; De-Ning, W.; Sheng-Kang, Y. *Macromolecules* **1997**, *30*, 4405. (b) Garrett, J. T.; Siedlecki, C. A.; Runt, J. *Macromolecules* **2001**, *34*, 7066. (c) Cheong, I. W.; Kong, H. C.; An, J. H.; Kim, J. H. *J. Polym. Sci. Part A: Polym Chem.* **2004**, *42*, 4353.

69. Wang, C.; Zhang, C.; Lee, M. S.; Dalton, L. R.; Zhang, H.; Steier, W. H. *Macromolecules* **2001**, *34*, 2359.

70. Yilgor, I.; Yustsever, E.; Erman, B. *Macromolecules* **2002**, *35*, 9825.

71. Yen, F-S.; Lin, L-L.; Hong, J-L. *Macromolecules* **1999**, *32*, 3068.

72. Murgasova, R.; Brantley, E. L.; Hercules, D. M.; Nefzger, H. *Macromolecules* **2002**, *35*, 8338.

73. Shahram, M-A.; Shahriar, K. *Polym. Int.* **2003**, *52*, 1487.

74. Cascella, C.; Malinconico, M.; Martuscelli, E.; Piermattei, A.; Ragosta, G.; Rizzo, A. *Die Angewandte Makromolekulare Chemie* **1995**, *231*, 79.

75. Ni, H.; Daum, J. L.; Thiltgen, P. R.; Soucek, M. D.; Simonsick Jr., W. J.; Zhong, W.; Skaja, A. D. *Prog. Org. Coat.* **2002**, *45*, 49.

76. Li, X.; Yee, A. F. *Macromolecules* **2003**, *36*, 9421.

77. Jayakannan, M.; Anilkumar, P. *J. Polym. Sci. Part A: Polym Chem.* **2004**, *42*, 3996.

78. Matuszak. M. L.; Frisch, K. C. *J. Polym. Sci. Polym. Chem. Ed.* **1973**, *11*, 637.

79. Srinivansan, R.; McGrath, J. E. *Polym Prepr.* **1992**, *33*, 503.

80. Vanhaecht, B.; Willem, R.; Biesemans, M.; Goderis, B.; Basiura, M.; Magusin, P. C. M. M.; Dolbnya, I.; Koning, C. E. *Macromolecules* **2004**, *37*, 421.

81. Cotter, R. J. *US Patent.* 3, 164, 571, **1965**.

82. Meltzer, A. D.; Spiess, H. W. *Macromolecules* **1992**, *25*, 993.

83. Nakamura, H.; Takata, T.; Endo, T. *Macromolecules* **1990**, *23*, 3032.

84. Bachmann, F.; Reimer, J.; Ruppenstein, M.; Thiem, J. *Macromol.Chem.Phys.* **2001**, *202*, 3410.

85. Joseph, M. D. ; Savina, M. R.; Harris, R. F. *J. Appl. Polym. Sci.* **1992**, *44*, 1125.

86. Adhikari, R.; Gunatillake, P. A.; Meijs, G. F.; McCarthy, S. J. *J. Appl. Polym. Sci.* **1999**, *73*, 573.

87. Tonelli, C.; Trombetta, T.; Scicchitano, M.; Castiglioni, G. *J. Appl. Polym. Sci.* **1995**, *57*, 1031.

88. Schmeizer, H. G. *Materials and Design* **1988**, *9*, 279.

89. Hergenrother, R. W.; Wabers, H. D.; Cooper, S. L. *Biomaterials* **1993**, *14*, 449.

90. Joseph, M. D.; Savina, M. R.; Harris, R. F. *J. Appl. Polym. Sci.* **1992**, *44*, 1125.

91. Byrne, C. A. *Polym. Mat. Sci. Engi.* **1988**, *58*, 962.

92. Barikani, M.; Hepburn, C. *Cellular Polymers* **1987**, *6*, 47.

93. Dieter, J. W.; Byrne, C. A. *Polym Engi. Sci.* **1987**, *27*, 673.

94. Le, T. P.; Viollaz, F.; Camberlin, Y.; Thanh, M. L.; Pascuali, J. P. *Makromol.Chem.* **1984**, *185*, 281.

95. Elabd, Y. A.; Sloan, J. M.; Tan, N. B.; Barbari, T. A. *Macromolecules* **2001**, *34*, 6268.

96. Lehn, J-M. *Polym. Int.* **2002**, *51*, 825.

97. Zhang, Y.; Jiang, M.; Zhao, J.; Wang, Z.; Dou, H.; Chen, D. *Langmuir* **2005**, *21*, 1531.

98. Widawski, G.; Rawiso, M.; Francois, B. *Nature* **1994**, *369*, 387.

99. a) Govor, L. V.; Bashmakov, I. A.; Kaputski, F. N.; Pientka, M.; Parisi, J. *Macromol. Chem. Phys.* **2000**, *201*, 2721. b) Govor, L. V.; Bashmakov, I. A.; Kiebooms, R.; Dyakonov, V.; Parisi, J. *Adv. Mater.* **2001**, *13*, 588.

100.   Stenzel-Rosenbaum, M. H.; Davis, T. P.; Fane, A. G.; Chen, V. *Angew. Chem. Int. Ed.* **2001**, *40*, 3428.

101.   Nishikawa, T.; Ookura, R.; Nishida, J.; Sawadaishi, T.; Shimomura, M. *RIKEN Review* **2001**, *37*, 43.

102.   Yabu, H.; Tanaka, M.; Ijiro, K.; Shimomura, M. *Langmuir* **2003**, *19*, 6297.

103.   Srinivasarao, M.; Collings, D.; Philips, A.; Patel, S. *Science* **2001**, *292*, 79.

104.   Karthaus, O.; Maruyama, N.; Cieren, X.; Shimomura, M.; Hasegawa, H.; Hashimoto, T. *Langmuir* **2000**, *16*, 6071.

105.   Bolognesi, A.; Mercogliano, C.; Yunus, S.; Civardi, M.; Comoretto, D.; Turturro, A. *Langmuir* **2005**, *21*, 3480.

106.   Cui, L.; Han, Y. *Langmuir* **2005**, *21*, 11085.

107.   Cui, L.; Xuan, Y.; Li, X.; Ding, Y. ; Li, B. ; Han, Y. *Langmuir* **2005**, *21*, 11696.

108.   Mitov, Z.; Kumacheva, E. *Phys. Rev. Lett.* **1998**, *81*, 3427.

109.   Park, M. S.; Kim, J. K. *Langmuir* **2004**, *20*, 5347.

110.   Wang, Y.; Liu, Z.; Huang, Y.; Han, B.; Yang, G. *Langmuir* **2006**, *22*, 1928.

111.   Cheng, C. X.; Tian, Y.; Shi, Y. Q.; Tang, R. P.; Xi, F. *Langmuir* **2005**, *21*, 6576.

112.   Park, M. S.; Joo, W.; Kim, J. K. *Langmuir* **2006**, *22*, 4594.

113.   Deepak, V. D.; Asha, S. K. *J. Phys. Chem. B* **2006**, *110*, 21450.

114.   a) Bormashenko, E.; Pogreb, R.; Musin, A.; Stanevsky, O.; Bormashenko, Y.; Whyman, G.; Barkay, Z. *J. Colloid and Interface Science* **2006**, *300*, 293. b) Bormashenko, E.; Pogreb, R.; Stanevsky, O.; Bormashenko, Y.; Tamir, S.; Cohen, R.; Nunberg, M.; Gaisin, V-Z.; Gorelik, M.; Gendelman, O. V. *Mater. Lett.* **2005**, *59*, 2461. c) Bormashenko, E.; Pogreb, R.; Stanevsky, O.; Bormashenko, Y.; Socol, Y.; Gendelman, O. *Polym. Adv. Technol.* **2005**, *16*, 299.

115.   a) Jenekhe, S. A.; Chen, X. L. *Science* **1998**, *279*, 1903. b) Chen, X. L.; Jenekhe, S. A. *Langmuir* **1999**, *15*, 8007. c) Jenekhe, S. A.; Chen, X. L. *Science* **1999**, *283*, 372.

116.   Lin, C-L.; Tung, P-H.; Chang, F-C. *Polymer* **2005**, *46*, 9304.

117.   Tzanetos, N. P.; Dracopoulos, V.; Kallitsis, J. K.; Deimede, V. A. *Langmuir* **2005**, *21*, 9339.

118.   Kuang, M.; Duan, H.; Wang, J.; Jiang, M. *J. Phys. Chem. B* **2004**, *108*, 16023.

119.   Lee, E.; Jeong, Y-H.; Kim, J-K.; Lee, M. *Macromolecules* **2007**, *40*, 8355.

120.   Hayakawa, T.; Horiuchi, S. *Angew. Chem. Int. Ed.* **2003**, *42*, 2285.

121.   Jabbari, E.; Khakpour, M. *Biomaterials* **2000**, *21*, 2073.

122.   Song, J-S.; Winnik, M. A. *Macromolecules* **2006**, *39*, 8318.

123.   Nagao, D.; Sakamoto, T.; Konno, H.; Gu, S.; Konno, M. *Langmuir* **2006**, *22*, 10958.

124.   Thandavamoorthy, S.; Gopinath, N.; Ramkumar, S. S. *J. Appl. Polym. Sci.* **2006**, *101*, 3121.

125.   Hong, K.; Park, S. *React. Funct. Polym.* **1999**, *42*, 193.

126.   Luhmann, B.; Feiring, A. E. *Polymer* **1989**, *30*, 1723.

127.   Hong, Y.; Gao, C.; Shi, Y.; Shen, J. *Polym. Adv. Technol.* **2005**, *16*, 622.

128.   Ma, Z.; Guan, Y.; Liu, X.; Liu, H. *Polym. Adv. Technol.* **2005**, *16*, 554.

129.   Wang, J.; Cormack, P. A. G.; Sherrington, D. C.; Khoshdel, E. *Angew. Chem. Int. Ed.* **2003**, *42*, 5336.

130.   Shim, S. E.; Yang, S.; Choi, H. H.; Choe, S. *J. Polym. Sci. Part A: Polym. Chem.* **2004**, *42*, 835.

131.   a) Park, S. H.; Xia, Y. *Adv. Mater.* **1998**, *10*, 1045. b) Park, S. H.; Xia, Y. *Chem. Mater.* **1998**, *10*, 1745.

132.   Yin, Y.; Li, Z-Y.; Xia, Y. *Langmuir* **2003**, *19*, 622.

133.   Batra, D.; Vogt, S.; Laible, P. D.; Firestone, M. A. *Langmuir* **2005**, *21*, 10301.

134.   Porrata, P.; Goun, E.; Matsui, H. *Chem. Mater.* **2002**, *14*, 4378.

135.   Chen, S.; Tian, Y.; Chen, L.; Hu, T. *Chem. Mater.* **2006**, *18*, 2159.

136.   Tan, K.; Obendorf, S. K. *J. Membrane Sci.* **2006**, *274*, 150.

137.   Frere, Y.; Danicher, L.; Gramain, P. *Eur. Polym. J.* **1998**, *34*, 193.

138.   Bouchemal, K.; Briancon, S.; Perrier, E.; Fessi, H.; Bonnet, I.; Zydowicz, N. *Inter. J. Pharm.* **2004**, *269*, 89.

139.   Hirose, M.; Zhou, J.; Kadowaki, F. *Colloids Surf. A* **1999**, *153*, 481.

140.   a) Ramanathan, L. S.; Shukla, P. G.; Sivaram, S. *Pure & Appl. Chem.* **1998**, *70*, 1295. b) Ramanathan, L. S.; Baskaran, D.; Shukla, P. G.; Sivaram, S. *Macromol. Chem. Phys.* **2002**, *203*, 998.

141. Phadtare, S.; Kumar, A.; Vinod, V. P.; Dash, C.; Palaskar, D. V.; Rao, M.; Shukla, P. G.; Sivaram, S.; Sastry, M. *Chem. Mater.* **2003**, *15*, 1944.

142. Phadtare, S.; Vyas, S.; Palaskar, D. V.; Lachke, A.; Shukla, P. G.; Sivaram, S.; Sastry, M. *Biotechnol. Prog.* **2004**, *20*, 1840.

143. Dong, A.; An, Y.; Feng, S.; Sun, D. *J. Colloid and Interface Science* **1999**, *214*, 118.

144. Kuo, C-H.; Peng, K-C.; Kuo, L-C.; Yang, K-H.; Lee, J-H.; Leung, M-K.; Hsieh, K-H. *Chem. Mater.* **2006**, *18*, 4121.

145. Lin, K-R.; Kuo, C-H.; Kuo, L-C.; Yang, K-H.; Leung, M-k.; Hsieh, K-H. *Eur. Polym. J.* **2007**, *43*, 4279.

146. Crenshaw, B. R.; Weder, C. *Macromolecules* **2006**, *39*, 9581.

147. (a) Wang, H-L.; Fu, C-M.; Gopalan, A.; Wen, T-C. *Thin Solid Films* **2004**, *466*, 197. (b) Wang, H-L.; Wen, T-C. *Mater. Chem. Phys.* **2003**, *82*, 341. (c) Wang, H-L.; Gopalan, A.; Wen, T-C. *Mater. Chem. Phys.* **2003**, *82*, 793.

148. Ikkala, O.; ten Brinke, G. *Science* **2002**, *295*, 2407.

149. Binder, W. H.; Kunz, M. J.; Kluger, C.; Hayn, G.; Saf, R. *Macromolecules* **2004**, *37*, 1749.

150. (a) Jorgenson, W. L.; Pranata, J. *J. Am. Chem. Soc.* **1990**, *112*, 2008. (b) Pranata, J.; Wierschke, S. G.; Jorgenson, W. L. *J. Am. Chem. Soc.* **1991**, *113*, 2810.

151. Kolotuchin, S. V.; Zimmerman, S. C. *J. Am. Chem. Soc.* **1998**, *120*, 9092.

152. Fouquey, C.; Lehn, J-M.; Levelut, A-M. *Adv. Mater.* **1990**, *2*, 254.

153. Lehn, J-M. *Makromol. Chem. Macromol. Symp.* **1993**, *69*, 1.

154. Beijer, F. H.; Sijbesma, R. P.; Kooijman, H.; Spek, A. L.; Meijer, E. W. *J. Am. Chem. Soc.* **1998**, *120*, 6761.

155. Kolomiets, E.; Buhler, E.; Candau, S. J.; Lehn, J-M. *Macromolecules* **2006**, *39*, 1173.

156. Moniruzzaman, M.; Sundararajan, P. R. *Langmuir* **2005**, *21*, 3802.

157. Moniruzzaman, M.; Sundararajan, P. R. *J. Phys. Chem. B* **2005**, *109*, 1192.

158.   Tuteja, B.; Moniruzzaman, M.; Sundararajan, P. R. *Langmuir* **2007**, *23*, 4709.

159.   Khanna, S.; Moniruzzaman, M.; Sundararajan, P. R. *J. Phys. Chem. B* **2006**, *110*, 15251.

160.   Kautz, H.; van Beek, D. J. M.; Sijbesma, R. P.; Meijer, E. W. *Macromolecules* **2006**, *39*, 4265.

161.   Brunsveld, L.; Folmer, B. J. B.; Meijer, E. W.; Sijbesma, R. P. *Chem. Rev.* **2001**, *101*, 4071.

Chapter-2

Design and Development of Solvent Free and Non-isocyanate Melt Transurethane Reaction

2.1. Introduction

From the beginning of the twentieth century many industrial research groups from all over the world have been looking for materials that can be used as an alternative for natural rubber. This led to the discovery of several types of thermo plastic elastomers (TPE) and among them thermoplastic polyurethanes (TPU) are the best known[1]. TPU possess many of the physical properties of rubbers i.e. softness, flexibility, and elasticity; but in contrast to conventional rubbers they can be melted and processed repeatedly as thermoplastic materials because of the reversible cross links.[2] Polyurethanes are usually synthesized through the polycondensation reaction between diisocyanates and diols. [1-4] These isocyanates are classified as one of the most hazardous chemicals to living organisms because continuous exposure to these can cause un-curable respiratory diseases.[5-6] The pollution and hazardous waste from chemical industries is a major concern to environmental safety and new synthetic strategies are very much required to reduce or eliminate the use and generation of substances which are hazardous to human health and environment. In the last few decades, various non-isocyanate polymerization routes were attempted for the synthesis of polyurethanes. The reaction of bis(chloroformates) with diamines via interfacial polycondensation is one of the oldest non-isocyanate routes known for the synthesis of polyurethanes (scheme-2.1).[7] Though the reaction is simple, the synthesis of bis(chloroformates) mostly involves the use of phosgene which is highly toxic.
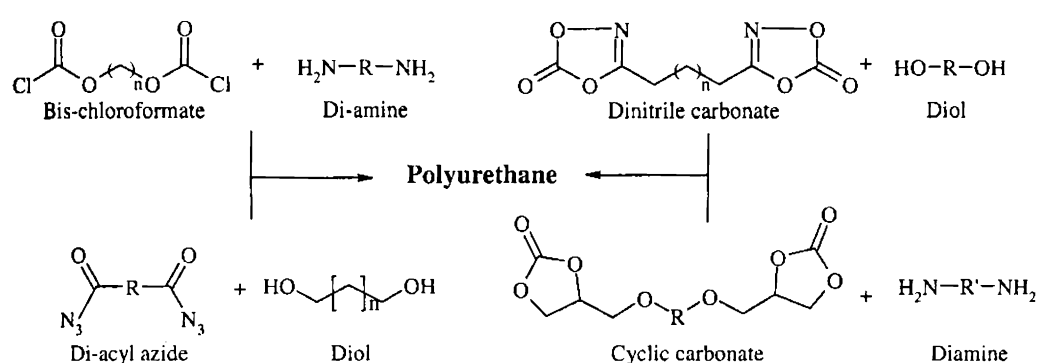
Scheme-2.1: Non-isocyanate routes known for the synthesis of Polyurethanes

Other indirect routes which are of less commercial importance for the synthesis of polyurethanes involves the reaction of dinitrile carbonate with diols or polyols in

presence of tin catalysts along with tertiary amine catalysts (scheme-2.1).[8] Foti, et al. reported a two step method for the synthesis of polyurethanes where in, the first step involves the reaction of piperazine with aromatic polycarbonates producing urethane diphenol which on further reaction with toxic phosgene yields the corresponding alternating copolymer.[9] Rokicki, et al. and Kihara et al. treated bifunctional cyclic carbonates with diamines and the intermediates were then reacted with diols to produce polyurethanes (scheme-2.1).[10] Another alternative route was the Curtius rearrangement which involves the conversion of an inert acyl azide group into a reactive isocyanate group, generated in situ which can then readily react with alcohols to generate urethane linkages (scheme-2.1). Kumar et al. and Okaniwa et al. have employed this reaction for the synthesis of hyperbranched polyurethanes and dendritic poly(amide urea)s.[11-12]Though these approaches have been widely explored for making oligomers or polyurethane coating applications, low degree of polymerization and difficulty in large scale preparation (explosive nature of the aryl azides) makes these processes less preferable over the conventional isocyanate-chemistry.[10] Blocking or masking of isocyanates with appropriate molecules such as phenols, oximes and alcohols and regenerating the isocyanate during the course of polymerization were also reported as shown in scheme-2.2.[13-21]
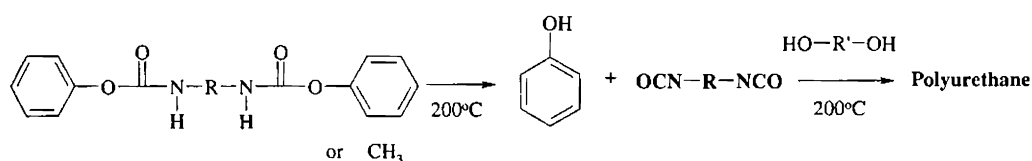
Scheme-2.2: Synthesis of polyurethanes by the blocked isocyanate approach

Bernard, et al. and Green performed the conversion of one urethane to another but their attempt ended up with insoluble and infusible gels which could not be processed.[13-14]A similar procedure was adopted by Wolgemuth, et al. to synthesize polyurethanes using organotin as catalyst in presence of inert solvent such as toluene.[15] A process for the manufacture of polyurethanes was described in which alkyl or phenyl diurethanes were reacted with diols but these procedures resulted in the formation of functional group end-capped low molecular weight polyurethanes.[16-21] All these reports suggested that masked-isocyanate approach was found to produce insoluble polymers due to the un-wanted cross-linking side reactions by the active

isocyanates (re-generated) in the high temperature polycondensation process. However, no clean and eco-friendly polymerization reactions were reported for polyurethanes, which is equivalent or superior to isocyanate chemistry in producing high molecular weight polymers.

In general, solvent free melt polymerization processes are highly preferred in engineering thermoplastics because of the direct utilization of the raw materials for processing into desired products. In the area of aliphatic or aliphatic-aromatic polyesters, aliphatic polyamides and aromatic polycarbonates, solvent free melt methodologies such as direct or transesterification were developed for manufacturing few million tons of these polymers every year.[22-24] A simple transesterification reaction is shown in scheme-2.3 where a diester reacts with a diol under melt conditions to obtain a polyester with the removal of low boiling alcohol from the equilibrium.
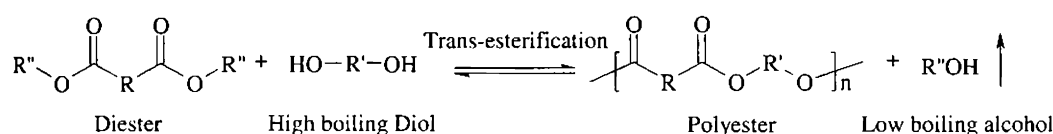
Scheme-2.3: Transesterification reaction for the synthesis of Polyesters

Recently, Jayakannan and Ramakrishnan reported another melt polymerization route for high molecular weight benzyl-aliphatic polyethers via transetherification reaction (scheme-2.4).[25-29] However, this approach was restricted to fully substituted bis-benzyl ethers due to the possible aromatic electrophilic substitution side-reaction in the polycondensation reactions.[26,30-31]
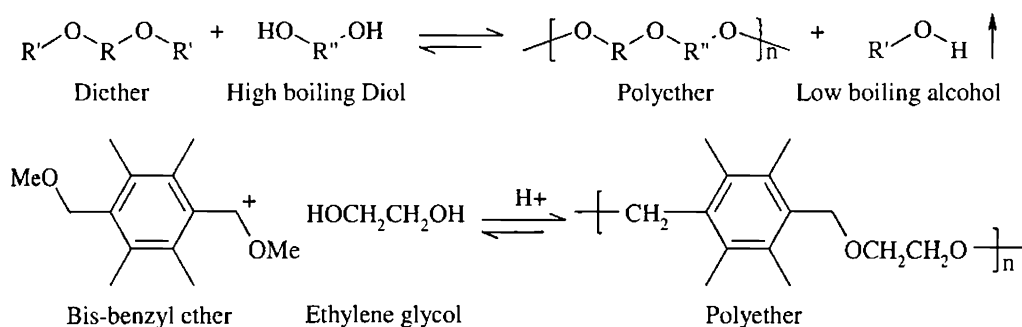
Scheme-2.4: Transetherification route for the synthesis of Polyethers

Other than these two melt polycondensation reactions, no other melt routes are known in the literature for the synthesis of polymers. Since polyurethanes are synthesized by employing a highly hazardous synthetic pathway, developing a melt route under non-isocyanate conditions would be very attractive.

The melt transurethane process is shown in scheme-2.5. The melt transurethane process involves the transformation of one urethane to another (or carbamate) by the reaction with an alcohol in the presence of a suitable catalyst.

Urethane-1   **Urethane-2**

Diurethane monomer   **Diol**   **Polyurethane**
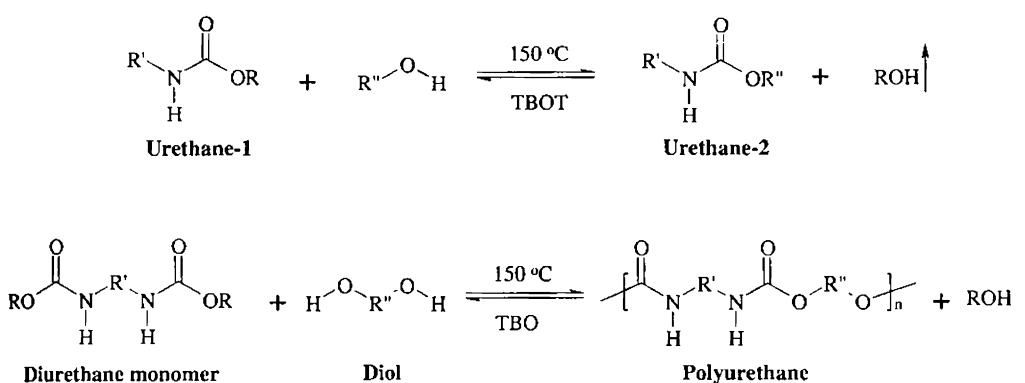
Melt Transurethane Process

Scheme-2.5: Novel Melt Transurethane Process for the Synthesis of Polyurethanes

In a polycondensation reaction, a di-urethane monomer reacts with equimolar amounts of diol in presence of a catalyst at high temperature under melt conditions to produce polyurethanes followed by the removal of low boiling alcohol. A urethane linkage can be considered as a half-ester-half-amide bond (ROCONHR') and during the transurethane process the ester bond in the diurethane monomer (or carbamate) cleaved selectively so as to form the new urethane linkage.

In this chapter the investigation is highlighted on the development of a novel melt transurethane process for the synthesis of polyurethanes. The mechanistic aspects of the process are studied in detail for sustainable and efficient alternative methodologies for polyurethanes under solvent free and non-isocyanate conditions. The di-urethane (also mono) monomers were easily synthesized by condensing a diamine (or mono-amine) with dimethyl carbonate in presence of a base in good yield and high purity.[32] The new process, melt transurethane polycondensation, was investigated for A + B; A-A + B and A-A + B-B (A-urethane and B-alcohol) type condensation reactions. Various primary and secondary aliphatic urethane monomers

were synthesized based on (i) 1, 6-hexamethylene diamine, 1, 3-cyclohexyl(bismethyl amine), benzyl amine and octyl amine (primary amines); (ii) cyclohexyl amine and isophorone diamine (secondary amines) and (iii) aromatic amines such as aniline, etc. Primary alcohols such as di-, tri-, tetra- ethylene glycols, polyethylene glycol-300, 1, 6-hexane diol, 1, 8-tricyclodecanedimethanol, 1, 4-cyclohexanedimethanol, benzyl alcohol, mono-glymes, tricyclodecanemethanol, and secondary alcohols such as 1, 4-cyclohexanediol, isosorbide and cyclohexanol were reacted under the melt transurethane conditions to study the reactivity differences and also the efficiency of the process (for more than 30 examples). Model reactions were carried out and the reaction products were subjected to ^{1}H-NMR, FAB-Mass spectrometer and MALDI-TOF Mass Spectrometer analysis to understand the mechanistic aspects of melt transurethane process.

2.2. Experimental Methods

2.2.1. Materials: 1, 6-hexamethylene diamine (HDA), isophorone diamine (IPDA), 1,3-cyclohexyl(bismethyl amine) (CHMA), octyl amine (OA), cyclohexyl amine (CHA), benzyl amine (BA), aniline (AA), diethylene glycol (DEG), triethylene glycol (TEG), tetraethylene glycol (TREG), polyethylene glycol-300 (PEG-300), 1, 4-cyclohexanedimethanol (CHDM), 1, 4-cyclohexanediol (CHD), isosorbide (IS), 1, 6-hexanediol (HD), benzyl alcohol (Bz), diethylene glycol monomethylether (DGME), triethylene glycol monomethylether (TGME), cyclohexanol (CH), titaniumtetrabutoxide (Ti(OBu)$_4$) and dimethyl carbonate (DMC) were purchased from Aldrich Chemicals and used without further purification. 1, 8-Tricyclodecanedimethanol (TCD-DM), and tricyclodecanemethanol (TCD) were kindly supplied by Celanese Chemicals. All other solvents were purchased locally and purified using standard procedures.[33] All the mono and di-alcohols were dried to 70 °C in a vacuum oven (0.1 mm of Hg) for 12 h prior to their use in the reaction.

2.2.2. Measurements: ^{1}H and ^{13}C-NMR spectra of the monomers, polymers and model compounds were recorded using 300-MHz Brucker NMR spectrophotometer in CDCl$_3$, or CF$_3$COOH/CDCl$_3$ containing small amount of TMS as internal standard. In the case of chloroform insoluble polymers, 10-15 mg of the samples were dissolved

by adding 3-4 drops of trifluoroacetic acid (TFA) and then diluted to 0.5 mL by adding CDCl$_3$. Infrared spectra of the samples were recorded using Perkin Elmer FT-IR spectrophotometer from 4000 to 600 cm^{-1}. For CHCl$_3$ soluble samples, the spectra were recorded by smearing a solution of the sample in CHCl$_3$ on a NaCl plate and for CHCl$_3$ insoluble samples the spectra were recorded for KBr pellets prepared by mixing 1-2 mg of the solid with KBr. The purity of the monomers and model compounds were determined by JEOL JSM600 fast atom bombardment (FAB) high-resolution mass spectrometry. The compound was dissolved in CHCl$_3$ and suspended in 3-nitrobenzylalcohol as a matrix for FAB-Mass measurements. The inherent viscosity (η_{inh}) of the polymers was measured for 0.5 wt % polymer solutions in acetic acid and the measurements were carried out using an Ubbelohde viscometer at 30 °C. The polymer solutions were filtered prior to measurements using a Whatmann no.1 filter paper and an average of three readings were taken for the calculation. The molecular weights of THF soluble polymers were determined by gel permeation chromatography (GPC) in tetrahydrofuran (THF) using polystyrene as standards. The flow rate of THF was maintained as 1 ml/min. The polymer solution was prepared by dissolving 10 mg of the sample in 1ml of THF, filtered and injected for recording the GPC chromatograms. The chromatograms were recorded using Waters 510 pump and Waters 410 differential RI detector. Three mixed styra-gel columns in series HT 6E (Linear) (THF) 7.8 x 30, HR 5E (Linear) (THF) 7.8x30, HR 4E (Linear) (THF) 7.8x30 were employed for the analysis. The MALDI-TOF MS were run on a Micromass TofSpec 2E instrument using a nitrogen 337 nm laser (4 ns pulse). At least 40-50 shots are summed up. The matrix used was 2, 5-dihydroxy benzoic acid dissolved in CHCl$_3$. The sample and the matrix were spotted on MALDI target and allowed to dry before introducing into the mass spectrometer. Elemental analyses of the monomers were carried out using Perkin Elmer-2400 CHNS analyzer. Thermal analysis of the polyurethanes was done using a Perkin Elmer Pyris 6 DSC instrument and the instrument was calibrated with indium, tin and lead standards. All the samples were first heated to melt prior to recording their thermograms to remove their previous thermal history and recorded using a heating/cooling rate of 10 °C/min, under 20 mL/min purge of nitrogen gas. The thermal stability of the polymers was determined using DTG-60 Shimadzu Thermogravimetric Analyzer at a heating rate of 10 °C/min in nitrogen.

2.2.3. Synthesis of Monomers

2.2.3.1. Synthesis of dimethyl 1, 6-hexamethylene dicarbamate (DHMD):
Dimethyl carbonate (7.8 g, 7.2 mL, 0.086 mol) and freshly prepared sodium methoxide (0.6 g, 0.01 mol) were taken in a 25 ml two necked flask equipped with a nitrogen inlet and refluxed for 5 minutes. 1, 6-hexamethylene diamine (1.0 g, 0.008 mol) was added to the above mixture under reflux and the reaction was proceeded for 6 h under nitrogen. It was cooled and precipitated into water. The solid was filtered, washed with methanol and was purified by recrystallization from hot methanol to obtain di-urethane monomer-**DHMD** as white crystalline solid. Yield = 3.6 g (88%). M.P. = 110 °C. ^{1}H NMR (300 MHz, CDCl$_3$) δ: 4.70 ppm (b, 2H, -NH), 3.65 ppm (s, 6H, OCH$_3$), 3.17 ppm (d, J = 6.2 Hz, 4H, -CH$_2$NH), 1.66 - 1.32 ppm (3xb, 8H). ^{13}C NMR (75 MHz, CDCl$_3$) δ: 157.32 (C=O), 52.11 (-OCH$_3$), 40.97, 30.03, 26.35 ppm. FT-IR (cm^{-1}): ν = 3340 (-NH $_{H\ bond}$), 2939, 2868 (-CH$_2$), 1687 (C=O $_{H\ bond}$), 1533 (-NH $_{bend}$), 1476, 1339, 1262, 1218, 1138, 1007 HRMS (FAB): calcd for C$_{10}$H$_{20}$N$_2$O$_4$ [M$^+$]: 233.28: found: 233.46. Elemental analysis: calcd for C$_{10}$H$_{20}$N$_2$O$_4$: C, 51.71; H, 8.68; N, 12.06; found: C, 52.16; H, 8.75; N, 12.15.

2.2.3.2. Synthesis of dimethyl isophorone dicarbamate (DIPD): Dimethyl carbonate (9.7 g, 9.1 mL, 0.100 mol) and sodium methoxide (0.7 g, 0.013 mol) were taken in a 25 ml two necked flask equipped with a nitrogen inlet and refluxed for 5 minutes. Isophorone diamine (1.8 g, 0.010 mol) was added to the above mixture under reflux and the reaction was proceeded for 6 h under nitrogen. It was cooled and poured into excess of chloroform, washed with brine and the organic layer was dried over anhydrous sodium sulphate. The solvent was evaporated to obtain the product as solid, which was purified by recrystallization from hot methanol to obtain di-urethane monomer-**DIPD** as white crystalline solid. Yield = 2.6 g (96%). M.P. = 113 °C. ^{1}H NMR (300 MHz, CDCl$_3$) δ: 4.77 ppm (s, 1H, -CH$_2$NH), 4.49 ppm (s, 1H, cy-CHNH), 3.81-3.65 ppm (s, 1H, cyCH-NH + d, J = 4.8 Hz, 6H,-OCH$_3$), 3.26, 2.93 ppm (d, J = 6.6 Hz, 2H,-CH$_2$NH), 1.73-0.82 ppm (15H, cy-H). ^{13}C NMR (75 MHz, CDCl$_3$) δ: 157.4, 156.3 (C=O), 54.8, 52.1, 51.8, 46.9, 46.3, 44.6, 42.5, 41.8, 36.3, 34.9, 31.7, 29.6, 27.5, and 23.1 ppm. FT-IR (cm^{-1}): ν = 3327 (-NH $_{H\ bond}$), 2952, 2853 (-CH$_2$), 1700 (C=O $_{H\ bond}$), 1538 (-NH $_{bend}$), 1247. HRMS (FAB): calcd for C$_{14}$H$_{26}$N$_2$O$_4$ [M$^+$]:

286.37: found: 287.41. Elemental analysis: calcd for $C_{14}H_{26}N_2O_4$: C, 58.72; H, 9.15; N, 9.78; found: C, 58.80; H, 9.65; N, 9.90.

2.2.3.3. Synthesis of dimethyl 1, 3-cyclohexyl dicarbamate (DCHD): Dimethyl carbonate (11.9 g, 11.09 mL, 0.132 mol) and sodium methoxide (0.86 g, 0.016 mol) were taken in a 25 ml two necked flask equipped with a nitrogen inlet and refluxed for 5 minutes. 1, 3-cyclohexyl(bismethyl amine) (1.89 g, 0.013 mol) was added to the above mixture and the reaction was performed as described for **DHMD** and the product was obtained as white crystalline solid. Yield = 2.1 g (69%). M.P. = 100 °C. ^{1}H NMR (300 MHz, CDCl₃) δ: 4.77 ppm (s, 2H, -CH₂NH), 3.66 ppm (s, 6H, -OCH₃), 3.02 ppm (s, 4H,-CH₂NH), 1.81-0.55 ppm (10H, cy-H). ^{13}C NMR (75 MHz, CDCl₃) δ: 157.4, 156.3 (C=O), 53.1, 52.3, 51.3, 49.5, 48.6, 47.4, 38.8, 38.5, 37.7, 37.5, 34.0, 33.6, 31.8, 31.2, 30.7, 30.2, 29.7, 29.2, 25.9, and 24.6 ppm. FT-IR (cm^{-1}): ν = 3332 (-NH $_{H\,bond}$), 2924, 2863 (-CH₂), 1698 (C=O $_{H\,bond}$), 1536 (-NH $_{bend}$), 1453, 1253, 1188, 1146. HRMS (FAB): calcd for $C_{12}H_{22}N_2O_4$ [M⁺]: 258.32: found: 259.56. Elemental analysis: calcd for $C_{12}H_{22}N_2O_4$: C, 55.80; H, 8.58; N, 10.84; found: C, 55.97; H, 9.93; N, 10.67.

2.2.3.4. Synthesis of methyl 1-octamethylene carbamate (MOC): Dimethyl carbonate (54.4 g, 50.5 mL, 0.600 mol) and sodium methoxide (3.91 g, 0.072 mol) were taken in a 100 ml two necked flask equipped with a nitrogen inlet and refluxed for 5 minutes. Octylamine (7.8 g, 10.0 mL, 0.060 mol) was added to the above mixture under reflux and the reaction was proceeded for 6 h under nitrogen. It was cooled and poured into excess of chloroform, washed with 5 vol % hydrochloric acid (carbamates are chemically stable towards acids) followed by brine and the organic layer was dried over anhydrous sodium sulphate. The solvent was evaporated to obtain the product as colourless viscous liquid. Yield = 10.1 g (89%). ^{1}H NMR (300 MHz, CDCl₃) δ: 4.85 ppm (s, 1H, -CH₂NH), 3.60 ppm (s, 3H, -OCH₃), 3.12 ppm (d, J = 6.3 Hz, 2H,-CH₂NH), 1.43-0.84 ppm (15H, others). ^{13}C NMR (75 MHz, CDCl₃) δ: 156.9, (C=O), 51.5, 41.3, 40.8, 31.5, 29.7, 29.0, 28.9, 26.4, 22.3, and 13.7 ppm. FT-IR (cm^{-1}): ν = 3339 (-NH $_{H\,bond}$), 2927, 2856 (-CH₂), 1706 (C=O $_{H\,bond}$), 1535 (-NH $_{bend}$), 1465, 1261, 1193, 1146. HRMS (FAB): calcd for $C_{10}H_{21}NO_2$ [M⁺]: 187.28: found: 188.30.

2.2.3.5. Synthesis of methyl cyclohexyl carbamate (MCHC): Dimethyl carbonate (84.9 g, 78.8 mL, 0.875 mol) and sodium methoxide (5.64 g, 0.104 mol) were taken in a 100 ml two necked flask equipped with a nitrogen inlet and refluxed for 5 minutes. Cyclohexyl amine (8.67 g, 10.0 mL, 0.087 mol) was added and the reaction was performed as described for **MOC** and the product was obtained as white crystalline solid. Yield = 12.7 g (92%). M.P. = 76 °C. ^{1}H NMR (300 MHz, CDCl$_3$) δ: 4.67 ppm (s, 1H, -CHNH), 3.61 ppm (s, 3H, -OCH$_3$), 3.44 ppm (s, 1H,-cyCHNH), 1.90-1.06 ppm (10H, cyclic). ^{13}C NMR (75 MHz, CDCl$_3$) δ: 156.0, (C=O), 51.5, 50.6, 49.6, 33.2, 25.3, and 24.6 ppm. FT-IR (cm^{-1}): ν = 3326 (-NH $_{H\ bond}$), 2932, 2855, (-CH$_2$), 1704 (C=O $_{H\ bond}$), 1537 (-NH $_{bend}$), 1451, 1316, 1275, 1253, 1233, 1057. HRMS (FAB): calcd for C$_8$H$_{15}$NO$_2$ [M$^+$]: 157.21: found: 158.23. Elemental analysis: calcd for C$_8$H$_{15}$NO$_2$: C, 61.12; H, 9.62; N, 8.91; found: C, 61.12; H, 10.10; N, 8.90.

2.2.3.6. Synthesis of methyl benzyl carbamate (MBzC): Dimethyl carbonate (82.5 g, 76.5 mL, 0.91 mol) and sodium methoxide (5.9 g, 0.11 mol) were taken in a 100 ml two necked flask equipped with a nitrogen inlet and refluxed for 5 minutes. Benzyl amine (9.8 g, 10.0 mL, 0.09 mol) was added and the reaction was performed as described for **MOC** and the product was obtained as viscous liquid. Yield = 13.3 g (88%). ^{1}H NMR (300 MHz, CDCl$_3$) δ: 7.33-7.22 ppm (m, 5H, aromatic), 5.29 ppm (s, 1H, -CH$_2$NH), 4.34 ppm (m, J = 5.7 Hz, 2H,-ArCH$_2$NH), 3.66 ppm (s, 3H, -OCH$_3$). ^{13}C NMR (75 MHz, CDCl$_3$) δ: 157.4, (C=O), 138.9, 128.4, 127.3, 52.1, 44.9, 31.8, 19.7, 13.6 ppm. FT-IR (cm^{-1}): ν = 3345 (-NH $_{H\ bond}$), 3060 (Ar-CH$_{str}$), 3027, 2943, 2851, (-CH$_2$), 1693, (C=O $_{H\ bond}$), 1537 (-NH $_{bend}$), 1452, 1316, 1275, 1253, 1230, 1053. HRMS (FAB): calcd for C$_9$H$_{11}$NO$_2$ [M$^+$]: 165.19: found: 166.26.

2.2.3.7. Synthesis of methyl phenyl carbamate (MPhC): Dimethyl carbonate (49.4 g, 45.8 mL, 0.55 mol) and sodium methoxide (3.5 g, 0.064 mol) were taken in a 100 ml two necked flask equipped with a nitrogen inlet and refluxed for 5 minutes. Aniline (5.11 g, 5.0 mL, 0.054 mol) was added and the reaction was performed as described for **MOC** and the product was obtained as viscous liquid. Yield = 5.5 g (66%). ^{1}H NMR (300 MHz, CDCl$_3$) δ: 7.39-7.07 ppm (m, 5H, aromatic), 6.85 ppm (s, 1H, -ArNH), 3.76 ppm (s, 3H, -OCH$_3$). ^{13}C NMR (75 MHz, CDCl$_3$) δ: 156.2, (C=O), 137.8, 128.8, 128.4, 123.0, 119.1, 118.1, 53.1 ppm. FT-IR (cm^{-1}): ν = 3321 (-NH $_H$

bond), 3139 (Ar-CH$_{str}$), 3059, 2952, 2841, (-CH$_2$), 1715, (C=O $_{H bond}$), 1601, 1538 (-NH bend), 1501, 1448, 1366, 1315, 1231, 1193, 1069, 1030. HRMS (FAB): calcd for C$_8$H$_9$NO$_2$ [M$^+$]: 151.17: found: 151.21.

2.2.4. Synthesis of Polymers

2.2.4.1. Melt Transurethane Process for Polyurethanes: (P-1 to P-16): Typical melt transurethane polymerization procedure is explained for polyurethane based on di-urethane monomer **DHMD** and 1, 8-tricylodecanedimethanol (TCD-DM) as diol **(P-5).** 1, 8-Tricylodecanedimethanol , (0.74 g, 0.003 mol) and di-urethane monomer **DHMD** (0.87 g, 0.003 mol) were taken in a test tube shaped polymerization apparatus and melted by placing in an oil bath at 100 °C with constant stirring. It was cooled and 3 drops of titaniumtetrabutoxide (Ti(OBu)$_4$) (40 mg, 0.1 mmol) was added as catalyst and the polycondensation apparatus was made oxygen and moisture free by nitrogen purge followed by vacuum. The polymerization tube was then immersed in the oil bath at 150 °C and the polymerization was carried out along with nitrogen purge for 4 h. The resultant viscous mass was further condensed by applying high vacuum (0.01 mm of Hg) at 150 °C for 2h. At the end of the polymerization, the polyurethane was obtained as a white mass. The polymer was purified by dissolving in minimum amount of acetic acid, filtered and precipitated into methanol to obtain polyurethane fibres. Yield = 1.16 g (85 %). Inherent viscosity (η_{inh}) = 0.74 dl/g. ^{1}H NMR (300 MHz, CDCl$_3$) δ: 4.84 ppm (b, 2H; -NH), 3.89 ppm (d, J = 10.4 Hz, 4H; -COOCH$_2$), 3.16 ppm (d, J = 4.8 Hz, 4H;-CH$_2$NH), 2.46 – 0.96 ppm (m, 3xb, 22H, others). ^{13}C NMR (75 MHz, CDCl$_3$) δ: 157.06 (C=O), 68.39, 44.91, 44.57, 43.78, 41.55, 40.73, 40.28, 39.23, 34.42, 33.61, 32.52, 29.90, 27.70, 26.25, 25.75, 25.19, 24.48 ppm. FT-IR (cm^{-1}) v = 3340 (-NH $_{H bond}$), 2934, 2862 (-CH$_2$), 1695(C=O $_{H bond}$), 1536 (-NH bend), 1462, 1251, 1031.

An identical procedure was adopted for the synthesis of polyurethanes **P-1** to **P-4** and **P-6** to **P-16**. GPC molecular weight and thermal data of all the polyurethanes are given in table-2.1.

P-1: Monomers used are diethylene glycol (0.79 g, 0.007 mol) and **DHMD** (1.74 g, 0.007 mol). Yield = 1.72 g (84%). Inherent viscosity (η_{inh}) = 0.33 dl/g. ^{1}H NMR (300 MHz, CDCl$_3$) δ: 5.09 ppm (b, 2H; -NH), 4.20 ppm (s, 4H; -COOCH$_2$), 3.67 ppm (d, J

= 17.7 Hz, 4H; -OCH$_2$), 3.16 ppm (d, *J* = 6.0 Hz, 4H; -CH$_2$NH), 1.75 - 1.32 ppm (3xb, 8H). ^{13}C NMR (75 MHz, CDCl$_3$) δ: 156.73 (C=O), 70.79, 69.86, 64.04, 41.07, 30.03, 26.50 ppm. FT-IR (cm^{-1}) ν = 3324 (-NH $_{H bond}$), 2945, 2857 (-CH$_2$), 1688 (C=O $_{H bond}$), 1538 (-NH $_{bend}$), 1476, 1338, 1265, 1130.

P-2: Monomers used are triethylene glycol (0.88 g, 0.006 mol) and **DHMD** (1.37 g, 0.006 mol). Yield = 1.50 g (80%). Inherent viscosity (η$_{inh}$) = 0.82 dl/g. ^{1}H NMR (300 MHz, CDCl$_3$) δ: 5.14 ppm (b, 2H; -NH), 4.20 ppm (s, 4H; -COOCH$_2$), 3.67 ppm (d, *J* = 9.0 Hz, 8H; -OCH$_2$), 3.15 ppm (d, *J* = 6.3 Hz, 4H; -CH$_2$NH), 1.88 - 1.32 ppm (3xb, 8H). ^{13}C NMR (75 MHz, CDCl$_3$) δ: 156.73 (C=O), 70.79, 69.86, 64.04, 41.07, 30.03, 26.50 ppm. FT-IR (cm^{-1}): ν = 3324 (-NH $_{H bond}$), 2934, 2857 (-CH$_2$), 1685 (C=O $_{H bond}$), 1539 (-NH $_{bend}$), 1476, 1341, 1262,1220,1130,1053.

P-3: Monomers used are tetraethylene glycol (0.90 g, 0.004 mol) and **DHMD** (1.00 g, 0.004 mol). Yield = 1.66 g (84%). Inherent viscosity (η$_{inh}$) = 0.62 dl/g. ^{1}H NMR (300 MHz, CDCl$_3$) δ: 5.07 ppm (b, 2H; -NH), 4.20 ppm (s, 4H; -COOCH$_2$), 3.64 ppm (s, 12H; -OCH$_2$), 3.17 ppm (q, *J* = 6.3 Hz, 4H; -CH$_2$NH), 2.00 - 1.32 ppm (3xb, 8H). ^{13}C NMR (75 MHz, CDCl$_3$) δ: 156.73 (C=O), 70.79, 69.86, 64.04, 41.07, 30.03, 26.50 ppm. FT-IR (cm^{-1}): ν = 3324 (-NH $_{H bond}$), 2934, 2868 (-CH$_2$), 1684 (C=O $_{H bond}$), 1536 (-NH $_{bend}$), 1459, 1338, 1264, 1111, 1070.

P-4: Monomers used are polyethylene glycol-300 (0.79 g, 2.6 mmol) and **DHMD** (0.62 g, 2.6 mmol). Yield = 1.01 g (82%). Inherent viscosity (η$_{inh}$) = 0.51 dl/g. ^{1}H NMR (300 MHz, CDCl$_3$) δ: 5.07 ppm (b, 2H; -NH), 4.20 ppm (s, 4H; -COOCH$_2$), 3.64 ppm (s, 20H; -OCH$_2$), 3.14 ppm (s, 4H; -CH$_2$NH), 1.48 - 1.25 ppm (2xb, 8H). ^{13}C NMR (75 MHz, CDCl$_3$) δ: 156.73 (C=O), 70.79, 69.86, 64.04, 41.07, 30.03, 26.50 ppm. FT-IR (cm^{-1}): ν = 3334 (-NH $_{H bond}$), 2931, 2862 (-CH$_2$), 1714 (C=O $_{H bond}$), 1537 (-NH $_{bend}$), 1462, 1349, 1253, 1107, 949.

P-6: Monomers used are 1, 4-cyclohexane dimethanol (0.74 g, 0.005 mol) and **DHMD** (1.19 g, 0.005 mol). Yield = 1.28 g (80%). Inherent viscosity (η$_{inh}$) = 0.87 dl/g. ^{1}H NMR (300 MHz, CDCl$_3$ + TFA) δ: 4.30-3.98 ppm (d, *J* = 14.1 Hz, cis + trans, 4H, -COOCH$_2$), 3.18 ppm (s, 4H, -CH$_2$NH), 1.83-1.03 ppm (m, 18H, others). FT-IR (cm^{-1}) ν = 3335 (-NH $_{H bond}$), 2928, 2852 (-CH$_2$), 1690 (C=O $_{H bond}$), 1530 (-NH $_{bend}$), 1465, 1338, 1254, 1138, 1048.

P-7: Monomers used are 1, 4-cyclohexane diol (0.53 g, 0.004 mol) and **DHMD** (1.00 g, 0.004 mol). Yield = 0.98 g (81%). Inherent viscosity (η$_{inh}$) = 0.46 dl/g. ^{1}H NMR

(300 MHz, CDCl$_3$ + TFA) δ: 4.78 ppm (s, 2H, -cyHOCO), 3.20 ppm (d, 4H, -CH$_2$NH), 1.99- 1.26 ppm (m, 16H, others). FT-IR (cm^{-1}) ν = 3341 (-NH $_{H bond}$), 2938, 2862 (-CH$_2$), 1688 (C=O $_{H bond}$), 1538 (-NH $_{bend}$), 1452, 1374, 1261, 1182, 1141, 1044.

P-8: Monomers used are isosorbide (0.57 g, 0.004 mol) and **DHMD** (1.00 g, 0.004 mol). Yield = 0.98 g (80%). Inherent viscosity (η_{inh}) = 0.30 dl/g. ^{1}H NMR (300 MHz, CDCl$_3$ + TFA) δ: 5.27 ppm (m, 2H, -cyHOCO), 5.05, 4.70 (2xs, 2H, -cyHOCH), 4.25, 4.11 ppm (2xm, 4H, -cyCH$_2$CHO), 3.18 ppm (d, 4H, -CH$_2$NH), 1.50- 1.32 ppm (2xs, 8H, others). FT-IR (cm^{-1}) ν = 3328 (-NH $_{H bond}$), 2933, 2860 (-CH$_2$), 1694 (C=O $_{H bond}$), 1548 (-NH $_{bend}$), 1466, 1377, 1268, 1148, 1092.

P-9: Monomers used are triethylene glycol (0.54 g, 0.003 mol) and **DIPD** (0.90 g, 0.003 mol). Yield = 1.1 g (82%). Inherent viscosity (η_{inh}) = 0.38 dl/g. ^{1}H NMR (300 MHz, CDCl$_3$) δ: 5.15 ppm (s, 1H, -CH$_2$NH), 4.87 ppm (s, 1H, cyCHNH), 4.19 ppm (s, 4H, -COOCH$_2$), 3.67 ppm (m, 8H, -OCH$_2$) 3.67 ppm (m, 1H, cyCH-NH), 3.26, 2.90 ppm (s + d, *J* = 6.2 Hz, 2H, -CH$_2$NH), 1.77-0.87 ppm (m, 15H, -cy-H, others). FT-IR (cm^{-1}): ν = 3309 (-NH $_{H bond}$), 2974, 2861 (-CH$_2$), 1725 (C=O $_{H bond}$), 1535 (-NH $_{bend}$), 1460, 1364, 1181, 1070.

P-10: Monomers used are tetraethylene glycol (0.59 g, 0.003 mol) and **DIPD** (0.90 g, 0.003 mol). Yield = 1.11 g (88%). Inherent viscosity (η_{inh}) = 0.30 dl/g. ^{1}H NMR (300 MHz, CDCl$_3$) δ: 5.12 ppm (s, 1H, -CH$_2$NH), 4.87 ppm (s, 1H, cyCHNH), 4.21 ppm (s, 4H, -COOCH$_2$), 3.68 ppm (m, 12H, -OCH$_2$) 3.68 ppm (s, 1H,cyCH-NH), 3.26, 2.92 ppm (s + d, 2H, -CH$_2$NH), 1.77-0.87 ppm (m, 15H, -cy-H, others). FT-IR (cm^{-1}): ν = 3309 (-NH $_{H bond}$), 2974, 2861 (-CH$_2$), 1725 (C=O $_{H bond}$), 1535 (-NH $_{bend}$), 1460, 1364, 1181, 1070.

P-11: Monomers used are 1, 8-tricylodecanedimethanol (0.55 g, 0.003 mol) and **DIPD** (0.90 g, 0.003 mol). Yield = 1.01 g (86%). Inherent viscosity (η_{inh}) = 0.46 dl/g. ^{1}H NMR (300 MHz, CDCl$_3$) δ: 4.85 ppm (s, 1H, -CH$_2$NH), 4.60 ppm (s, 1H, cy-CHNH), 3.79 ppm (s, 4H, -COOCH$_2$), 3.79 ppm (s, 1H, cy-CH-NH), 3.24, 2.89 ppm (s, 2H, -CH$_2$NH), 2.46-0.87 ppm (29H, cy-H, others). FT-IR (cm^{-1}): ν = 3321 (-NH $_{H bond}$), 2952, 2879 (-CH$_2$), 1707 (C=O $_{H bond}$), 1669, 1509(-NH $_{bend}$), 1299, 1222 (C-N).

P-12: Monomers used are 1, 4-cyclohexane dimethanol (0.55 g, 0.004 mol) and **DIPD** (1.09 g, 0.004 mol). Yield = 1.2 g (84%). Inherent viscosity (η_{inh}) = 0.41 dl/g. ^{1}H NMR (300 MHz, CDCl$_3$) δ: 4.80 ppm (s, 1H, -CH$_2$NH), 4.53 ppm (s, 1H, cyCHNH), 3.95 ppm (b, 4H,-COOCH$_2$), 3.95 ppm (s, 1H, cyCH-NH), 3.25, 2.90 ppm (s, 2H,-

CH$_2$NH), 1.79-0.87 ppm (25H, cy-**H**, others). ^{13}C NMR (75 MHz, CDCl$_3$) δ: 157.2, 156.0, 128.9, 69.8, 54.8, 47.0, 46.4, 44.5, 41.9, 40.0, 38.0, 37.4, 36.3, 34.8, 31.8, 30.8, 25.3, 23.2 ppm. FT-IR (cm^{-1}): ν = 3330 (-NH $_{H bond}$), 2921, 2853 (-CH$_2$), 1703 (C=O $_{H bond}$), 1533 (-NH $_{bend}$), 1237.

P-13: Monomers used are 1, 6-hexane diol (0.43 g, 0.004 mol) and **DIPD** (1.09 g, 0.004 mol). Yield = 1.11 g (89%). Inherent viscosity (η$_{inh}$) = 0.31 dl/g.^{1}H NMR (300 MHz, CDCl$_3$) δ: 4.95 ppm (s, 1H, -CH$_2$NH), 4.70 ppm (s, 1H, cyCHNH), 4.01 ppm (s, 4H, -COOCH$_2$), 3.77 ppm (s, 1H, cyCH-NH), 3.26, 2.89 ppm (s, 2H, -CH$_2$NH), 2.25-0.85 ppm (24H, -CH$_2$&Cy-**H**). FT-IR (cm^{-1}): ν = 3334 (-NH $_{H bond}$), 2947 (-CH$_2$), 1694 (C=O $_{H bond}$), 1535 (-NH $_{bend}$), 1243.

P-14: Monomers used are tetraethylene glycol (0.40 g, 0.002 mol) and **DCHD** (0.53 g, 0.002 mol). Yield = 0.65 g (81%). ^{1}H NMR (300 MHz, CDCl$_3$) δ: 5.15 ppm (s, 2H, -CH$_2$NH), 4.20 ppm (s, 4H, -COOCH$_2$), 3.65 ppm (d, *J* = 10.8 Hz, 12H, -OCH$_2$), 3.00 ppm (s, 4H, -CH$_2$NH), 1.81-0.55 ppm (10H, cy-**H**, others). FT-IR (cm^{-1}): ν = 3334 (-NH $_{H bond}$), 2921, 2865 (-CH$_2$), 1701 (C=O $_{H bond}$), 1538 (-NH $_{bend}$), 1457, 1246, 1120, 1035.

P-15: Monomers used are 1, 8-tricylodecanedimethanol (0.42 g, 0.002 mol) and **DCHD** (0.53 g, 0.002 mol). Yield = 0.70 g (83%). Inherent viscosity (η$_{inh}$) = 0.30 dl/g. ^{1}H NMR (300 MHz, CDCl$_3$) δ: 4.82 ppm (s, 2H, -CH$_2$NH), 3.97 ppm (s, 4H, -COOCH$_2$), 3.02 ppm (s, 4H, -CH$_2$NH), 1.81-0.56 ppm (20H, cy-**H**, others). FT-IR (cm^{-1}): ν = 3341 (-NH $_{H bond}$), 2925, 2853 (-CH$_2$), 1696 (C=O $_{H bond}$), 1529 (-NH $_{bend}$), 1457, 1252, 1151, 1017.

P-16: Monomers used are 1, 4-cylohexanedimethanol (0.50 g, 0.003 mol) and **DCHD** (0.90 g, 0.003 mol). Yield = 0.96 g (81%). ^{1}H NMR (300 MHz, CDCl$_3$) δ: 4.89 ppm (s, 2H, -CH$_2$NH), 3.84 ppm (s, 4H, -COOCH$_2$), 3.01 ppm (s, 4H, -CH$_2$NH), 2.46-0.81 ppm (24H, cy-**H**, others). FT-IR (cm^{-1}): ν = 3334 (-NH $_{H bond}$), 2935, 2861 (-CH$_2$), 1696 (C=O $_{H bond}$), 1529 (-NH $_{bend}$), 1455, 1248, 1142, 1011.

2.2.5. Synthesis of Model Compounds

2.2.5.1. Melt Transurethane Process for simple urethanes or carbamates (Model reaction-A-A+B Type):

Typical melt transurethane procedure for simple condensation reaction is described for benzyl alcohol (**Bz**) with the di-urethane

monomer (**DHMD**) (for compound **M-4**). Benzyl alcohol (0.87g, 8.0 mmol) and di-urethane monomer (0.93g, 4.0 mmol) were taken in a test tube shaped polymerization apparatus and melted by placing in an oil bath at 100 °C with constant stirring. It was cooled and 3 drops of Ti(OBu)$_4$ (40 mg, 0.1 mmol) was added as catalyst and the polycondensation apparatus was made oxygen and moisture free by nitrogen purge followed by vacuum. The tube was then immersed in the oil bath at 150 °C and the condensation reaction was carried out with nitrogen purge for 4 h. The resultant viscous mass was further condensed by applying controlled vacuum (1 mm of Hg) at 150 °C for 2 h. At the end of the condensation reaction the product was obtained as white powder. Yield= 1.3 g (88 %). ^{1}H NMR (300 MHz, CDCl$_3$) δ: 7.32 ppm(s, 10H, **Ar-H**), 5.06 ppm (s, 4H, -COOCH$_2$), 4.74 ppm (b, 2H, -NH), 3.16 ppm (s, 4H, -CH$_2$NH), 1.72 – 1.30 ppm (3xb, 8H, others). ^{13}C NMR (75 MHz, CDCl$_3$) δ: 156.49(C=O), 136.33, 128.57, 128.15, 66.67, 52.07, 40.89, 29.91, 26.24 ppm. FT-IR (cm^{-1}) ν = 3328 (-NH $_{H bond}$), 3032, 2934, 2862 (-CH$_2$), 1684 (C=O $_{H bond}$), 1537 (-NH $_{bend}$), 1456, 1336, 1265, 1218. HRMS (FAB): calcd for C$_{22}$H$_{28}$N$_2$O$_4$ [M$^+$]: 384.5: found: 385.5.

An identical procedure was adopted for the synthesis of model compounds **M-1** to **M-3** and **M-5**. The percent conversion and the FAB-HRMS data are given in table-2.2.

M-1: Monomers used are diethylene glycol monomethyl ether (0.97 g, 0.008 mol) and **DHMD** (0.93 g, 0.004 mol). Yield = 1.3 g (84%). ^{1}H NMR (300 MHz, CDCl$_3$) δ: 4.85 (b, 2H, -NH), 4.23 (s, 4H, -COOCH$_2$), 3.61-3.57 (m,18H, -OCH$_2$CH$_2$OCH$_2$CH$_2$OCH$_3$), 3.18 (d, 4H, -CH$_2$NH), 1.85 - 1.32 (3xb, 8H, others). ^{13}C NMR (75 MHz, CDCl$_3$) δ: 156.73 (C=O), 70.59, 69.74, 64.04, 41.07, 30.03, 26.50 ppm. FT-IR (cm^{-1}): ν = 3328 (-NH $_{H bond}$), 2932, 2868(-CH$_2$), 1705(C=O $_{H bond}$), 1624, 1537(-NH $_{bend}$), 1458, 1250,1135, 1107. HRMS (FAB): calcd for C$_{18}$H$_{36}$N$_2$O$_8$ [M$^+$]: 408.50: found: 409.50.

M-2: Monomers used are triethylene glycol monomethyl ether (1.16 g, 0.007 mol) and **DHMD** (0.82 g, 0.0035 mol). Yield = 1.3 g (82%). ^{1}H NMR (300 MHz, CDCl$_3$) δ: 4.96 (b, 2H, -NH), 4.21 (s, 4H, -COOCH$_2$), 3.65-3.57 (m, 26H,-OCH$_2$CH$_2$OCH$_2$CH$_2$OCH$_2$CH$_2$OCH$_3$), 3.16 (d, 4H, -CH$_2$NH), 2.03 - 1.33 (3xb, 8H, others). ^{13}C NMR (75 MHz, CDCl$_3$) δ: 156.73 (C=O), 70.59, 69.74, 64.04, 41.07, 30.03, 26.50 ppm. FT-IR (cm^{-1}): ν = 3309 (-NH $_{H bond}$), 2933, 2873(-CH$_2$), 1719(C=O

$_{H\ bond}$), 1678, 1626, 1537(-NH $_{bend}$), 1458, 1351, 1200, 1109. HRMS (FAB): calcd for $C_{22}H_{44}N_2O_{10}$ [M$^+$]: 496.60: found: 496.60.

M-3: Monomers used are tricyclodecanemethanol (0.86 g, 0.005 mol) and **DHMD** (0.60 g, 0.0025 mol). Yield = 1.01 g (83%). ^{1}H NMR (300 MHz, CDCl$_3$) δ: 4.66 (b, 2H, -NH), 3.82 (s, 4H, -COOCH$_2$), 3.17 (d, 4H, -CH$_2$NH), 2.10– 0.91 (4xb, 38H, others). ^{13}C NMR (75 MHz, CDCl$_3$) δ: 157.06 (C=O), 68.39, 44.91, 44.57, 43.78, 41.55, 40.73, 40.28, 39.23, 34.42, 33.61, 32.52, 29.90, 27.70, 26.25, 25.75, 25.19, 24.48 ppm. FT-IR (cm^{-1}): ν = 3327 (-NH $_{H\ bond}$), 2936, 2857(-CH$_2$), 1693(C=O $_{H\ bond}$), 1615, 1538(-NH $_{bend}$), 1459, 1251. HRMS (FAB): calcd for $C_{30}H_{48}N_2O_4$ [M$^+$]: 500.73: found: 501.54.

M-5: Monomers used are cyclohexanol (0.79 g, 0.0078 mol) and **DHMD** (0.91 g, 0.0039 mol). Yield = 1.06 g (78%). ^{1}H NMR (300 MHz, CDCl$_3$) δ: 4.76 (b, 2H, -NH), 3.79 (s, 2H, -COOCH$_{cyc}$), 3.24 (d, 4H, -CH$_2$NH), 1.86– 1.35 (4xb, 30H, others). FT-IR (cm^{-1}): ν = 3336 (-NH $_{H\ bond}$), 2933, 2859(-CH$_2$), 1712(C=O $_{H\ bond}$), 1690, 1537(-NH $_{bend}$), 1451, 1252. HRMS (FAB): calcd for $C_{20}H_{36}N_2O_{10}$ [M$^+$]: 368.52: found: 369.42.

2.2.5.2. Melt Transurethane Process for simple urethanes or carbamates: (Model reaction-A+B Type): Typical melt transurethane procedure for simple condensation reaction is described for benzyl alcohol (**Bz**) with simple urethane monomer **MOC** (for compound **M-6**). Benzyl alcohol (0.29g, 0.0027 mol) and **MOC** (0.50g, 0.0027 mol) were taken in a test tube shaped polymerization apparatus and melted by placing in an oil bath at 100 °C with constant stirring. It was cooled and 3 drops of Ti(OBu)$_4$ (40 mg, 0.1 mmol) was added as catalyst and the polycondensation apparatus was made oxygen and moisture free by nitrogen purge followed by vacuum. The tube was then immersed in the oil bath, the temperature of which was increased gradually to 150 °C over a period of 0.5 h and the condensation reaction was carried out with nitrogen purge for 4 h. The resultant viscous mass was further condensed by applying controlled vacuum (1 mm of Hg) at 150 °C for 2 h. At the end of the condensation reaction the product was obtained as viscous liquid. Yield= 0.5 g (81 %). ^{1}H NMR (300 MHz, CDCl$_3$) δ: 7.36 (m, 5H, Ar), 5.09 (s, 2H, -OCH$_2$Ar), 4.70 (s, 1H, -NH), 3.19 (d, 2H, -CH$_2$NH), 1.48-0.85 (others). FT-IR (cm^{-1}) ν = 3329 (-NH $_{H\ bond}$), 3032,

2926, 2851 (-CH$_2$), 1704 (C=O $_{H\,bond}$), 1537 (-NH $_{bend}$), 1458, 1250, 1017cm^{-1}. HRMS (FAB): calcd for C$_{16}$H$_{25}$NO$_2$ [M$^+$]: 263.38: found: 264.33.

An identical procedure was adopted for the synthesis of model compounds **M-7 to M-9**. The percent conversion and the FAB-HRMS data are given in table-2.2.

M-7: Monomers used are benzyl alcohol (0.36 g, 0.003 mol) and **MCHC** (0.53 g, 0.003 mol). Yield = 0.65 g (85%). ^{1}H NMR (300 MHz, CDCl$_3$) δ: 7.36 (m, 5H, Ar), 5.08 (s, 2H, -OCH$_2$-Ar), 4.70 (s, 1H, -NH), 3.49 (s, 1H, -cyHNH), 1.95-1.06 (others). FT-IR (cm^{-1}): ν = 3324 (-NH $_{H\,bond}$), 2923, 2862(-CH$_2$), 1684(C=O $_{H\,bond}$), 1508(-NH $_{bend}$), 1451, 1220, 1023. HRMS (FAB): calcd for C$_{14}$H$_{19}$NO$_2$ [M$^+$]: 233.31: found: 234.42.

M-8: Monomers used are benzyl alcohol (0.36 g, 0.003 mol) and **MBzC** (0.51 g, 0.003 mol). Yield = 0.64 g (85%). ^{1}H NMR (300 MHz, CDCl$_3$) δ: 7.37- 7.25 (m, 10H, Ar), 5.13 (s, 2H, ArCH$_2$OCO-), 5.08 (s, 1H, NH), 4.39 (t, 2H, ArCH$_2$NH-). FT-IR (cm^{-1}): ν = 3324 (-NH $_{H\,bond}$), 3027, 2934, 2862(-CH$_2$), 1693(C=O $_{H\,bond}$), 1508(-NH $_{bend}$), 1451, 1240, 1130. HRMS (FAB): calcd for C$_{15}$H$_{15}$NO$_2$ [M$^+$]: 241.29: found: 242.54.

M-9: Monomers used are benzyl alcohol (0.36 g, 0.003 mol) and **MPhC** (0.50 g, 0.003 mol). Yield = 0.59 g (80%). ^{1}H NMR (300 MHz, CDCl$_3$) δ: 7.39-7.04 (m, 10H, Ar), 6.71 (d, 1H, ArNH), 5.20 (ArCH$_2$OCO-). FT-IR (cm^{-1}): ν = 3302 (-NH $_{H\,bond}$), 3060, 3027, 2939, 2868(-CH$_2$), 1705(C=O $_{H\,bond}$), 1596, 1517(-NH $_{bend}$), 1440, 1308, 1217, 1050. HRMS (FAB): calcd for C$_{14}$H$_{13}$NO$_2$ [M$^+$]: 227.27: found: 228.46.

2.3. Results and Discussion

2.3.1. Synthesis of Monomers

The design of the di-urethane monomer is very crucial for successful melt transurethane process. We have adapted a methyl urethane derivative since it is very easy to remove methanol from the melt during the polycondensation process. The mono and bis-methyl urethane (**A** and **A-A** type) were synthesized as shown in scheme-2.6. Commercially available monoamines or diamines were reacted with excess of dimethyl carbonate in presence of freshly prepared sodium methoxide as base.[32] Three di-urethane monomers dimethyl- 1, 6-hexamethylene dicarbamate (**DHMD**), dimethyl isophorone dicarbamate (**DIPD**) and dimethyl 1, 3-cyclohexyl(bis

methylene dicarbamate (**DCHD**) were prepared from 1, 6-hexamethylene diamine, isophorone diamine and 1, 3- cyclohexyl(bismethyl amine), respectively.
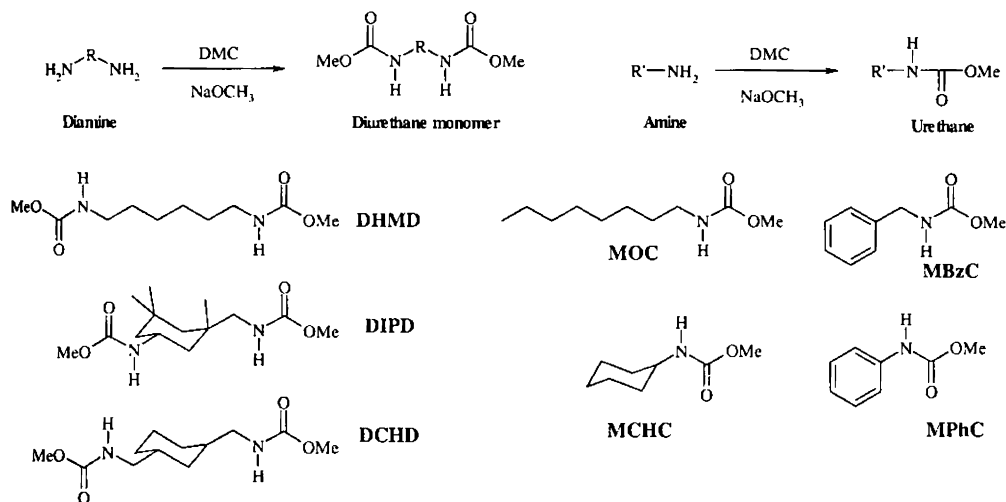
Scheme-2.6: Synthesis of Monomers

Four simple urethane monomers such as methyl 1-octamethylene carbamate (**MOC**), methyl cyclohexyl carbamate (**MCHC**), methyl benzyl carbamate (**MBzC**) and methyl phenyl carbamate (**MPhC**) were synthesized from octyl amine, cyclohexyl amine, benzyl amine and aniline, respectively. These urethane monomers bear difference in their functionality: for example primary (**DHMD, DCHD, MOC** and **MBzC**), secondary (**MCHC**), primary + secondary (**DIPD**) and aromatic urethane linkage (**MPhC**). The structure of the monomers was confirmed by ^{1}H and ^{13}C-NMR spectroscopies, HR-MS and elemental analysis. The ^{1}H-NMR spectra of few monomers are represented in figure-2.1. The peaks corresponding to different types of protons in the monomers are assigned alphabetically. Figure-2.1a corresponds to the ^{1}H-NMR of **DHMD**. The –NH peak for the compound appears at 4.70 ppm (a), the –OCH$_3$ peak lies at 3.65 ppm (b) and –CH$_2$NH peak appears at 3.17 ppm (c). All the other aliphatic protons appear between 1.66-1.32 ppm. In the case of **DIPD**, there are two –NH peaks for the primary and secondary urethane linkages at 4.77 (a) and 4.49 (b) ppm, respectively as seen in figure-2.1b. The –OCH$_3$ and the cyHNH are seen to appear together as a multiplet between 3.81-3.65 ppm (c+d) whereas –CH$_2$NH proton appeared as two separate peaks at 3.26 and 2.93 ppm (e). The ^{1}H-NMR spectra of **MCHC** is shown in figure-2.1c. The peak at 4.67 ppm (a) corresponds to the –NH

proton, the peak at 3.61 ppm (b) corresponds to $-OCH_3$ proton and a peak at 3.44 ppm (c) is assigned to the -cyHNH proton.
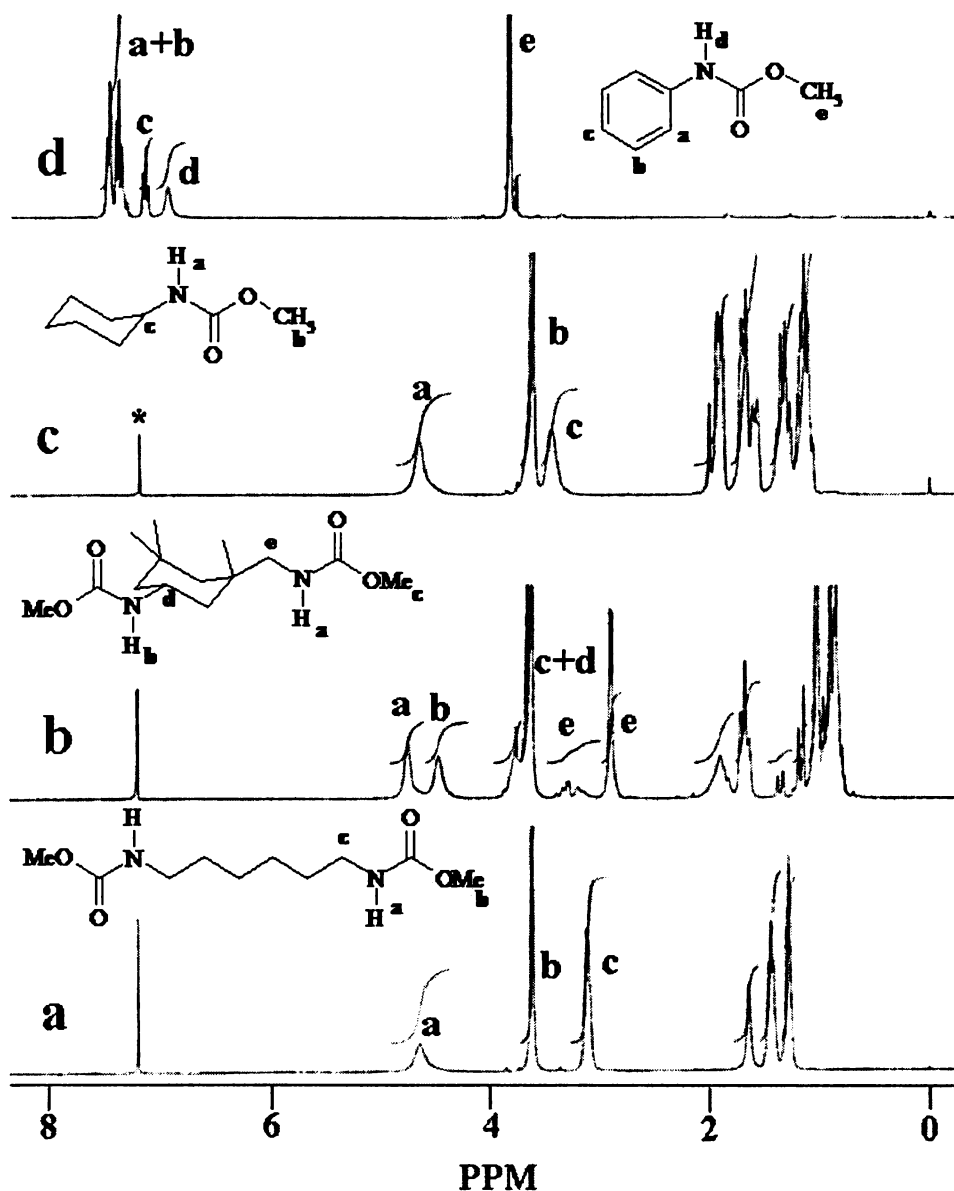
Figure-2.1:^{1}H-NMR spectra of DHMD (a), DIPD (b), MCHC (c) and MPhC (d). The peak at the asterisk corresponds to the solvent peak

In the case of **MPhC**, there are three peaks within the aromatic region from 7.39 to 7.07 ppm which are assigned to the three protons a, b and c as shown in figure-2.1d. The aromatic $-NH$ proton appears downfield at 6.85 ppm (d). The spectra of all the other monomers were compared similarly and confirmed the formation of the compounds.

2.3.2. Thermal Stability of Monomers

The thermal stability of the monomers was studied by TGA analysis under nitrogen atmosphere and shown in figure-2.2.
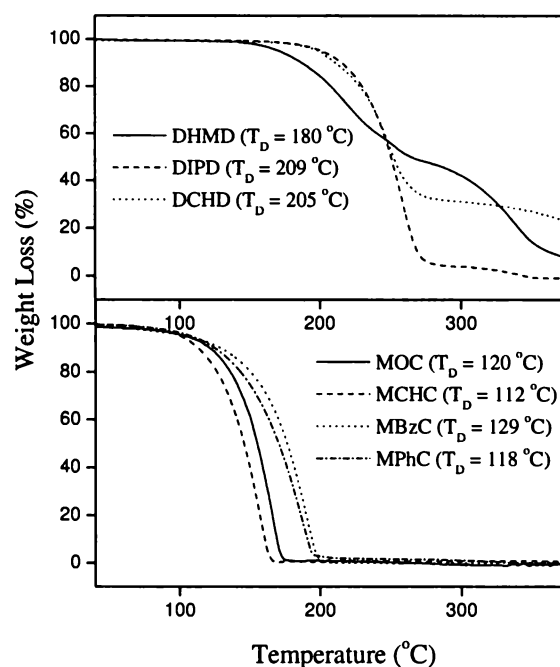

Figure-2.2: TGA plots of Monomers

The di-urethane monomers (**DHMD, DIPD** and **DCHD**) were found thermally more stable (up to 180-210 °C) compared to that of the simple urethanes (**MOC, MCHC, MBzC** and **MPhC**), (up to 120-130 °C). Based on the TGA-analysis the polycondensation temperatures were chosen as 150 and 100 °C for di-urethane and mono-urethane monomers, respectively. The polymerization reaction temperatures were chosen 20-30 °C less than that of the decomposition temperature in order to avoid any possible cross-linking reaction.[10] TGA analysis only provides the thermal stability of the monomers under static conditions; however, these urethane monomers were expected to undergo vigorous stirring during the high temperature melt polymerization. Therefore it is very important to study the thermal stability of the monomers under the mechanically stirred melt condensation conditions. **DHMD** was melted at 150 °C, stirred under nitrogen atmosphere for 6 h and aliquots collected at various intervals were subjected to NMR, FT-IR and HR-MS analysis. The NMR plot of the 3 h heated sample was exactly identical to that of the original one (figure-2.3).
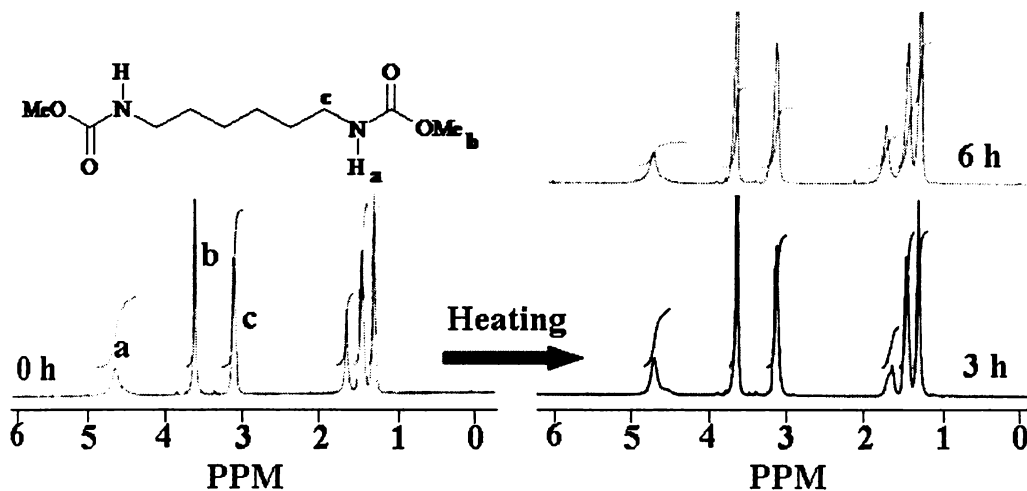
Figure-2.3: ^{1}H-NMR spectra of various fractions of DHMD heated at 150 °C without Ti-catalyst

Also HR-MS and FT-IR did not show the formation of isocyanate groups (which may occur due to thermal decomposition).[10] If the isocyanate would have formed during the course of the reaction, it would be clearly indicated in the FTIR spectra. For this the above fractions were subjected to FTIR analysis by smearing their solution in CHCl$_3$ on NaCl plate (figure-2.4). A peak at 2264 cm^{-1} was absent which clearly indicates that during the transformation no isocyanate linkage was formed. These control experiments confirmed that all the urethane monomers designed for investigating melt transurethane process are thermally stable under melt conditions.

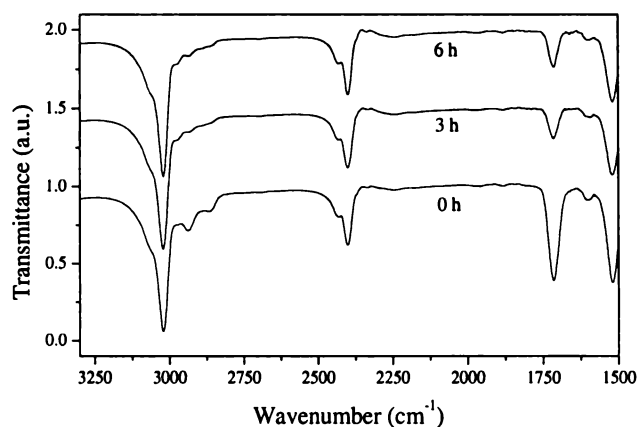*Figure-2.4: FTIR spectra of various fractions of DHMD heated at 150 °C without Ti-catalyst*

2.3.3. Melt Transurethane Process

The melt transurethane reaction was investigated for a wide range of alcohols (mono and diols of primary and secondary) consisting of oligoethylene glycols such as di-, tri-, tetra- ethylene glycols, PEG-300, mono-glymes, 1, 8-tricyclodecanedimethanol (TCD-DM), 1, 4-cyclohexanedimethanol (CHDM), 1,6-hexanediol (HD), benzyl alcohol (Bz), tricylodecanemethanol (TCD) and secondary alcoholic linkages such as 1, 4-cyclohexanediol (CHD), isosorbide (IS) and cyclohexanol (CH). The melt transurethane reaction was carried out in a cylindrical shaped home-made polymerization apparatus (figure-2.5). For A-A + B-B type polycondensation, equimolar amounts of di-urethane monomer and diol were taken and melted under nitrogen atmosphere at 100 °C. To the melt 0.1 mmol of catalyst was added under nitrogen atmosphere and the polymerization vessel was made oxygen and moisture free by purging with nitrogen followed by evacuation. The transurethane polycondensation was performed in one-pot but two stages: initially the polymerization was proceeded by stirring the reactants at 150 °C for 4 h under nitrogen purge (stage-I) and subsequently the viscous oligomers were condensed by applying high vacuum (stage-II, 0.05 mm of Hg) for 2 h. At the end of the polymerization, the polyurethane was obtained as a white solid mass.
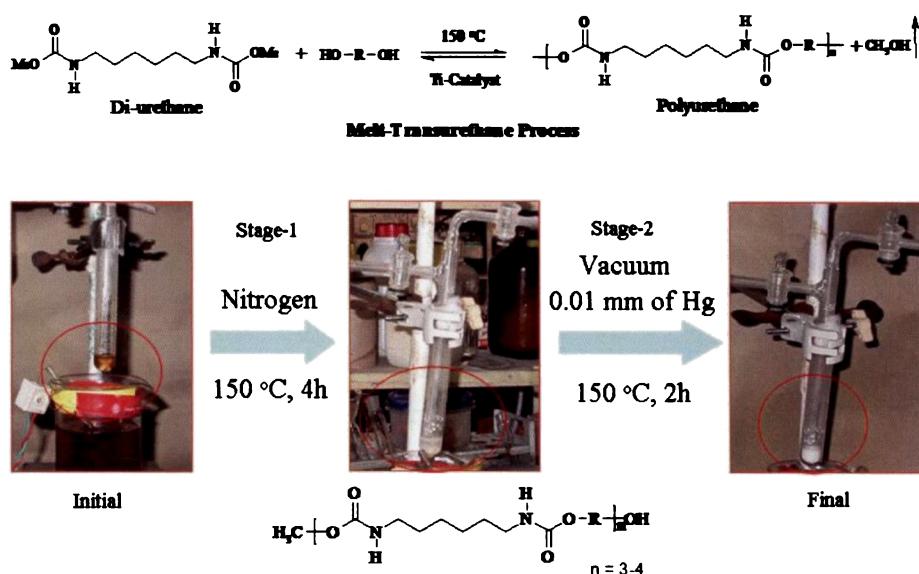
Figure-2.5: Pictures of different stages in the melt transurethane reaction for P-6

The polymerization was investigated for three di-urethane monomers **DHMD**, **DIPD**, **DCHD** with various diols and more than 15 structurally different polyurethanes were prepared as shown in scheme-2.7.
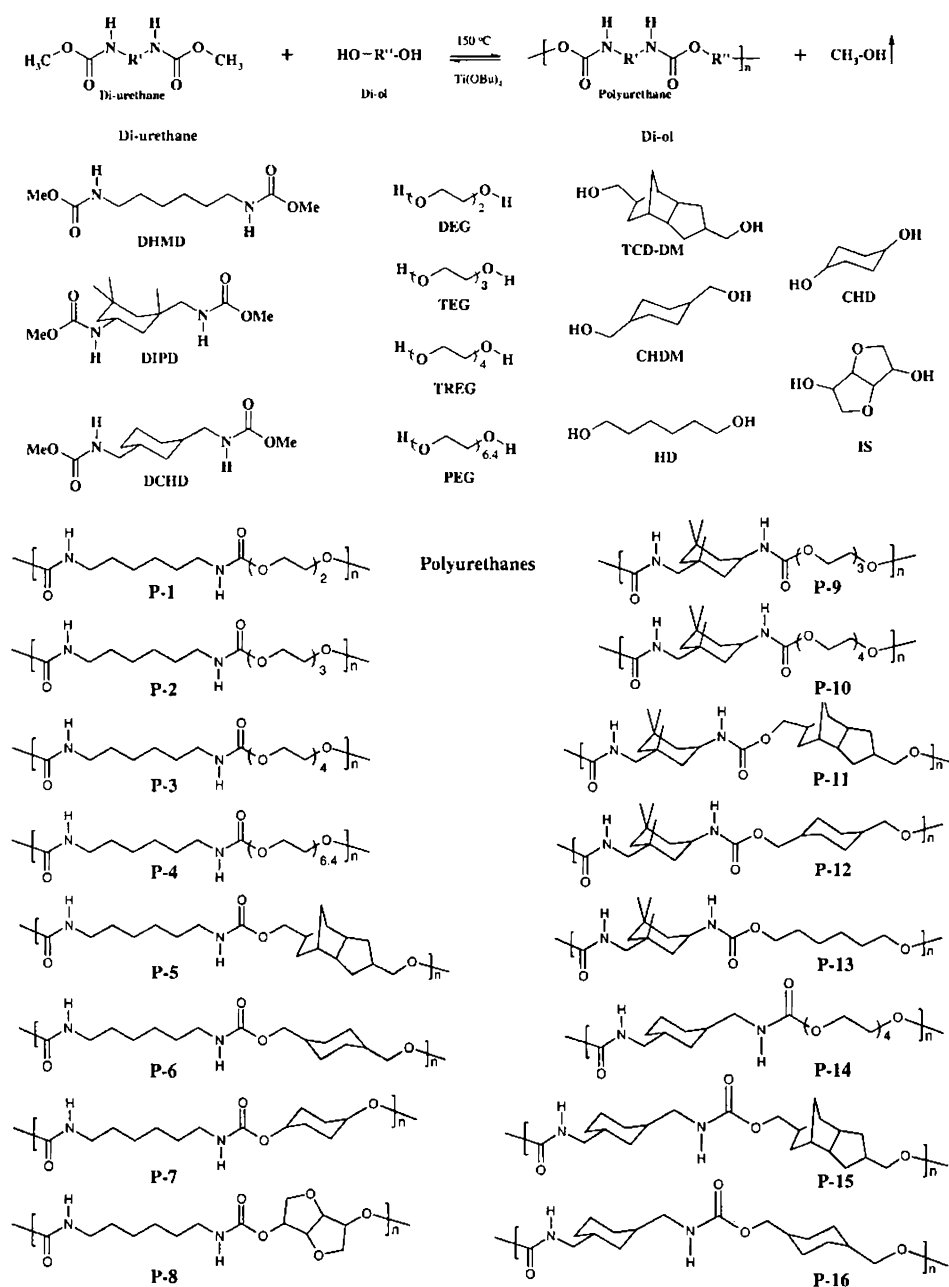
Scheme-2.7: Melt Transurethane Process and Structure of Polyurethanes

The melt transurethane process and the structures of the new polyurethanes were analyzed by ^1H and ^{13}C NMR spectroscopies. ^1H and ^{13}C NMR spectra of monomer

DHMD and one example for A-A+B-B type condensation product (**P-5**) is shown in figure-2.6.
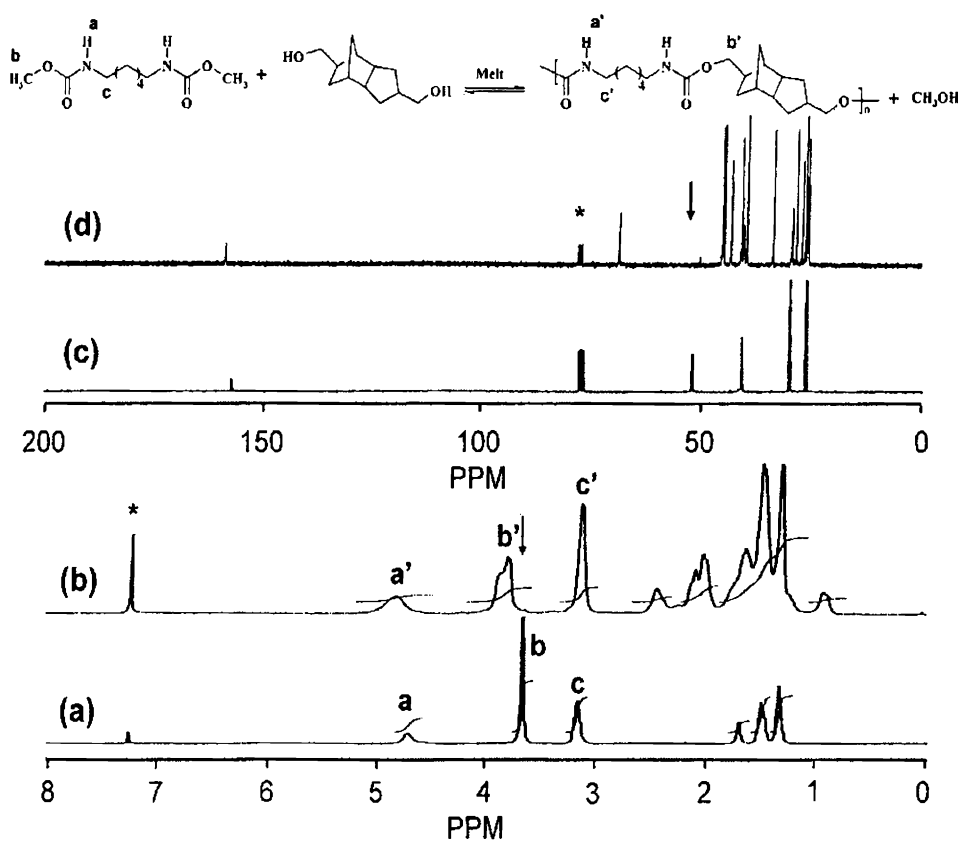
Figure-2.6: ^1H & ^{13}C NMR of diurethane monomer DHMD (a), (c) and polyurethane P-5 (b), (d). The peak at the asterisks corresponds to the solvent peaks.

The peaks for the different types of protons in the monomer and polymer are assigned by alphabets. The melt transurethane process can be easily confirmed by comparing the appearance or disappearance of $-OCH_3$, N-H and $-NHCOOCH_2-$ protons. In figure-2.6a, the N-H proton (a), $-OCH_3$ proton (b) and $-CH_2NH$ proton (c) in the di-urethane monomer appeared at 4.70, 3.65 and 3.17 ppm, respectively. Up on polymerization one would expect that the $-OCH_3$ peak in the di-urethane monomer (at 3.65 ppm), should vanish in the polymer. It is very clear from the figure-2.6b that the $-OCH_3$ peak of the monomer completely disappeared in the polyurethane spectra and a new peak for $-NHCOOCH_2-$ protons appeared at 3.89 ppm, which confirmed the formation of high molecular weight polyurethanes without any end groups.[29]

Similarly the N-H proton (a) of the monomer also disappeared and a new peak at 4.84 ppm appeared for **P-5** (a') corresponding to the N-H proton of the new urethane linkage. In order to confirm the process still further ^{13}C-NMR spectra of the monomer **DHMD** and **P-5** are also compared and shown in figure-2.6. Interestingly, the –OCH$_3$ carbon at 52 ppm in the monomer (figure-2.6c) disappeared and a new peak at around 68 ppm for the methylene carbon (NHCOOCH$_2$-) was observed in the polymer (figure-2.6d), which confirm the occurrence of melt transurethane process resulting in the formation of polyurethanes. The molecular weights of the polymers were determined by both solution viscosity techniques in acetic acid using automatic Ubbelohde viscometer and GPC in tetrahydrofuran. The inherent viscosity data of the polyurethanes are given in the experimental methods and polymer molecular weights are summarized in table-2.1.

Table-2.1: Monomers, Molecular weights, Decomposition temperature and Glass Transition of the Polyurethanes

Sample Code	Diurethane monomer	Diol	$M_n{}^a$	$M_w{}^a$	M_w/M_n	n	$T_D{}^d$	$T_g{}^e$
P-1	DHMD	DEG	3,200^b	3,900	1.25	12^b	280	2.2^f
P-2	DHMD	TEG	11,500	14,900	1.30	37	280	-3.3^f
P-3	DHMD	TREG	12,500	16,200	1.30	35	283	-23^f
P-4	DHMD	PEG	7,500	14,200	1.91	16	280	-31
P-5	DHMD	TCD-DM	20,000	42,000	2.10	55	282	59
P-6	DHMD	CHDM	-^{c}	-	-	-	297	46^f
P-7	DHMD	CHD	-	-	-	-	270	75
P-8	DHMD	IS	-	-	-	-	254	61^f
P-9	DIPD	TEG	4,700	10,900	2.36	12	270	59
P-10	DIPD	TREG	5,300	9,300	1.78	12	260	27
P-11	DIPD	TCD-DM	8,400	13,200	1.58	20	281	118
P-12	DIPD	CHDM	9,100	18,200	2.01	25	288	91
P-13	DIPD	HD	19,200	47,700	2.49	56	279	78
P-14	DCHD	TREG	3,800^b	6,700	1.80	9^b	268	1.3
P-15	DCHD	TCD-DM	6,400	19,800	3.11	16	276	96
P-16	DCHD	CHDM	4,100^b	7,000	1.70	12^b	280	43

a. Molecular weights as determined by gel permeation chromatography in THF at 30 °C using polystyrene standards for calibration.
b. Partially soluble in THF for molecular weight determination
c. Insoluble in THF for molecular weight determination
d. Temperatures represent 10 % weight loss in TGA measurements at heating rate of 10°/min in nitrogen.
e. Measured for the quenched sample in the second heating cycle at 10 ° C /min.
f. Detailed thermal analytical data are given in table-2.3.

The solution viscosity values of the polymers were obtained as η_{inh} = 0.4 - 0.7 dl/g which is typically in the range of thermoplastics obtained by melt polymerization routes. GPC chromatograms of the polyurethanes are shown in figure-2.7 and all the polyurethanes have shown a mono-modal distribution indicating the formation of uniform molecular weight polymers in the melt transurethane process.[25] The molecular weight of the polymers (table-2.1) were obtained in the range of M_n = 10 - 15 x 10^3 and M_w = 15 - 45 x 10^3 g/mol with the polydispersity in the range of 1.5 - 3.0. GPC molecular weights of the polymers indicate the formation of moderate to high molecular weight polymers and the values also proved that the melt transurethane process was superior to the conventional isocyanate route for the synthesis of polyurethanes.[34]
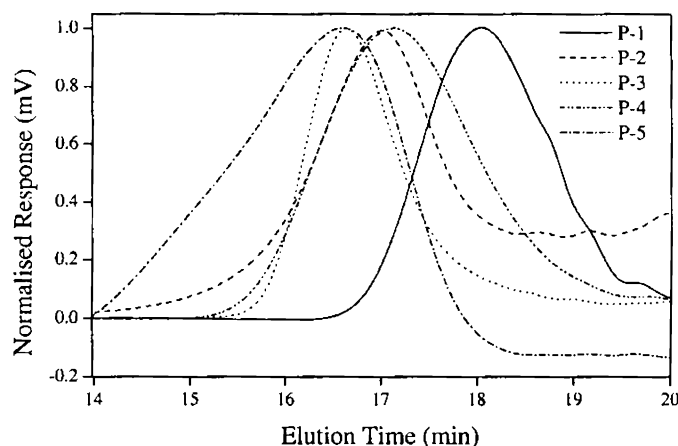
Figure-2.7: Representative GPC chromatograms of Polyurethanes

The polymers prepared from the cycloaliphatic diols (TCD-DM and CHDM) showed much higher molecular weights compared to that of oligoethylene glycols, which may be due to the difference in the hydrodynamic volume for the polymers in THF solvent. The molecular weight data gave clear evidence that the nature (primary and secondary) of the carbamate monomer did not make much difference compared to that of the nature of the diols in the formation of higher molecular weight chains. For example: the di-urethanes **DHMD, DCHD** (only primary) and **DIPD** (primary+ secondary) produce almost equivalent molecular weights for TCD-DM, CHDM and oligoethylene glycols. On the other hand the reaction of isosorbide or cyclohexanediol (secondary cycloaliphatic alcohols) produced low molecular weight (low viscosity)

polymers compared to that of CHDM (high viscosity), which is a primary diol. The number average degree of polymerization for the polymers were calculated from their GPC-data and the values were obtained for most of the polymers in the range of n = 25-50. According to the Carothers equation for equimolar amount of A-A + B-B type polycondensation: n = 1/1-P (where P is the extent of the reaction), the extent of the melt transurethane process was obtained as 95 - 98 %.[35] This indicates that the melt transurethane process developed here for polyurethanes is very efficient like other melt routes such as transesterification (for polyesters and polycarbonates) and transetherification (for polyethers).[22,25]

2.3.4. Model Reactions

Model reactions were performed under the transurethane conditions for A-A + B and A + B type condensation (A-urethane and B-alcohol). The different monomers such as simple urethanes (A) and diurethanes (A-A) and the alcohols (B) used for the model reactions are given in table-2.2.

Table-2.2: Monomers, percent conversion and FAB-Mass data for Model reactions

Sample Code	Monomers		Nitrogen Purge (1)	Vacuum (2)	
	Urethane	Alcohol	%conversion[a]	%conversion[a]	Mass[b]
A-A + B type					
M-1	DHMD	DGME	63	90	409.31
M-2	DHMD	TGME	65	90	496.6
M-3	DHMD	TCD	69	96	501.54
M-4	DHMD	Bz	65	97	385.5
M-5	DHMD	CH	40	70	369.42
A + B type					
M-6	MOC	Bz	53	63	264.33
M-7	MCHC	Bz	54	74	234.42
M-8	MBzC	Bz	58	75	242.54
M-9	MPhC	Bz	58	87	228.46

a. Determined by ^{1}H-NMR
b. Molecular mass (in amu) determined by FAB-HRMS.

It is very important to mention that in the case of model reactions, during the second stage the vacuum was controlled at ~ 1 mm of Hg (not very high as in the case of polymers, 0.01 mm of Hg) due to the low boiling point of the mono-alcohols. The

structures of the model compounds are shown in scheme-2.8. These structures were confirmed by ^{1}H-NMR, FTIR and FAB-HRMS analysis and the data are given in table-2.2.

AA +B Type Reaction

A + B Type Reaction
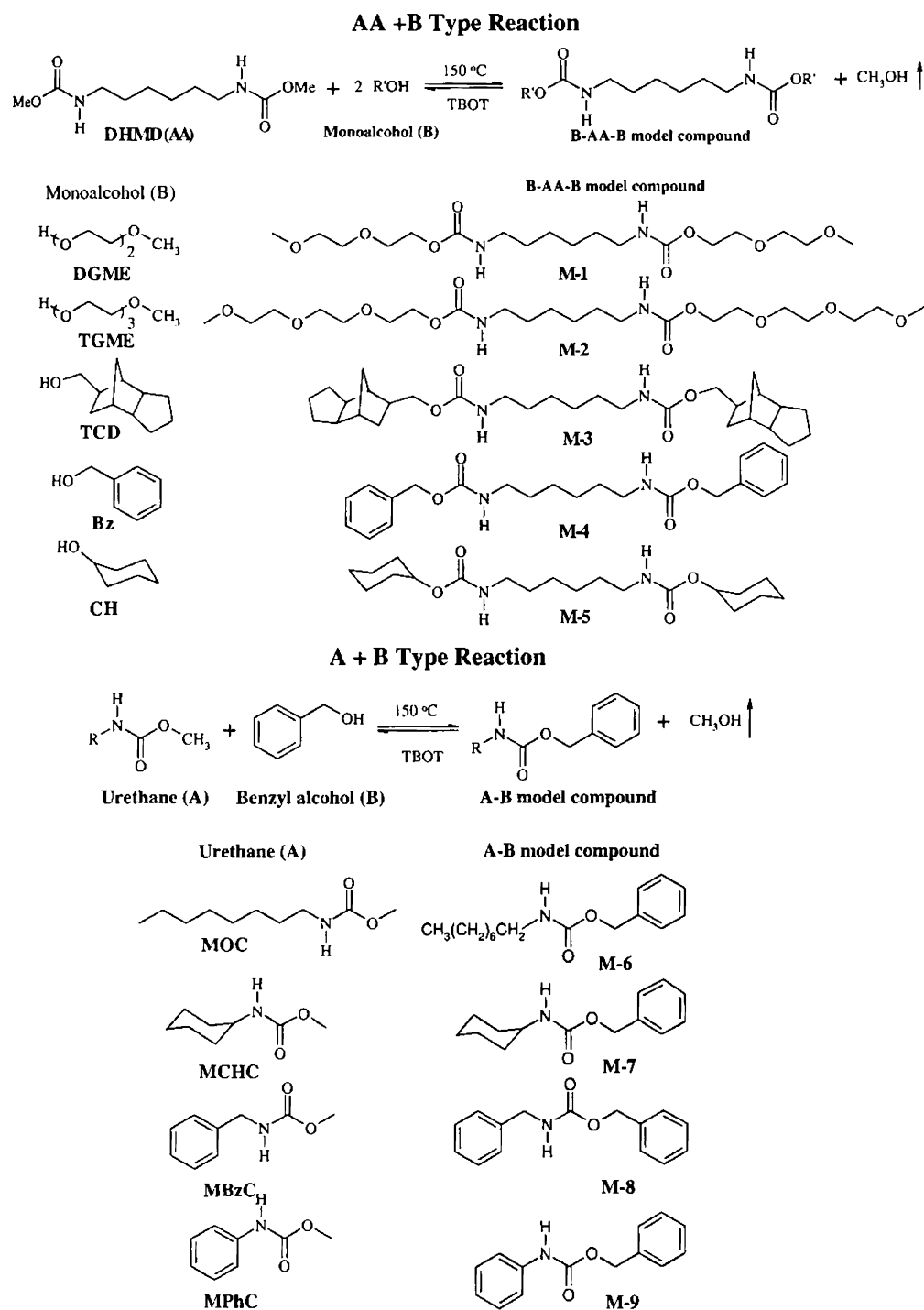
Scheme-2.8: Synthesis of A-A+B and A+B Type Model Compounds

^{1}H-NMR spectra of monomer **DHMD** and one representative A-A+B type model compound **M-4** are shown in figure-2.8. The peaks for the different types of protons in the monomer and model compound are assigned by alphabets.
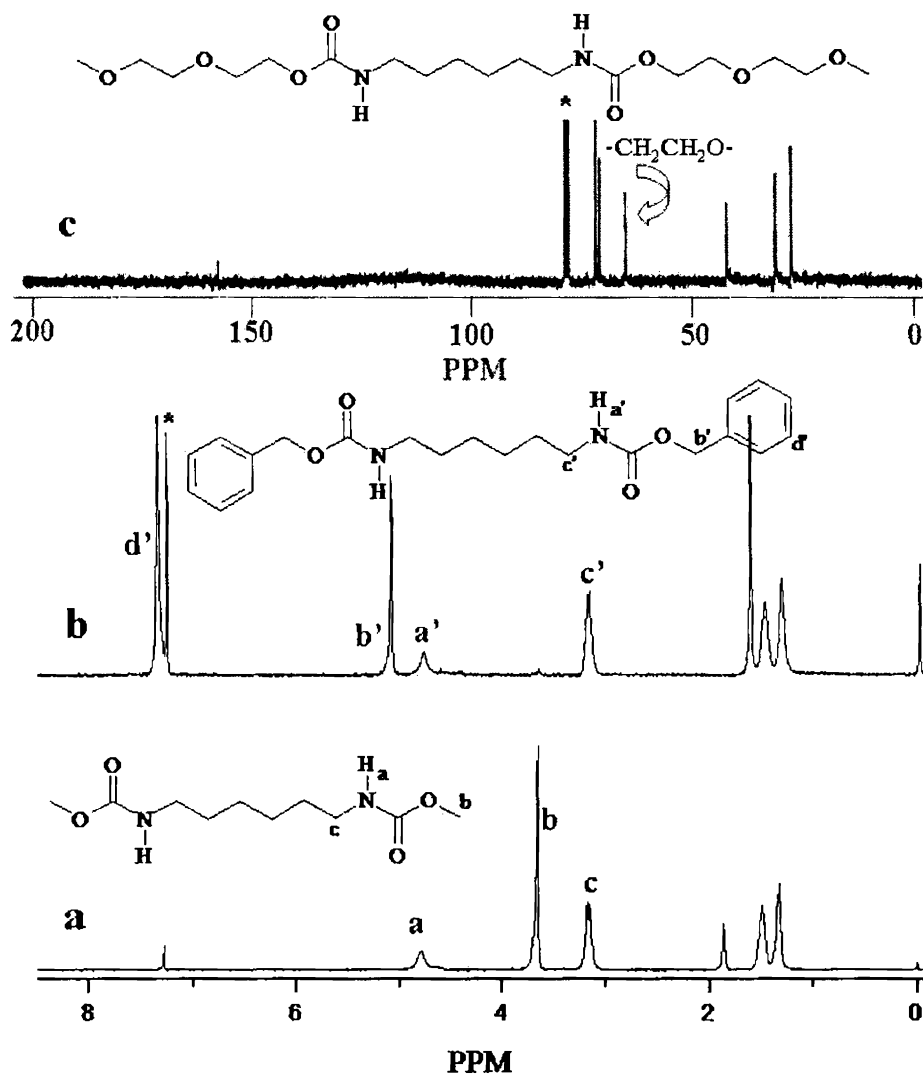
Figure-2-8: ^{1}H-NMR of diurethane monomer DHMD (a), model compound M-4 (b) and ^{13}C-NMR of model compound M-1(c).The peak at the asterisks corresponds to the solvent peaks.

The melt transurethane process for the model compounds can be easily confirmed by comparing the appearance or disappearance of $-OCH_3$, N-H and $-NHCOOCH_2$- protons. In figure-2.8a, the N-H proton (a), $-OCH_3$ proton (b) and $-CH_2NH$ proton (c) in **DHMD** appeared at 4.70, 3.65 and 3.17 ppm, respectively. With the formation of the model compound **M-4**, the peak at 3.65 ppm vanished and a new peak at 5.06

ppm corresponding to the NHCOOCH$_2$- protons (b') appeared as shown in figure-2.8b. The other peaks for **M-4** were corresponding to the aromatic protons (d') at 7.32 ppm, N-**H** proton (a') at 4.74 ppm and the –CH$_2$NH proton (c') at 3.16 ppm. For the model compounds with the oligoethylene spacers the confirmation for the formation of the products could not be done solely by comparing the ^{1}H-NMR peaks. This is because the –OCH$_3$ proton in **DHMD** merged with the oligoethylene protons (-NHCOOCH$_2$CH$_2$O-) in the model compound. In order to confirm the reaction in the oligoethylene based alcohols, the ^{13}C-NMR spectra of the compounds were taken and the spectrum of one such model compound (**M-1**) is shown in figure-2.8c. Since the difference in the chemical shift values for –OCH$_3$ and -NHCOOCH$_2$CH$_2$O- carbon atoms are large, the ^{13}C-NMR was very efficient for confirming the transurethane process in the oligo-ethylene based compounds. Interestingly, the –OCH$_3$ carbon at 52 ppm in the monomer (figure-2.6c) has disappeared and a new peak at around 70 ppm for the methylene carbon (NHCOOCH$_2$-) were observed in the model compound (figure-2.8c), which confirm the occurrence of melt transurethane process in model compounds.

2.3.5. Role of Catalyst and Mechanistic Aspects

In order to study the role of the catalyst and the mechanism of the melt transurethane process, model compound **M-4** prepared via A-A+B condensation between **DHMD** and benzyl alcohol was chosen. This particular combination was selected because of easy identification of various types of protons in the starting materials as well as the products by ^{1}H-NMR spectroscopy. To study the role of the catalyst, **DHMD** (di-urethane monomer) was reacted with twice the amount (in moles) of benzyl alcohol in presence of Ti-catalyst. Aliquots were collected at various intervals during the nitrogen purge as well as under controlled vacuum and subjected to NMR and HR-MS analysis. The ^{1}H-NMR plots are shown in figure-2.9. The -OCH$_3$ proton (at 3.65 ppm) in the di-urethane monomer slowly vanish over reaction time and a new peak corresponding to PhCH$_2$-O-CO-NH-CH$_2$- protons appeared at 5.06 ppm indicating the formation of transurethane product. The broad peak at 4.74 ppm is the combination of the un-reacted Ph-CH$_2$OH and N-**H** protons in the urethane linkage. The decrease in the intensity of the sharp peak and the clear visibility of the

broad N-H peak over reaction time also gives indication for the vanishing of free Ph-CH_2OH during the reaction.
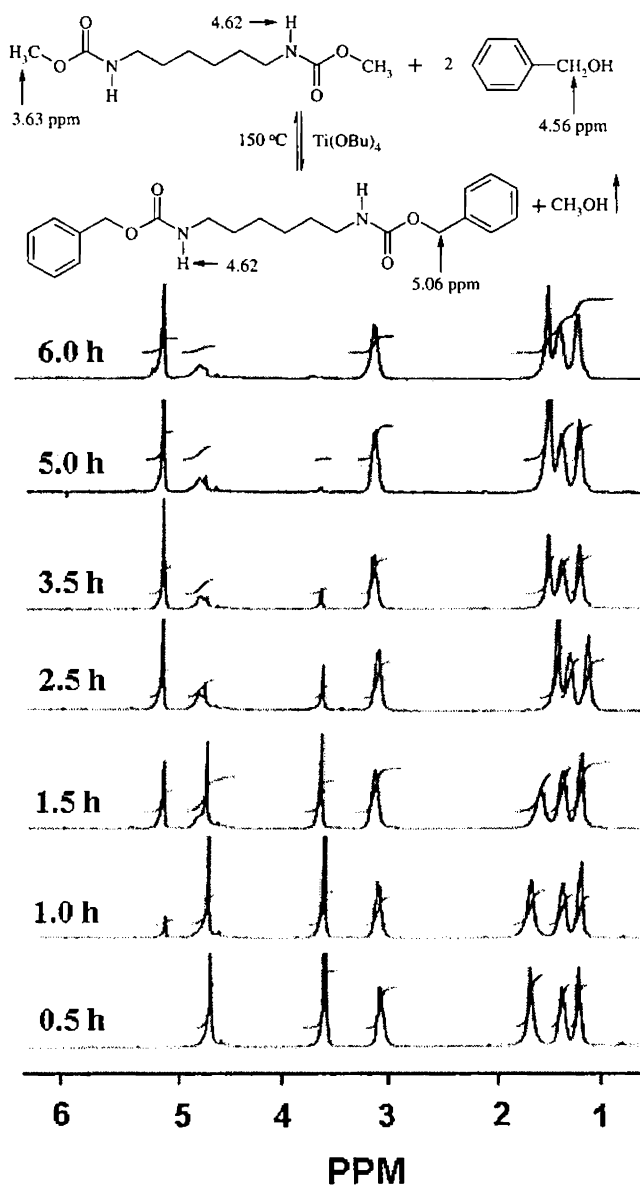
Figure-2.9: ^1H-NMR spectra for various fractions of M-4 in presence of catalyst

In order to determine the extent of the reaction, the intensities (peak integration) of the peaks $-CO-OCH_3$ and $PhCH_2-O-CO-NH-CH_2-$ were compared and the values are plotted and shown in figure-2.10. The plot confirmed the conversion of the reaction to almost 88 % under the nitrogen purge (stage-1) and almost 97 % at the end of the reaction (stage-2). This % conversion value for the model reaction is almost matching

with that of the value obtained from the M_n-data of polymerization reactions using Carothers equation. It confirms that the conditions employed for the synthesis of polymers as well as model reactions are comparable and the % conversion data obtained for model reaction would be sufficient enough for studying the kinetics of the melt transurethane reaction. The same model reaction was then carried out without Ti-catalyst and aliquots were analysed using ^{1}H-NMR spectroscopy. The plot for the % conversion versus time for reaction without catalyst (figure-2.10) indicates the formation of less than 2 % reaction. It clearly demonstrates that the melt transurethane process is mediated via Ti-catalyst and in the absence of catalyst no transurethane reaction or polymerization took place.
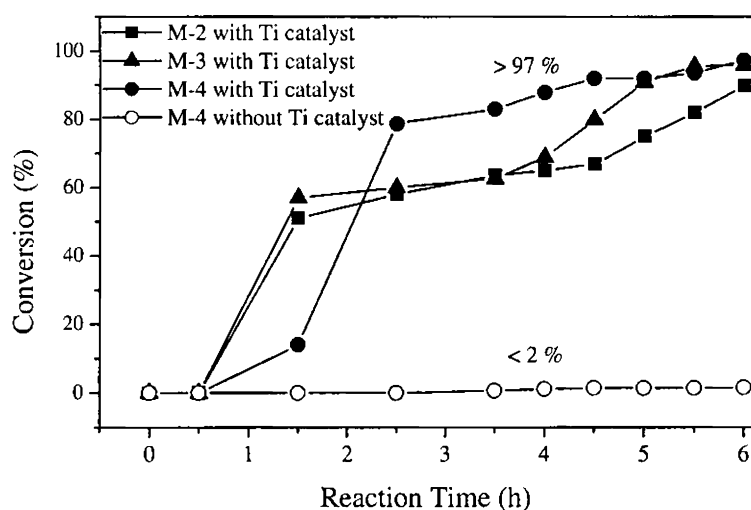
*Figure-2.10: Percent conversion versus reaction time for various model reactions with catalyst and for **M-4** without catalyst.*

Similarly model reactions were also performed for TCD, di- and tri-ethyleneglycol monomethyl ether (all are primary alcohols) (figure-2.10) and cyclohexanol (secondary alcohol) and the data are summarized in table-2.2. It is very clear from the table that the primary alcohols has 65-70 % conversion at the end of nitrogen purge and the reaction was completed with almost 96-97 % conversion in the second stage. On the other hand the cyclohexanol (secondary alcohol) showed only 40 and 70 % conversion for stage-1 and stage -2, respectively indicating the lower reactivity of the secondary alcohols under the transurethane conditions. This observation further supports the formation of lower molecular weight polymers for isosorbide and

cyclohexanediol in the polycondensation with **DHMD** (table-2.1). Similarly model reactions (A+B type) were also carried out between various mono urethanes bearing octyl, cyclohexyl, benzyl and phenyl groups with benzyl alcohol to study urethane-exchange reaction (table-2.2). It indicates that almost all carbamates (both aliphatic and aromatic) undergo exchange reaction under the solvent free and melt transurethane reaction conditions and produce almost 58 % of product under the nitrogen purge and subsequent application of vacuum gave almost 75-80 % yield.

The thermal stability of the polymers was investigated by TGA, and the onset of degradation was calculated for 10 % weight loss under nitrogen atmosphere and the values are summarized in table-2.1. All the polymers are stable up to 270-300 °C and suggested that the polymers prepared in the present investigation are very stable and can be processed under the conventional melt processing techniques for high temperature applications. Another important point to be mentioned here is that as the reaction proceeds, the transurethane reaction results in the formation of thermally stable species. A representative TGA plot for polyurethane (**P-14**) prepared using di-urethane monomer **DCHD** and tetraethylene glycol under the two stages, i.e., after nitrogen purge and after vacuum are shown in figure-2.11. The plot shows that as monomer gets converted into oligomer (stage 1, nitrogen purge) the thermal stability of the oligomers increases in comparison to the di-urethane monomer. With the formation of higher molecular weight polymer (stage 2, vacuum), the thermal stability is found to increase still further compared to that of the oligomers. This clearly indicates that the process drives the reaction towards the formation of thermally stable and high molecular weight polyurethanes.
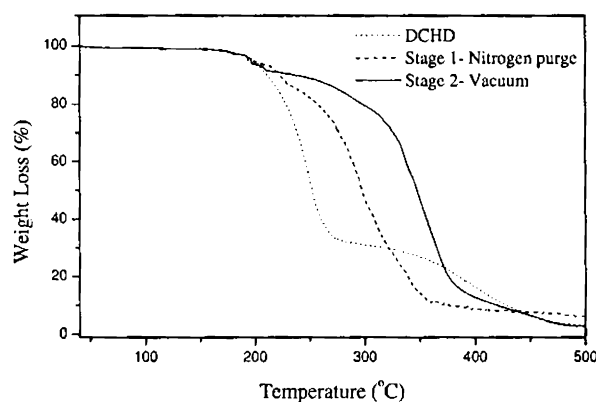

*Figure-2.11: TGA plots of diurethane monomer **DCHD** and fractions of **P-14** taken out after nitrogen purge (stage 1) and after applying vacuum (stage 2)*

Based on the above studies the mechanism for the melt transurethane process has been proposed and shown in scheme-2.9. Initially the catalyst, titanium tetrabutoxide reacts with the alcohol to form the new titanium tetraalkoxide. This then reacts with the urethane-1 and cleaves the ether bond of the half ester part in the urethane linkage and forms an intermediate (1). An exchange of bonds takes place within this intermediate to form a rearranged product (2) which then transforms into a more stable urethane-2 and a new active species (3) which then performs the next cycle of reactions.

$$R-OH \ + \ Ti(OBu)_4 \ \longrightarrow \ Ti(OR)_4$$
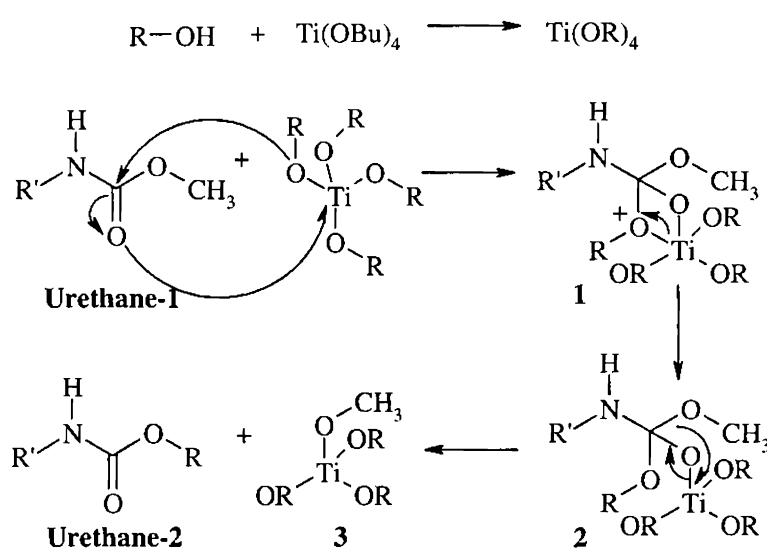
Scheme-2.9: Possible Mechanism for Melt Transurethane Reaction

2.3.6. End Group Analysis by MALDI-TOF-MS

In a typical A-A + B-B type polycondensation reaction (A-urethane, B-alcohol), there are four types of end groups possible in the polymer chains: (i) both the ends with A-functionality (chain-AA), (ii) both the ends with B-functionality (chain-BB), (iii) each end with either A or B-functionality (chain-AB) and (iv) formation of macrocycles followed by the reaction between two chain-AB.[36] In the absence of any side reaction, the polymer chains are expected to posses any one or all these chain ends. The polymerization product of the reaction between **DIPD** and **CHDM** (samples collected at the end of the nitrogen purge, stage-1) was subjected to MALDI-TOF mass spectrometry analysis. The MALDI-TOF spectrum was obtained using 2, 5-dihydroxy benzoic acid as a matrix and maintaining the matrix to sample

ratio as 1000 (in moles).[37-39] MALDI-TOF spectra showed various mass peaks in the range of m/z = 700 to 1000 corresponding to the repeating units 1-2 (figure-2.12).
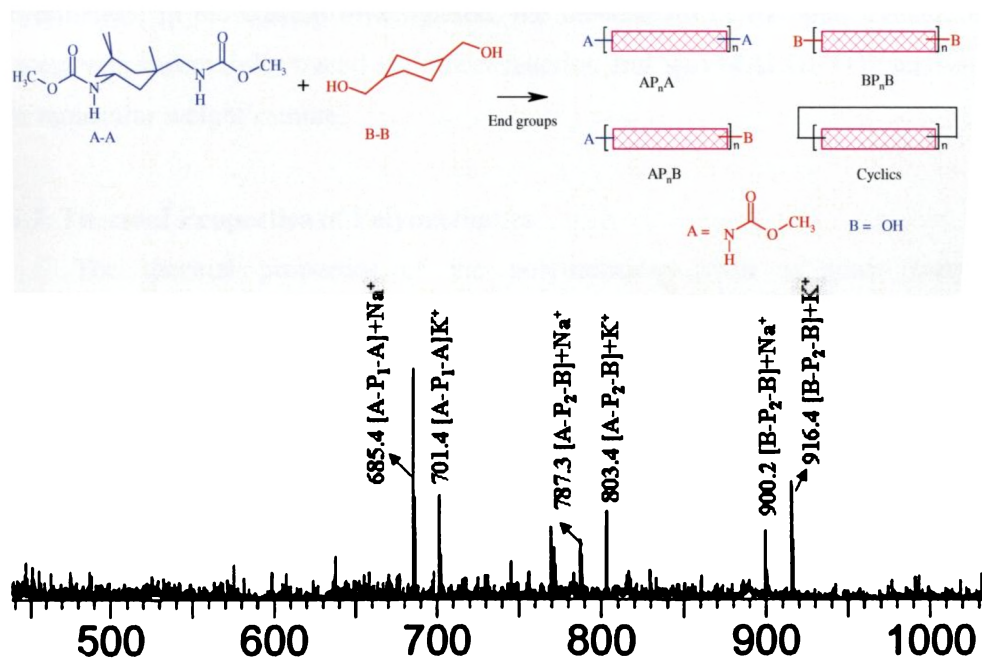

*Figure-2.12: MALDI-TOF spectrum of **P-12** after nitrogen purge (stage I of Transurethane Reaction)*

The polyurethane chains have appeared either as a sodium or potassium ion in the mass spectra. The mass peaks at m/z= 685.4 and 701.4 are assigned to the sodium and potassium ions for the polymer chain having carbamate functionality (type-A) at both the ends, respectively. The peaks at 787.3 and 803.4 are corresponding to the sodium ion and potassium ion of hydroxyl terminal chains (B-type), respectively. The two peaks at m/z 900.2 and 916.4 are corresponding to the chains with two repeating units and having both A and B type chains ends. There were no peaks corresponding to macrocyclics, which may be due to the analysis of low molecular weight polymer chains. Interestingly, the mass spectrum is completely devoid of any isocyanate group and also the isocyanate cross-linked compounds such as biuret.[4] It is evident that the melt transurethane process completely follows a non-isocyanate pathway. The presence of carbamate end groups (type AA) in the MALDI-TOF spectrum also gives direct evidence that the carbamate linkage is thermally stable under the high temperature melt transurethane process. Unfortunately, all efforts to obtain good and

reliable MALDI-TOF spectra for the high molecular weight polyurethane samples were not successful which may be due to the high polydispersity of the samples. Nevertheless, in the current investigation, the mechanism of the melt transurethane process was successfully traced via model reaction and also MALDI-TOF analysis of low molecular weight sample.

2.3.7. Thermal Properties of Polyurethanes

The thermal properties of the polyurethanes such as glass transition temperature (T_g), melting transition temperature (T_m), crystallization temperature (T_c) and their enthalpies were determined by DSC. The DSC thermograms for the second heating cycle of all the polyurethanes (except **P-4**) are shown in figure-2.13.
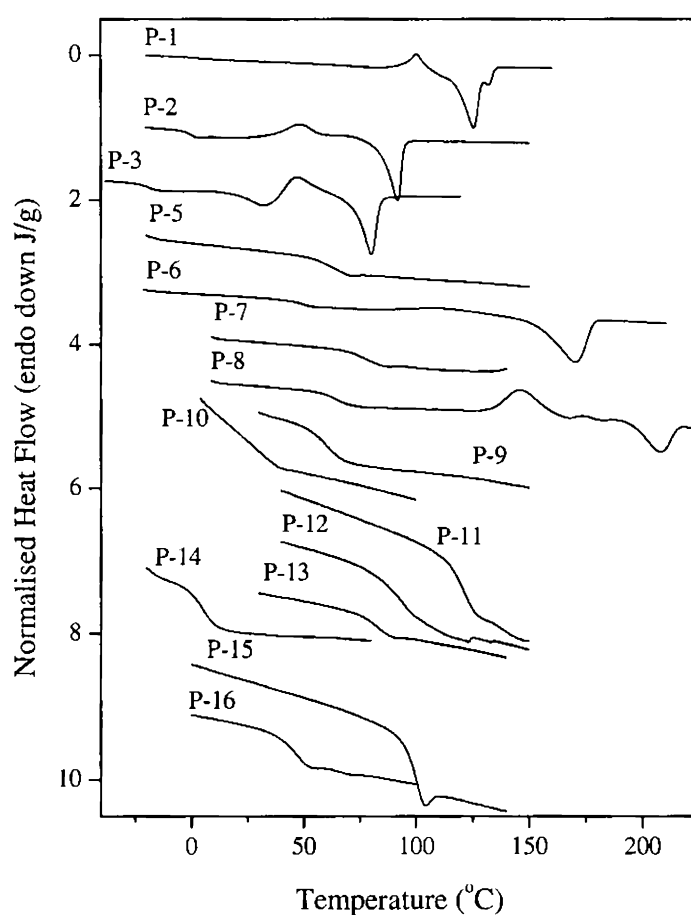

Figure-2.13: DSC thermograms of quenched samples of Polyurethanes at 10 °C/min

Most of the polyurethanes were sluggish to crystallise (except **P-1, P-2, P-3, P-6** and **P-8**) under the 10 °C/min heating/cooling cycle and showed only T_g and the T_g values

are summarized in table-2.1. By comparing the T_g values of the polymers, it is clear that irrespective of the diurethane monomers employed, the polyurethanes obtained from TCD-DM are having the maximum T_g values and the T_g trend observed is in the order TCD-DM > CHDM > HD > oligoethylene glycols. This suggests that cycloaliphatic units makes the polymer chains more rigid compared to linear alkyl chains. Among the ethylene glycols used, the values for T_g are found to decrease with the increase in the length of the oligo ethylene spacers in the polyurethane backbone. On comparing the different diurethane monomers used, polyurethanes based on **DIPD** are having the maximum T_g values and the trend observed is in the order **DIPD** > **DCHD** > **DHMD**. **DIPD** and **DCHD** have 1, 3 linkages along the polymer chains and this kinked structure makes the polymer chains sluggish to chain fold due to the loss in chain symmetry. Also in the case of **DIPD**, due to the presence of methyl groups this effect would be more predominant and hence the T_g values would be very high. This would further suggest that the polymers synthesized using **DHMD** would be less rigid and so they should show a tendency to chain fold due to the flexible nature of the bonds present in them. This is very much clear from the DSC thermograms that those polyurethanes synthesized from **DHMD** (**P-1** to **P-3**, **P-6** and **P-8**) showed melting and crystallisation peaks. The corresponding temperature and enthalpy values are given in table-2.3.

Table-2.3: DSC data of few polyurethanes synthesized from DHMD

Sample	T_m $(^{\circ}C)^a$	ΔH_m $(J/g)^a$	T_c $(^{\circ}C)^b$	ΔH_c $(J/g)^b$
P-1	123	61.35	75	37.63
P-2	89	31.58	39	6.22
P-3	77	28.38	24	9.53
P-6	167	34.16	117	18.83
P-8	208	17.42	-	-

a. Measured for the quenched sample in the second heating cycle at 10 °C/min.
b. Measured for first cooling cycle from the melt at 10 °C/min.

The thermal properties such as T_m, T_c, ΔH_c and ΔH_m decrease with the increase in the length of the oligo ethylene spacers in the polyurethane backbone whereas the value is found to be high when oligo ethylene spacer is replaced by a cycloaliphatic diol (**P-6**). Among all the polyurethanes prepared from **DHMD**, the T_m value was found to be

highest in the case of **P-8**. Among **P-1** to **P-3**, **P-6** and **P-8**, the latter polyurethane **P-8** has the highest T_g value (table-2.1) and it exhibits sluggishness to crystallise. This is evident in the cooling cycle of the polymer as there is no peak corresponding to the crystallization of the polymer but instead the sample exhibited a cold crystallisation peak at 145 °C during the second heating cycle (for 10 °C/min cooling rate). The thermal data suggested that by choosing appropriate diurethane monomers and diols, polyurethanes possessing a wide spectrum of thermal characteristics could be obtained. The thermal properties of the polyurethanes can be easily fine-tuned by designing suitable monomer molecules for the synthesis of polyurethanes.

2.4. Conclusion

A novel melt transurethane process was designed and developed for the preparation of polyurethanes under solvent free and isocyanate free conditions. Simple commercially available amines were converted into methyl carbamate monomers (urethane monomers) by reaction with dimethyl carbonate in presence of a base. These urethane monomers were condensed with variety of alcohols to produce transurethane products. The present work has many advantages and unique novelty: (i) melt transurethane reaction was developed for the synthesis of aliphatic and cycloaliphatic polyurethanes, (ii) the effect of functionality on the transurethane reaction was investigated for monomers bearing primary and secondary diurethanes and diols, (iii) the transurethane was performed for A+B, A-A + B and A-A + B-B type condensations consisting of aliphatic, cycloaliphatic and aromatic urethane linkages, (iv) thermal stability experiments confirmed that all the urethane monomers designed from commercially available amines were thermally stable under melt conditions and the reaction proceeds without decomposition, (v) model kinetic reactions revealed that the reaction proceeded up to 97 % in the presence of catalysts whereas less than 2 % product was formed in the absence of catalyst, (vi) melt transurethane process was confirmed by ^{1}H and ^{13}C NMR spectroscopies and inherent viscosity and GPC analysis of the polymers suggested the formation of moderate to high molecular weight polymers with the number average degree of polymerization obtained in the range of n = 25-50, (vii) both the polycondensation and model reactions revealed that the diurethane monomer is less sensitive to the functionality whereas the primary diol (or alcohol) produce much higher molecular weight compared to that of secondary alcohols, (viii) the end group analysis of the polymers by MALDI-TOF MS indicated the presence of chain ends of the type AA, BB and AB (A-urethane and B-hydroxyl) and confirmed the non-isocyanate pathway for melt transurethane process, (ix) the polymers were found to be thermally stable up to 270-300 °C and thermal properties particularly T_g of the polyurethanes can be easily fine-tuned from -30 to 120 °C by using appropriate diols in the melt transurethane process. The new melt transurethane process has potential for large scale industrial application of polyurethanes as similar to other thermoplastics such as polyester and polycarbonates. This approach can be extended to non-linear polymeric architectures such as dendrimers, hyperbranched and random branched polymers.

2.5. References

1. Frisch, K. C.; Klempner, D. *In Comprehensive Polymer Science*; Eastmond, G. C.; Ledwith, A.; Russo, S.; Sigwalt, P., Eds.; Pergamon: Oxford, **1989**; Vol. 5, Chapter 24, p. 413.

2. Petrovic, Z. S.; Ferguson, J. *Prog. Polym. Sci.* **1991**, *16*, 697.

3. Eisenbach, C. D.; Nefzger, H. *In Hand Book of Polymer Synthesis, Part-A*; Kricheldorf H. R., Ed.; Marcel Dekker, Inc.: New York, **1992**; Chapter-12, p.685.

4. Caraculacu, A.A.; Coseri, S. *Prog. Polym. Sci.* **2001**, *26*, 799.

5. Figovsky, O. *In Interface Phenomena in Polymer Coating. Encyclopedia of Surface and Colloid Science*, Marcel Dekker Inc.: New York, **2002**; p. 2653.

6. (a) Kebir, N.; Morandi, G.; Campistron, I.; Laguerre, A.; Pilard, J-F. *Polymer* **2005**, *46*, 6844. (b) Creely, K. S.; Hughson, G. W.; Cocker, J.; Jones, K. *Ann. Occup. Hyg.* **2006**, *50*, 609.

7. Hoff, G. P.; Wicker, D. B. *In Perlon U. Polyurethanes at I. G. Farben*, Boringen, Augsburg, P. B. Report 1122, Sept. 12, **1945**.

8. Dieter, J. A.; Frisch, K. C.; Wolgemuth, L. G. *J. Paint Technol.* **1975**, *47*, 65.

9. Foti, S.; Giuffrida, M.; Maravigna, P. Montaudo, G. *J. Polym. Sci. Polym. Chem. Ed.*, **1983**, *21*, 1599.

10. (a) Rokicki, G.; Piotrowska, A. *Polymer* **2002**, *43*, 2927. (b) Kihara, N.; Endo, T. *J. Polym. Sci., Part A: Polym. Chem.* **1993**, *31*, 2765. (c) Kihara, N.; Kushida, Y.; Endo, T. *J. Polym. Sci., Part A: Polym. Chem.* **1996**, *34*, 2173.

11. Kumar, A.; Ramakrishnan, S. *J. Polym. Sci., Part A: Polym. Chem.* **1996**, *34*, 839.

12. (a) Okaniwa, M.; Takeuchi, K.; Asai, M.; Ueda, M. *Macromolecules* **2002**, *35*, 6224. (b) Okaniwa, M.; Takeuchi, K.; Asai, M.; Ueda, M. *Macromolecules* **2002**, *35*, 6232.

13. Bernard, J-M. ; Jousseaume, B.; Laporte, C.; Toupance, T. US-20040044242, **2004**.

14. Green, M. J. US-4,663,472, **1987**.

15. Wolgemuth, L. G. US-3,950,285, **1976**.

16. Haggis, G. A.; Lambert, A. GB-944,310, **1963**.

17. Caldwell, J. R. US-2,801,231, **1957**.

18. Dreyfus, H US-2,623,867, **1952**.

19. Dreyfus, H GB-620,116, **1949**.

20. Sato, M.; Komatsu, F.; Takeno, N.; Mukaida, K-i. *Makromol.Chem. Rapid Commun.* **1991**, *12*, 167.

21. Miyake, Y.; Ozaki, S.; Hirata, Y. *J. Polym. Sci. Part A-1*, **1969**, *7*, 899.

22. Whinfield, J. R. *Nature* **1946**, *158*, 930.

23. Pilati F. *In Comprehensive Polymer Science*; Eastmond, G. C.; Ledwith, A.; Russo, S.; Sigwalt, P., Eds.; Pergamon: Oxford, **1989**; Vol. 5, Chapter 17, p. 279.

24. Clagett, D. C.; Shefer S. J. *In Comprehensive Polymer Science*; Eastmond, G. C.; Ledwith, A.; Russo, S.; Sigwalt, P., Eds.; Pergamon: Oxford, **1989**; Vol. 5, Chapter 20, p. 347.

25. Jayakannan, M.; Ramakrishnan, S.; *Chem. Commun.* **2000**, *19*, 1967.

26. Jayakannan, M.; Ramakrishnan, S. *Macromol. Chem. Phys.* **2000**, *201*, 759.

27. Jayakannan, M.; Ramakrishnan, S. *J. Polym. Sci. Part A: Polym. Chem.* **2001**, *39*, 1615.

28. Jayakannan, M.; van Dongen, J. L. J.; Behera, G. C.; Ramakrishnan, S. *J. Polym. Sci. Part A: Polym. Chem.* **2002**, *40*, 4463.

29. Jayakannan, M.; Ramakrishnan, S. *Macromol. Rapid Commun.* **2001**, *22*, 1463.

30. Behera, G. C.; Ramakrishnan, S. *J. Polym. Sci. Part A: Polym. Chem.* **2004**, *42*, 102.

31. (a) Behera, G. C.; Ramakrishnan, S. *Macromolecules* **2004**, *37*, 9814. (b) Behera, G. C.; Saha, A.; Ramakrishnan, S. *Macromolecules* **2004**, *37*, 9814.

32. Tundo, P.; Rossi, L.; Loris, A. *J. Org. Chem.* **2005**, *70*, 2219.

33. Armarego, W. L. F.; Perrin, D. D. *Purification of Laboratory Chemicals*, 4th ed.; Butterworth-Heinemann: Oxford, **2000**.

34. Deepa, P.; Jayakannan, M. *J. Polym. Sci. Part A: Polym. Phys.* **2006**, *44*, 1296.

35. Odian, G. *In Principles of Polymerization*; John Wiley & Sons. Inc.: New York, **1991**; Third Ed., Chapter 2, p. 53.

36. Jayakannan, M.; van Dongen, J. L. J.; Janssen, R. A. J. *Macromolecules* **2001**, *34*, 5386.

37. Borda, J.; Bodnar, I.; Keki, S.; Sipos, L.; Zsuga, M. *J. Polym. Sci. Part A: Polym. Chem.* **2000**, *38*, 2925.

38. Krol, P. ; Pilch-Pitera, B. *Polymer* **2003**, *44*, 5075.

39. Puapaiboon, U.; Taylor, R. T. *Rapid Commun. Mass Spectrom.* **1999**, *13*, 508.

Chapter-3

# Solvent Induced Self-organization of Polyurethanes for Nanostructures

3.1. Introduction

Self-organization of polymer chain through non-covalent forces to construct polymeric assemblies with one or three dimensional regularity has attracted great significance in the area of micro-and nanotechnology.[1-5] Zubarev et al. designed a novel dendron rod-coil molecule (DRC) capable of self assembling into one-dimensional nano-structures in solvent such as dichloromethane (scheme-3.1). The self-organization was aided by non-covalent hydrogen bonding interaction among the hydroxyl groups along the periphery of the dendron synergistically supported by the π-π stacking of the biphenyl aromatic segments. Crystal structures of the model compounds of the DRC revealed that the supramolecular structure consisted of a nano-ribbon 10 nm wide and 2 nm thick.[6]
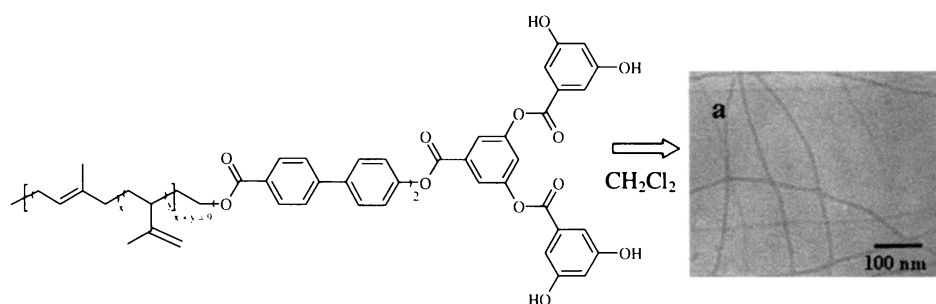

Scheme-3.1: TEM image of nano-ribbons (a) of DRC formed in CH₂Cl₂ (adapted from ref. 6)

Anisotropy combined with dynamic nature makes liquid crystalline polymers really promising for various applications in the field of information, charge transportation, molecular sensing, etc.[7] Liquid crystalline polymers possessing hydrogen bonding moieties along the main chain or side chain have been synthesized for the formation of molecularly assembled structures. These secondary interactions increase the aspect ratio of the liquid crystalline polymers making them more stable. The degree of polymerization is enhanced by imparting strong cooperativity between the association through hydrogen bonding and the induction of liquid crystalline phase.[8] One such example is shown in scheme-3.2 wherein a supramolecular hydrogen bonded liquid crystal exhibiting a nematic phase upto 252 °C has been prepared by the complexation of polyacrylate containing a benzoic acid moiety in the side chain with stilbazole.[9]
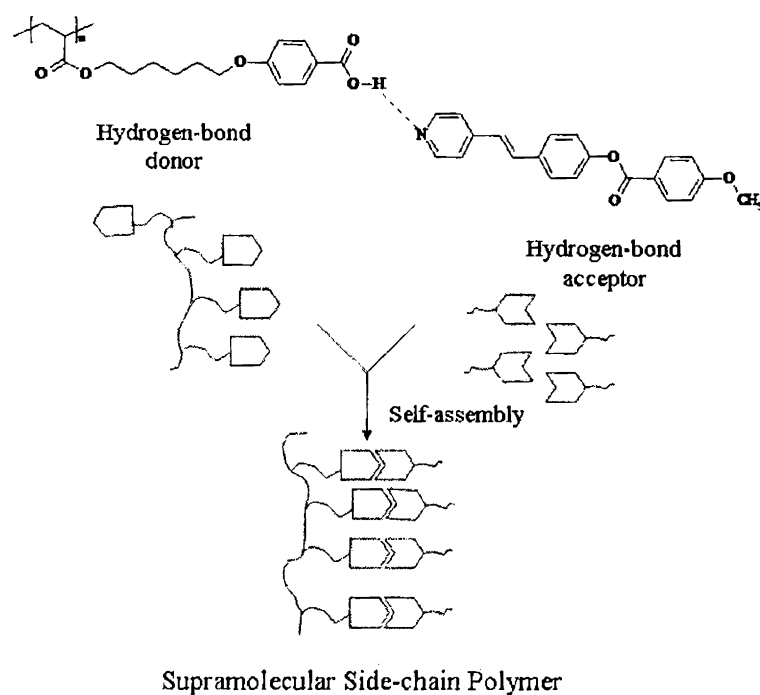
Scheme-3.2: Example for a supramolecular side-chain hydrogen bonded liquid crystalline polymer (adapted from ref. 9)

Self-assembled porous polymeric materials of sub-micrometer and nanometer scales are employed as templates, as solid support for catalysis, micro-structured electrode surfaces and as vehicles for sustained and targeted delivery of drugs and biologically active agents.[10-16] Porrata et al. have utilized polycarbonate membranes as templates for the growth of monodisperse peptide nanotubes from a peptide bolaamphiphile molecule as shown in scheme-3.3.[10]Various processing methodologies such as electro-spinning,[17-19] phase separation with supercritical CO_2,[20] melt processing of immiscible blends,[21-22] metal oxide monoliths of polymer foams,[23] isothermal immersion precipitation,[24] graft polymerization[25-27] and self-organization of polymer chains via solvent evaporation[28-46] have been reported for the preparation of one and three dimensional (micro or nano) polymeric porous materials. Among all the approaches, a great deal of effort has been taken to study the solvent induced self-organization in polymer chains not only because of its simple experimental conditions but also it is a powerful tool in understanding the fundamentals of polymer chain interactions.[29-32] It is also readily adaptable to large scale applications compared to other supramolecular approaches which involve tedious synthesis and purification.

Bis(N-α-amido-glycylglycine)-1,7-heptane dicarboxylate

Peptide nanotube   Polycarbonate membrane
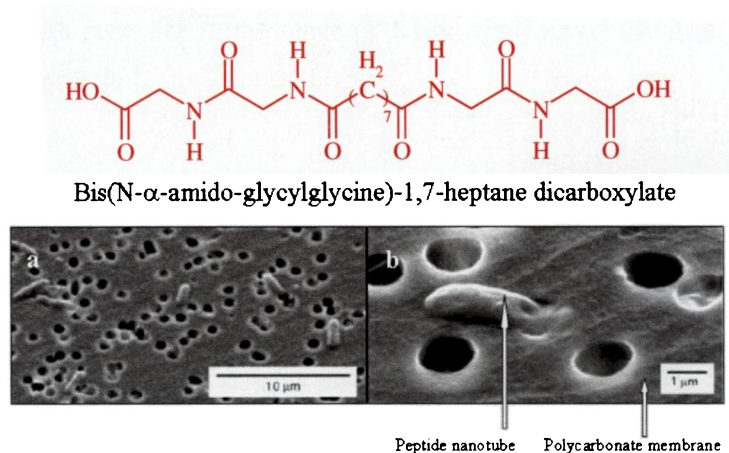
Scheme-3.3: Peptide nanotubes produced from a bolaamphiphile molecule in solution grown on polycarbonate templates lower magnification (a) and higher magnification (b) (adapted from ref. 10)

Three dimensionally arranged honey-comb type hexagonal morphology have been produced through self-organization route by adapting suitable experimental conditions or using molecules with specific structural backbone.[29-30] Breath figure patterns have also been fabricated by spin coating polymer solutions either in water or water miscible solvents containing water.[31, 33] Micro-patterned surfaces were also generated by evaporating polymer solution containing small amount of non solvent of polymer in air, where phase separation and breath figure effect together played a significant role in producing such morphologies.[42-43] Micro-patterning of polymer surfaces have been examined for a range of rod-coil diblock and triblock coil-rod-coil copolymers,[28-30, 34-37] amphiphilic and dendronized block copolymers,[38] polystyrene,[39-41] polyacrylates,[44] cellulose acetate butyrate[45] and star polymers[46] etc. Few examples of such polymers are given in scheme-3.4. Lin et al. obtained regularly porous honey-comb structured films of poly(phenylquinoline)-b-poly(methyl methacrylate) ($PPQ_{52}PMMA_{800}$) copolymers solution cast from dichloromethane with pore size of 2.6 μm (scheme-3.4a).[28b] Lee et al. synthesized a rod-coil molecule consisting of two biphenyls and a phenyl group connected through ester linkages as the rod and polypropylene oxide as the coil. These copolymers produced honey-comb supramolecular structure when cast from dilute chloroform solution as revealed by the TEM images as shown in scheme-3.4b.[35] Star polymers have produced honey-comb

morphology with pore size in the range of 1 μm from carbon disulfide solution as shown in scheme-3.4c.[46]

(a)

Poly(phenyl quinoline)-b-poly(methyl methacrylate)

Coil-rod polymer

(b)

(c)

α-D-glucose-polystyrene star polymer
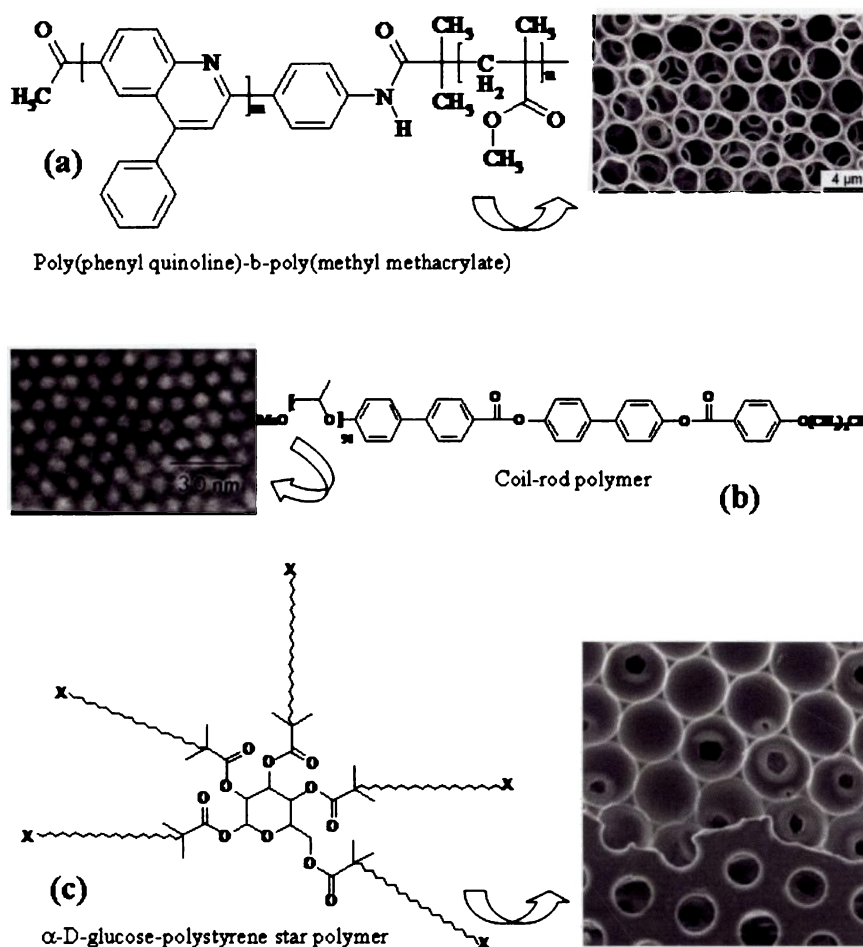
Scheme-3.4: Few examples of polymers showing honey-comb morphology

(adapted from ref. 28b(a) 35(b) and 46(c))

Deepak et al.[47] had recently reported the existence of a three-dimensional honey-comb pattern in methacrylic comb polymer bearing hydrogen bonded urethane (or carbamate) and hydrophobic bulky anchoring groups. The unique advantage of polyurethane is that the presence of reversible hydrogen bonding network in the polymeric matrix behaves as physical cross links for thermo-elastic properties. Few synthetic approaches have been reported in the literature for morphology control in

polyurethanes such as UV-light curing of liquid polyurethane precursor,[48-49] epoxy resin mediated polyurethane hybrid network,[50-51] nano-fibers through electro-spinning[52] and micro spheres via interfacial,[53] precipitation[54] and suspension polymerization techniques,[55] etc. However, the potential of reversible hydrogen bonding network in polyurethane backbone has not been explored for simple solvent induced self-organization to produce one or three dimensional molecular architectures.

This chapter deals with the solvent induced self-organization of new class of polyurethanes into micro-pores and the conversion of these porous templates into their higher ordered polymeric hexagons and spheres of micro to nano-meter scale. The present study is emphasized on investigating the effect of chemical structures on the morphology of new cycloaliphatic polyurethanes and the role of solvent combination in the self-organization process. The polyurethanes employed for the present survey were synthesized through the novel solvent free and isocyanate free melt transurethane methodology as described in chapter-2. These polyurethanes are pristine in their chemical structure, soluble in common organic solvents, thermally stable and possess high molecular weight for utilizing them in the present solvent induced self-organization study. Micro-pores and polymeric hexagons and micron or nanometer sized polymeric spheres were produced by the hydrogen bonded self-organization process. The effect of chemical structure of the polymer backbone, solvent polarity, water + organic solvent bi-phase combinations and concentration of the polymer solutions were investigated to understand the morphology formation. The different morphologies such as micro-pores, polymeric hexagons and spheres produced by the solvent induced self-organization were investigated by scanning electron microscope (SEM) and transmission electron microscope (TEM). SEM and TEM analysis revealed that the morphology of polyurethane films is highly sensitive to their chemical structure and solvent combinations. Concentration dependant solution FT-IR, ^{1}H-NMR measurements, differential scanning calorimetry (DSC), and AM1 calculation were employed as tools to trace the mechanistic aspects and the factors that control the hydrogen bond assisted self-organization process.

3.2. Experimental Methods

3.2.1. Materials: The polyurethanes used for the solvent induced self-organization studies have been adapted from chapter-2. These polyurethanes were synthesized by utilising the solvent free and non-isocyanate melt transurethane reaction as reported in chapter-2. The polyurethanes which were selected for the present study are:

1. **P-12** prepared by the reaction between **DIPD** and **CHDM**
2. **P-11** prepared by the reaction between **DIPD** and **TCD-DM**
3. **P-13** prepared by the reaction between **DIPD** and **HD**
4. **P-10** prepared by the reaction between **DIPD** and **TREG**
5. **P-5** prepared by the reaction between **DHMD** and **TCD-DM**

For simplicity these polymers will be denoted as **P-1**, **P-2**, **P-3**, **P-4** and **P-5** in the ascending order. Similarly an A-A+B type model compound, **M-3** prepared by the melt transurethane reaction between **DHMD** and TCD-M from chapter-2 was also used for the studies in this chapter. Its name will be retained as such in this chapter. Isophorone diisocyanate (IPDI), 1-decanol (Dec) and dibutyl tin dilaurate (DBTDL) were purchased from Aldrich Chemicals and used without further purifications. Tricyclodecanemethanol (TCD-M) was kindly supplied by Celanese Chemicals. High purity HPLC grade tetrahydrofuran (THF) was purchased locally (Merck India Ltd) and dried using standard procedures prior to further analysis.

3.2.2. Measurements: ^{1}H and ^{13}C-NMR spectra of the model compounds were recorded using 300-MHz Brucker NMR spectrometer in CDCl$_3$ containing small amount of TMS as internal standard. ^{1}H NMR titration studies of the model compounds and polyurethanes were recorded in CDCl$_3$ containing small amount of TMS as internal standard. Sample solutions of different concentrations were prepared by fixing the volume of the solvent (0.5 ml of CDCl$_3$) and varying the amount of sample added (2, 10, 25, 50 mg). The hydrogen bonding association constants were determined by Scatchard equation[56]

$$\Delta/[S] = -K\Delta + \Delta_o K,$$

where, $\Delta = \delta_{obs} - \delta_{free}$, [S] is the concentration of the sample in M and K is the association constant in M^{-1}. For each concentration the Δ-value was calculated by taking δ_{obs} as the value of the -NH peak obtained from the NMR spectra for that particular concentration. The value for δ_{free} was obtained from the δ value of the -NH peak from the NMR spectra of structurally similar model compound with the least concentration (2 mg/0.5 ml). Such a low concentration was chosen because under these conditions the probability for a molecule to come in the vicinity of another molecule to undergo hydrogen bonding would be the least. So the molecule can be considered to be in the free state with relevance to hydrogen bonding. The association constant (K) was obtained from the straight line slope of the plot of Δ/[S] versus Δ. For compounds containing two –NH peaks, the Δ values were calculated for both the –NH peaks but the K values were obtained from the primary urethane –NH peak (value with least error bar). Infrared spectra of the samples were recorded using Perkin Elmer Fourier Transform Infrared (FTIR) spectrophotometer. To record solution FT-IR spectra, sample solution of various concentrations ranging from 10^{-2} to 10^{-4} were prepared by dissolving appropriate amounts of the sample in tetrahydrofuran (THF). The solution was filtered and a constant volume of the solution (50μL) was injected between two NaCl plates held together in a sample holder and the spectra were recorded from 4000 to 600 cm^{-1}. For scanning electron microscopy (SEM) measurements, polymer samples were prepared by dissolving the polymers in THF or THF/water solvent combinations (5 wt %). The solution of the polyurethanes in THF was filtered using Whatmann No.1 filter paper to remove any unwanted materials. For THF/water solvent combinations, water was added drop wise from a syringe into a known amount of the polymer solution in THF. These solutions were drop cast on a glass plate and the probing side was inserted into JEOL JSM-5600 LV scanning electron microscope for taking photographs. Transmission electron microscope (TEM) images were recorded using JEOL-JEM-1011 instrument at 80 KV. For TEM measurements, the polymer solutions were prepared similar to SEM and a drop of the polymer solution (1 wt % solution) was deposited directly on Formvar coated copper grid and the samples were allowed to dry under ambient conditions.

3.2.3. Synthesis of Model compounds

3.2.3.1. Synthesis of model compound (M-1): Tricyclodecanemethanol (TCD-M) (3.35 g, 0.02 mol) was placed in dried toluene (15 ml) in a 50 ml two necked flask blanked with nitrogen. Two drops of DBTDL was added as catalyst and the flask was cooled to -20 °C using an ice-salt bath. IPDI (2.24 g, 2.14 ml, 0.01 mol) was added in drops and the reaction was proceeded in the ice bath for 1 h. It was warmed and stirred at 30 °C for 3 h and then the vessel was immersed in an oil bath at 75 °C and stirred for another 18 h. After the reaction, the contents were poured into 100 ml hexane, filtered and washed well with methanol/hexane mixture to remove the un-reacted materials and the product was obtained as white solid. It was dried in an oven at 50 °C (0.5 mmHg) for 12 h prior to further analysis. Yield: 4.08 g (73%), M.P.= 65 °C. ^{1}H NMR (300 MHz, CDCl$_3$) δ: 4.74 ppm (s, 1H, -CH$_2$NH), 4.45 ppm (s, 1H, cy-CHNH), 3.77 ppm (s, 4H, -COOCH$_2$), 3.77 ppm (s, 1H, cy-CH-NH), 3.24, 2.91 ppm (s, 2H, -CH$_2$NH), 2.35-0.93 ppm (45H, cy-H, others). ^{13}C NMR (CDCl$_3$) δ: 157.46, 128.38 68.74, 54.99, 47.24, 46.60, 45.67, 45.34, 43.78, 42.09, 41.36, 40.22, 36.58, 35.22, 34.29, 32.03, 29.12, 27.87, 27.81, 27.11, 23.39 ppm. FT-IR (cm^{-1}): ν = 3348 (-NH $_{H\,bond}$), 2948, 2863 (-CH$_2$), 1688 (C=O $_{H\,bond}$), 1528 (-NH $_{bend}$), 1452, 1273 (C-N), 1216. HRMS (FAB): calcd for C$_{34}$H$_{54}$N$_2$O$_4$ [M$^+$]: 554.8: found: 555.6

3.2.3.2. Synthesis of model compound (M-2): 1-decanol (Dec) (3.16 g, 0.02 mol) was placed in dried toluene (15 ml) in a 50 ml two necked flask blanked with nitrogen. Two drops of DBTDL was added as catalyst and the flask was cooled to -20 °C using an ice-salt bath. IPDI (2.22 g, 2.12 ml, 0.01 mol) was added in drops and the reaction was performed as described for **M-1**. The product was obtained as a white viscous mass. Yield: 1.2 g (22%). M.P. = No (highly viscous) ^{1}H NMR (300 MHz, CDCl$_3$) δ: 4.77 ppm (s, 1H, -CH$_2$NH), 4.49 ppm (s, 1H, cy-CHNH), 4.02 ppm (s, 4H, -COOCH$_2$), 3.77 ppm (s, 1H, cy-CH-NH), 3.25, 2.91 ppm (s, 2H, -CH$_2$NH), 2.00-0.84 ppm (53H, cy-H, others). ^{13}C NMR (CDCl$_3$) δ: 157.39, 65.27, 65.06, 55.04, 42.14, 36.57, 35.23, 32.07, 29.72, 29.48, 29.25, 27.80, 26.08, 23.40, 22.84 ppm. FT-IR (cm^{-1}): ν = 3321 (-NH $_{H\,bond}$), 2919, 2851 (-CH$_2$), 1683 (C=O $_{H\,bond}$), 1539 (-NH $_{bend}$), 1471, 1344, 1263 (C-N), 1223, 1144, 1056. HRMS (FAB): calcd for C$_{32}$H$_{62}$N$_2$O$_4$ [M$^+$]: 538.9: found: 541.2

3.3. Results and Discussion

3.3.1. Structure of Polyurethanes

All the polyurethanes used for studying the solvent induced self-organization process were prepared using the solvent free and non-isocyanate melt transurethane route as reported in chapter-2. The structures of the polyurethanes are given in scheme-3.5.

P-1

P-2

P-3

P-4

P-5
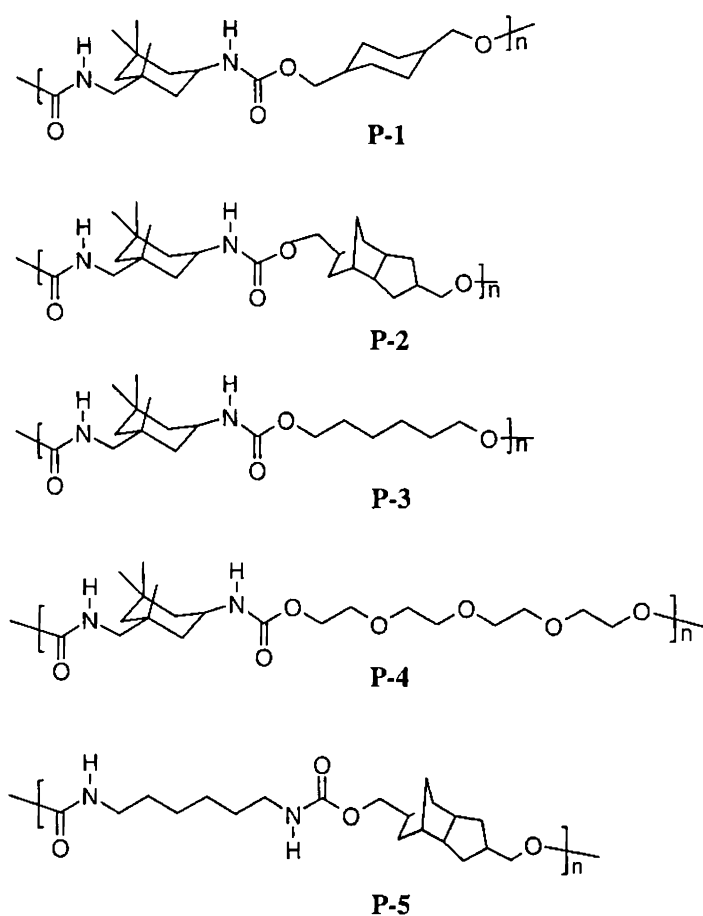
Scheme-3.5: Structure of Polyurethanes

3.3.2. Strategy for Solvent Induced Self-organization of Polymers

The strategy employed for the solvent induced self-organization of polyurethanes is described in figure-3.1. The polymer solution was prepared by dissolving the polymer in a suitable solvent such as THF (or chloroform) and this solution was filtered to remove any unwanted particles. It was then drop cast on a

glass substrate and allowed to evaporate very slowly under ambient conditions at room temperature resulting in the formation of stable polymer films. Similarly, water was added drop wise into the clear polymer solution in THF and shaken well to obtain a homogeneous polymer solution. This solution was also drop cast on a glass substrate and evaporated very slowly as said above. These stable films were then observed under the scanning electron microscope to determine the evolution of different types of morphologies based on two stipulations: (i) backbone structure of the polymers selected and (ii) the solvent combinations used for the sample preparation.
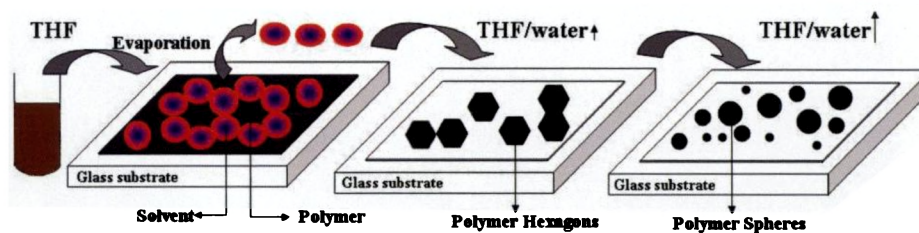

Figure-3.1: Strategy used for the solvent induced self-organization of polyurethanes into various morphologies

3.3.3. Scanning Electron Microscopy (SEM) Analysis

The morphological properties of the cycloaliphatic polyurethanes were studied for solvent evaporated polymer samples using JEOL JSM- 5600 LV scanning electron microscope. The polymer films were prepared by dissolving the polymer in dry THF (5 wt % solution), filtered through Whatmann no.1 filter paper and drop cast on a glass substrate. All the polymer films were allowed to evaporate slowly for 24 h under ambient conditions in air.[43] SEM images of the polymer films **P-1** to **P-5** are shown in *figure-3.2. It is very clear from the SEM pictures that all the five polymers produce different morphology. The polymers P-1 and P-2 showed a typical polymer micro-* porous membrane type texture whereas the polymers **P-3** to **P-5** did not show any features. **P-1** has almost same pore sizes (0.50 - 0.75 μm) separated by 1.25 - 3.00 μm. **P-2** has much smaller pores (0.26 - 0.53 μm) and the pores are more closely packed (0.79 - 1.3 μm) compared to **P-1**. In both the samples, only straight through pores were observed and no trace of honey-comb pattern is noticed in the entire film. The porous morphology was not confined to small domains or edges.
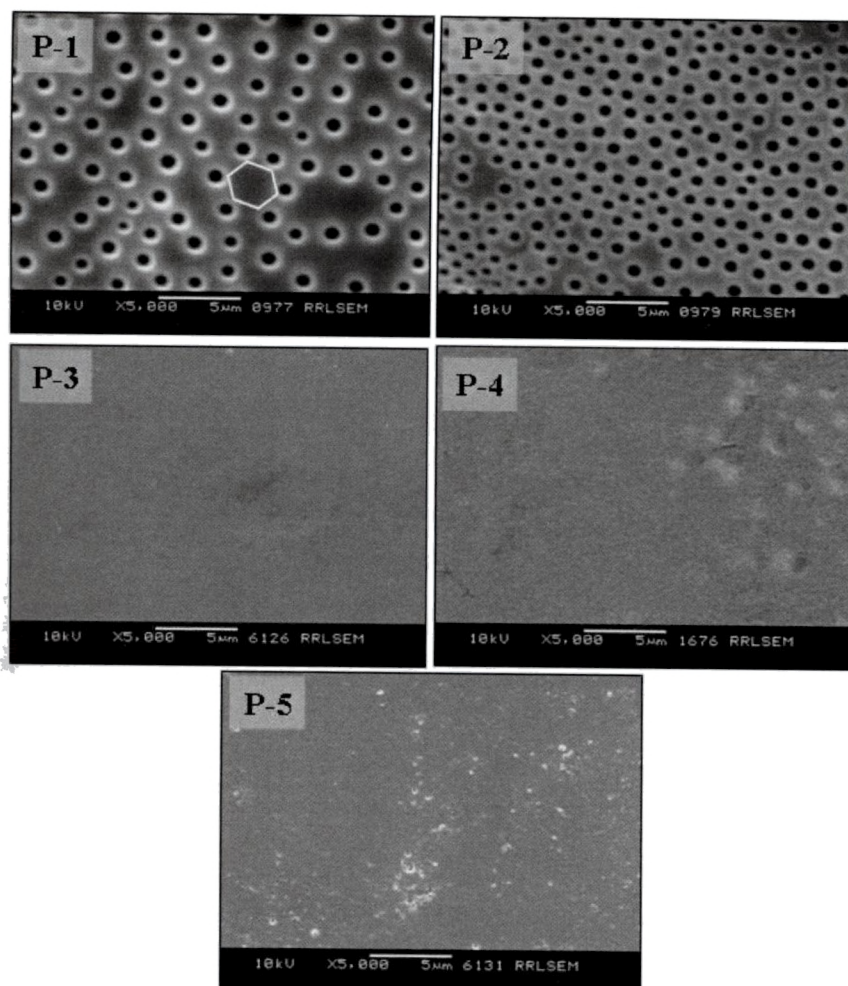
Figure-3.2: SEM images of polyurethanes prepared from THF solution (5 wt %)
at ambient conditions

It appeared throughout the sample for more than 100 micron square meters. On close observation a definite pattern is seen for the arrangement of pores, for example, in **P-1** (figure-3.2) a group of six pores together forms a hexagonal arrangement. It is also very important to mention that **P-1** and **P-2** produced similar porous-morphology from chloroform solution with much larger pore sizes (figure-3.3). For instance **P-1** has pores ranging from 4 - 6 μm where as **P-2** produced much larger pores with sizes ranging from 1 - 8 μm with the distance between the pores to be ~15 μm. It was also observed that **P-3** and **P-5** did not show any special morphology in chloroform as shown in figure-3.3.
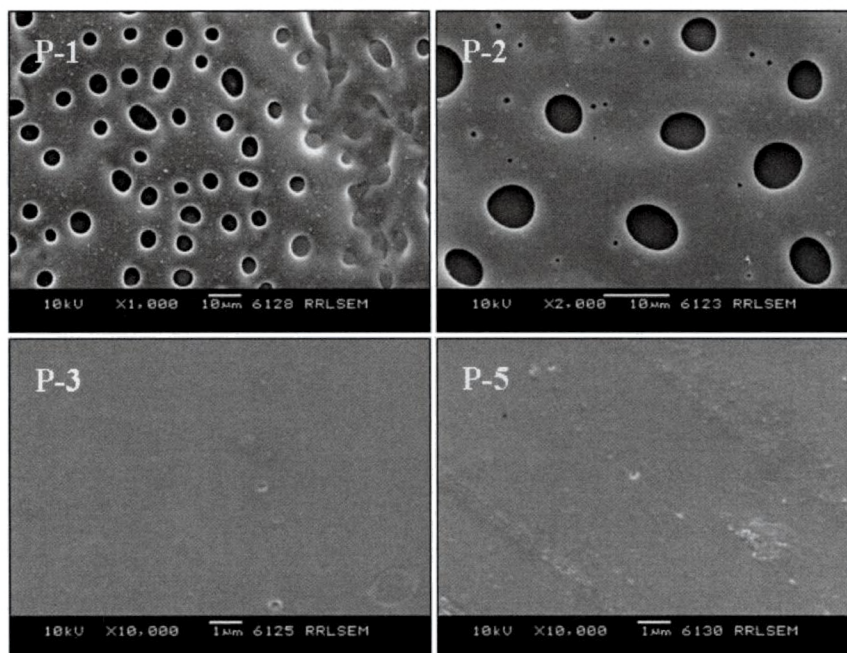
Figure-3.3: SEM images of polyurethanes prepared from CHCl₃ solution (5 wt %)
at ambient conditions

It suggested that the tendency for the pore formation in the polyurethanes is not restricted to water loving solvents like THF and even water-immiscible solvent like chloroform may also be useful for creating micro-patterns. Therefore, difference in the SEM morphology of **P-1** to **P-5** primarily arose from the difference in the chemical structure of the polyurethane backbone and the solvent type has less influence on the micro-pattern formation.

3.3.4. Effect of Water on Morphology

In order to study the effect of water (or humid atmosphere) on the morphology of the polymers, polyurethane films were prepared from THF + water solvent combinations. The composition of THF and water were varied from 95:5, 90:10 and 85:15 (v/v %, 5 wt % solutions) and the films were prepared under identical ambient conditions. When the amount of water was higher, i.e. 80: 20, v/v THF: water, it was found that the polymer solution became hazy and the polymer began to precipitate. The SEM images of the film of **P-1** prepared from water/THF solvent combinations are shown in figure-3.4.
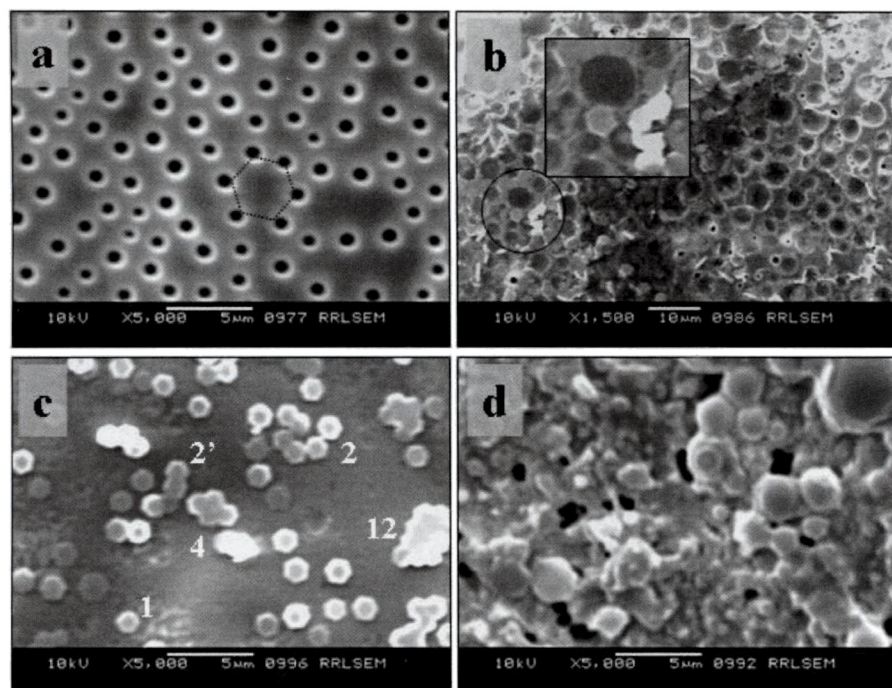
*Figure-3.4: SEM images of **P-1** in THF alone (a), 95:5 THF/water (b), 90:10 THF/water (c) and 85:15 THF/water (d)*

In figure-3.4a, the micro-porous membrane type morphology of the polymer with hexagonally patterned polymeric matrix in between the solvent pores is visible. With the addition of small quantities of water into the polymer solution in THF (95:5, v/v, THF: water), the pore sizes significantly increases (~ 3.5 μm, see figure-3.4b) and the solid polymer matrix surrounded by the pores emerged as perfectly edged micron size polymeric hexagons. Further increase in the amount of water in the solvent mixture (90:10, v/v, THF: water) results in the formation of more hexagonal morphologies and no traces of pores were noticed (see figure-3.4c). The size of the hexagons (diagonal) ranges from 1.30 to 1.95 μm which is almost identical to the distance between the adjacent pores in figure-3.4a. It confirms that the increase in the water content in the solvent mixture increases the sizes of the hexagonally packed pores formed by solvent coalescence and the solid polymer matrix isolated as polymer hexagons. It is very interesting to notice that like fused aromatic rings, the polymer hexagons also appeared as fused 2, 3, 4, 5…12 hexagons (figure-3.5).
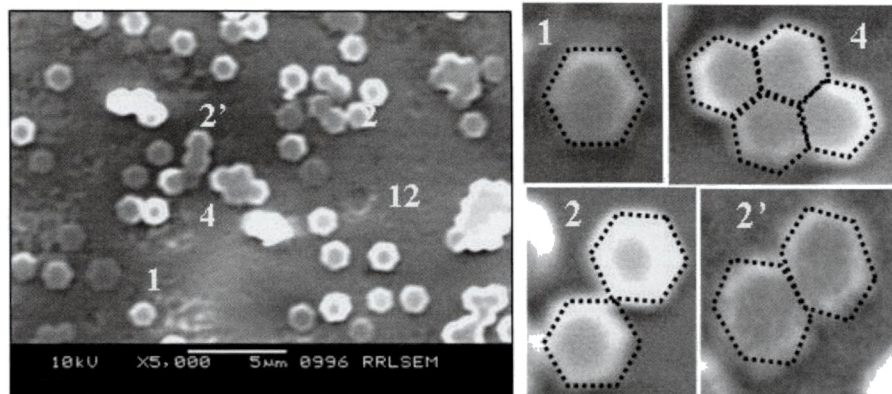
Figure-3.5: Expanded SEM images of polymeric hexagons of P-1 in THF: water-90:10

The fused linkages were formed either edge-on (2) or face-to- face (2'). This is for the first time that such perfect hexagonal morphologies are observed for solvent induced self-organization process for any type of polymers in the literature. In the presence of very high amount of water in the polymer solution (85:15, v/v, THF: water), the edges of the hexagons curved and results in the formation of spheres (figure-3.4d). It is also clear from figure-3.4d that the hexagons and spheres co-exist in some domains and gives evidence for the formation of spheres from the polymeric hexagons. The diameter of spheres is in the range of 1.25 - 1.50 μm, which is almost similar to that of the diagonals of the hexagons (1.30 to 1.95 μm). It suggests that the hexagonal packing of the pores is assumed to drive the formation of solid polymeric hexagons. The solid hexagons are not consistently seen throughout the SEM images because of the irregular packing of pores in the hexagonal array in the entire polymer film. The SEM images of **P-2** in THF and THF + water combinations are shown in figure-3.6. In this case also the microporous morphology in THF (figure-3.6a) gets converted into polymeric hexagons with the increase in the water content in the solvent mixture. The addition of water induces phase separation in the porous film for the formation of hexagons of sizes in the range of 0.52 - 1.05 μm as seen in fugure-3.6b. When the amount of water in the solvent mixture is increased still further, the polymeric hexagons subsequently evolve into polymeric spheres (1.34 - 1.63 μm) as evident in figure-3.6c and 3.6d.
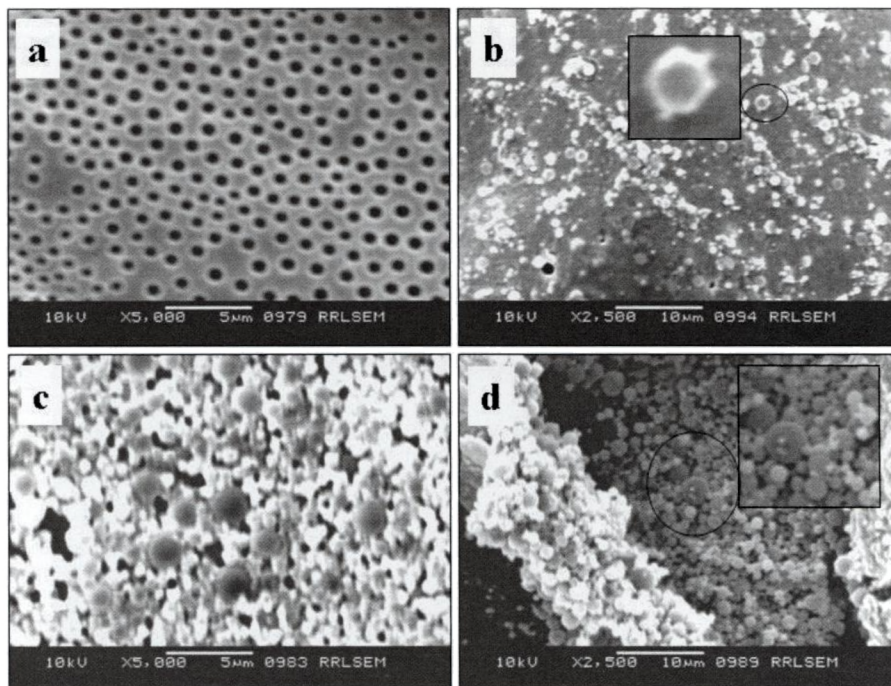
*Figure-3.6: SEM images of **P-2** in THF alone (a), 95:5 THF/water (b), 90:10 THF/water (c) and 85:15 THF/water (d)*

The density of the spheres is found to be more in the case of **P-2** when compared to **P-1** (figure-3.6d and 3.4d). This may be due to the greater density of pores in the former case than in the latter (figure-3.2). Surprisingly, **P-3**, **P-4** and **P-5** (figure-3.7) did not show any types of pores, hexagons or spheres either in THF alone or for increasing the water content in the solvent mixture. It is evident that only those polyurethanes bearing fully cycloaliphatic chemical structure have tendency to form straight through pores and produces higher ordered hexagons and spheres for higher water content in the solvent combinations. On the other hand, the replacement of one of the cycloaliphatic ring by linear units such as hexyl (in **P-3** and **P-5**) or oligoethyleneoxy (in **P-4**) failed to show any types of morphology for THF or THF + water. Therefore, the morphological evolutions of polyurethanes are highly dependent on the chemical structure of their backbone. Concentration dependent studies were also carried out for **P-2** (for 50 mg, 35 mg and 20 mg/mL polymer solutions) for 90:10 v/v of THF: water solvent combination. SEM morphologies of the films are shown in figure-3.8 which confirmed the presence of spheres which indicated that the self-organization of

polyurethane chains were highly selective to their structure and less influenced by the concentration of the polymer solution.
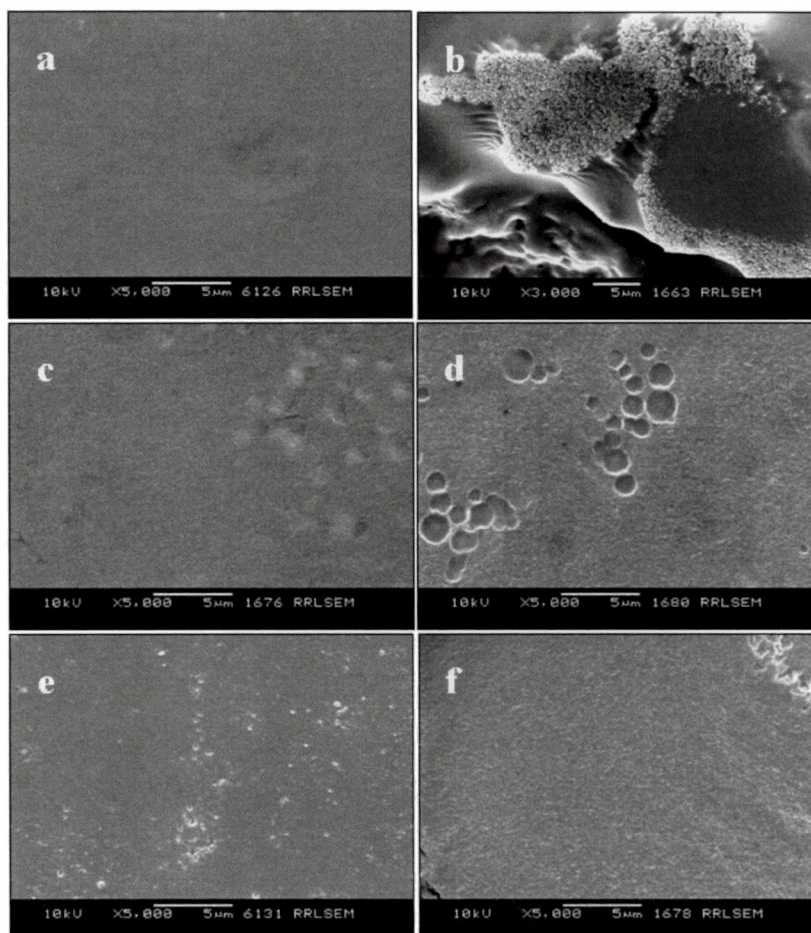
*Figure-3.7: SEM images in THF alone for **P-3** (a), **P-4** (c) and **P-5** (e) and in THF: water-85:15 for **P-3** (b), **P-4** (d) and **P-5** (f)*
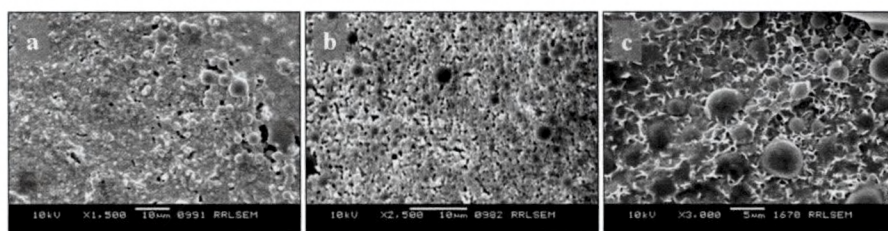

*Figure-3.8: SEM images at various concentrations of **P-2** for 90:10 v/v of THF: water - 50 mg (a), 35 mg (b) and 20 mg /mL (c)*

This is the first time that such diverse morphologies are observed for main chain polyurethanes under solvent evaporation process. From the above discussions it is clear that only certain polyurethanes have a remarkable tendency for the evolution of complex morphologies in presence of different solvent combinations in the microscopic scale.

3.3.5. Transmission Electron Microscopy (TEM) Analysis

The polymer samples were subjected to transmission electron microscopic (TEM) analysis since SEM has limitation that it can not distinguish a solid or hollow sphere (or hexagon). The TEM images of **P-1** and **P-2** were recorded for samples prepared from 95:5 and 85:15 v/v THF/water solvent combinations (1 wt % solution), respectively. The polymer films were prepared by drop casting the above solution on the top of Formvar coated copper grid at ambient conditions. The TEM images of **P-1** and **P-2** are shown in figure-3.9. The TEM image of **P-1** has supported the formation of perfect hexagons (as similar to their SEM images in figure-3.4b for same solvent combination) and they are filled solid species and there is no hollow domain. Though sharp edges could not be pictured for the hexagon, they were clearly visible through the microscope. In figure-3.9b, the polymer sample **P-2** has only solid spheres and no traces of hexagons are noticed (similar to the SEM in figure-3.6d). The diagonals of the hexagons in **P-1** are found in the range 60-80 nm and the diameters of the spheres in **P-2** exist from 200 nm to 1 μm.
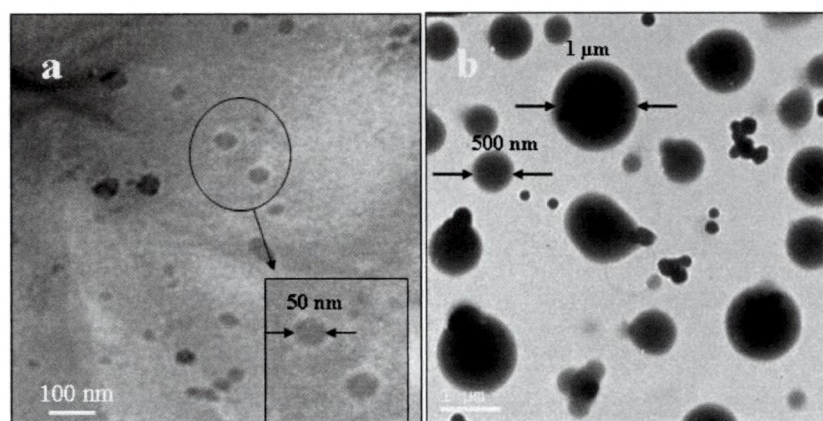

Figure-3.9:TEM images of P-1 in THF/water- 95:5 (a) and P-2 in THF/water-
85:15 (b)

In both the cases, the sizes of species are much smaller compared to that of their SEM-images. It may be due to the variation in the concentration of the polymer solution used for the sample preparation in the SEM and TEM. A similar trend has been normally been noticed in the area of polymeric nano- materials since both the microscopic techniques largely differed in the sample preparation.[57]There are reports in the solvent induced process that the patterns observed in SEM were difficult to reproduce by TEM mainly because of the large variation in the concentration of the polymer solution employed for both the techniques.[47, 58-59] Interestingly in the present investigation, though, there is a significant difference in the concentration of the polymer solution employed for SEM and TEM, the solvent induced self-organization of polyurethanes is very unique to their chemical structure and produce similar morphological pattern in both SEM and TEM techniques. Therefore, the self-organization of polyurethanes was dominated by their chemical structure and solvent combinations rather than their concentration in solution.

3.3.6. Mechanism for the Morphological Evolution

The possible mechanism for the formation of micro-pores, hexagons and spheres is given in figure-3.10. When a polymer is dissolved in a good solvent, the solvent molecules solvate the polymer chains and the chains expanded from coil to freely extended conformation (figure-3.10a). The pore formation in the polyurethane film is the result of phase separation of these polymer chains from the solution. During the slow evaporation, the polymer solution is thermodynamically unstable and undergoes phase separation to form polymer rich and polymer lean phases (figure-3.10b). The concentrated phase solidifies shortly after phase separation and forms the continuous matrix whereas the polymer lean solvent rich phase forms the pores (figure-3.10c). Unlike polyacrylics or polystyrene, the polyurethane chains have strong intra or inter-molecular hydrogen bonding interaction in the backbone and this strong secondary interaction dominate the entire phase separation process and diminish the three dimensional array of air (or solvent) bubbles formation for honey-comb patterns, as reported earlier.[29-32] In the present investigation no honey-comb pattern is observed and the solvent evaporation produces only straight through pores. Interestingly, the pores produced by the phase separation process are arranged into a hexagonal packing, however, they are not connected together (figure-3.10c).
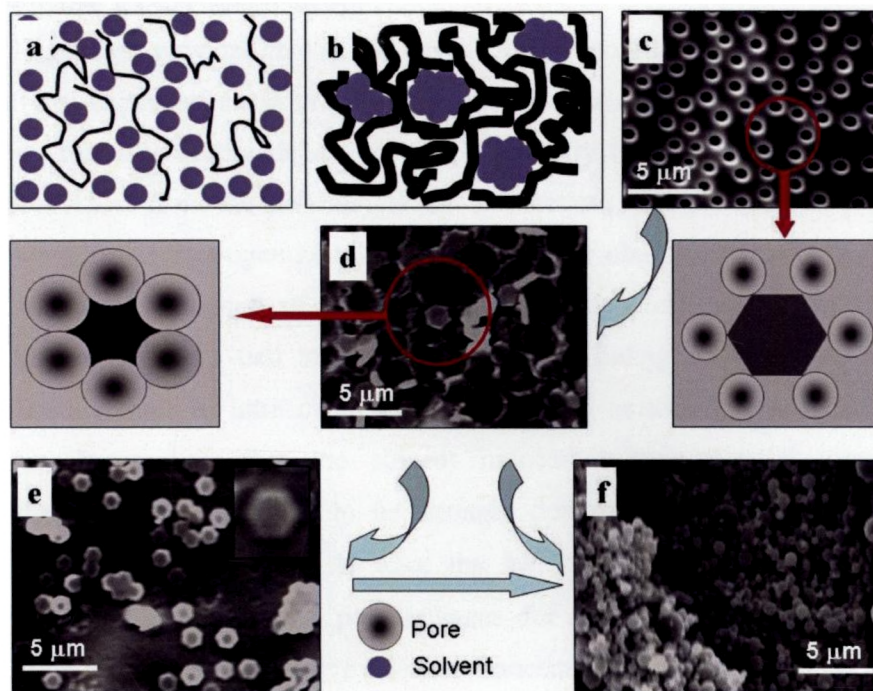
Figure-3.10: Plausible mechanism for the formation of micro-pores, polymeric hexagons and spheres in polyurethane through solvent induced self-organization

When trace amounts of water are present, the sizes of the pores (the solvent occupied domains in figure-3.10b) significantly increase from 1 to 3.4 µm, which brings the pores together to form connected hexagonal porous arrangements (figure-3.10d). It was recently reported that the increase in the water content in the solvent mixture increases the pore sizes in the honey-comb pattern for polyacrylics,[47] which supports the increase in the pore sizes in the present case as well. There are two pathways for the evaporation of packed hexagonal solvent pockets: (i) evaporate to isolate the solid matrix as a perfect hexagon (figure-3.10e) which is subsequently converted into a sphere at a much higher proportion of water or (ii) the formation of spheres directly from the porous materials (figure-3.10f). The current morphological trend in **P-1** and **P-2** (in figure-3.4, figure-3.6 and figure-3.10) and the sizes of the species (from SEM and TEM) support the first mechanism that the hexagons are converted to spheres. The present investigation has clearly demonstrated that the solvent induced process can be successfully utilized to self-organize polyurethane chains to form pores, hexagons and spheres of micron to nano-meter size.

3.3.7. Solution FT-IR Spectroscopy

In general, polymer chains adopt two kinds of conformations when dissolved in a solvent: expanded chain or coil-like conformation and the degree or extent of these two forms is highly dependent on the polarity (also nature) of the solvent molecules. Apart from the polymer-solvent interactions, the presence of secondary interaction such as hydrogen bonding in the polymer chain may also significantly influence the conformation of polymer chains. In main chain polyurethanes, the molecular sub-units are tied together by carbamate linkages (-HN-COO-), which induces strong inter or intra chain hydrogen bonded networks for its elastomeric behaviour. It suggests that the solvent induced self-organization process in polyurethanes is also expected to be strongly determined by hydrogen bonding. Therefore, it is very important to trace the factors which are influenced by the hydrogen bonding network in polyurethanes for better understanding the self-organization induced morphology evolution. Concentration dependant solution FT-IR and ^{1}H-NMR titration measurements are very important tools to gain more knowledge about the polymer segregation process during the slow evaporation of solvents. During solvent evaporation, the amount of solvent decreases which in-turn increase the concentration of polymer chains. Therefore the concentration dependent FT-IR and NMR experiments directly give evidence for the intra or inter molecular hydrogen bonding interaction in polyurethanes, which are chemically different and also differed largely in their morphological properties.

Polyurethanes **P-1** to **P-4** was subjected to solution FT-IR analysis. The expanded region of the N-H stretching vibration of FT-IR spectra of the polyurethanes for 2×10^{-2} M^{-1} in THF are shown in figure-3.11a. The two peaks at higher wave numbers (3572 and 3500 cm^{-1}) are corresponding to the free anti-symmetric and symmetric stretching vibrations of the N-H group in the urethane linkage, respectively.[60] The peak at lower wavenumber (3329 cm^{-1}) is corresponding to the hydrogen-bonded N-H stretching vibration. The hydrogen bonded peaks are more intense in **P-1** and **P-2** and they are almost absent in **P-3** and **P-4**. It confirmed that the fully cycloaliphatic polyurethanes (**P-1** and **P-2**) exist in a strong hydrogen bonded form in THF compared to the partially cycloaliphatic structures **P-3** and **P-4**. It further supports the mechanism proposed in figure-3.10 that the strong hydrogen bonded polyurethane undergoes phase separation process to form porous templates (as noticed

in **P-1** and **P-2**, figure-3.2) whereas the weakly bonded chains fail to produce any significant morphology (**P-3** and **P-4** in figure-3.2).
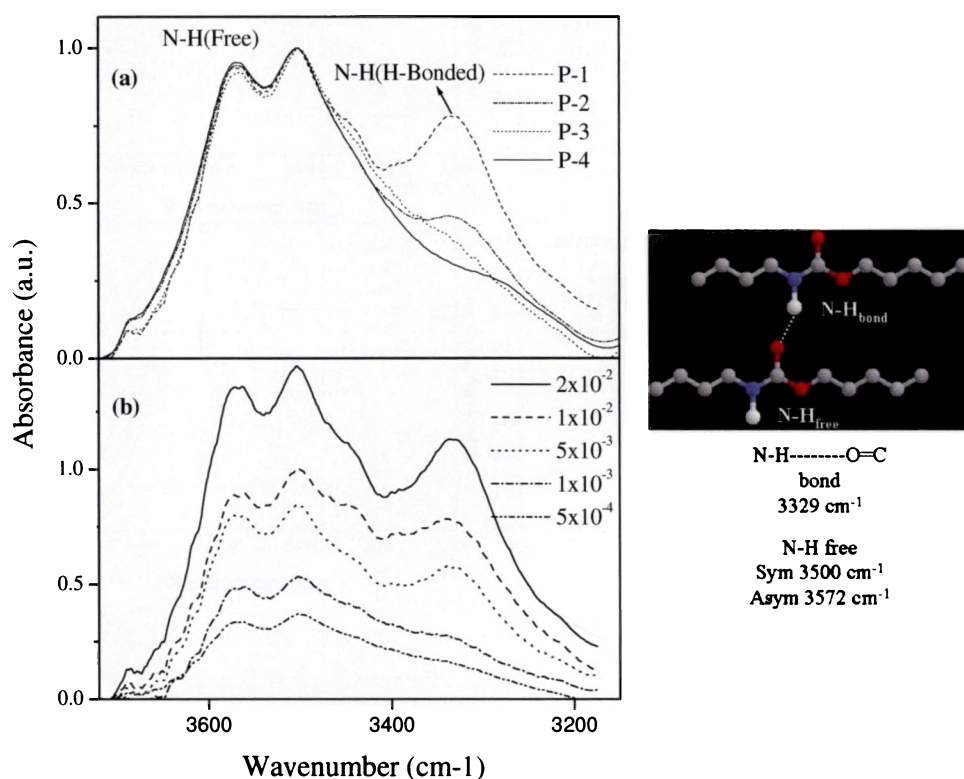

*Figure-3.11: Solution FT-IR spectra of Polymers **P-1** to **P-4** at $2x10^{-2}$ M^{-1} in THF (a) and concentration dependant FT-IR for **P-1** in THF (b) at 25 °C. Various FTIR stretching vibrations in the N-H region*

A concentration dependant FT-IR spectrum of **P-1** is shown in figure-3.11b. It is clear that at higher concentration (2×10^{-2} M^{-1}) there is a significant amount of hydrogen bonding corresponding to a shoulder at 3329 cm^{-1} but the intensity of this shoulder is found to decrease as the concentration keeps on decreasing below 5×10^{-3} M^{-1}. A similar observation is noticed for **P-2** to **P-4** (figure-3.12). A plot of the ratio of the intensity of the hydrogen bonded N-H band (I_{3329}) to that of the non-hydrogen bonded band (I_{3572}) as a function of concentration is also shown in figure-3.12.[60] As expected the intensity ratios increases with the increase in concentration due to the existence of strong hydrogen bonding at higher concentrations.
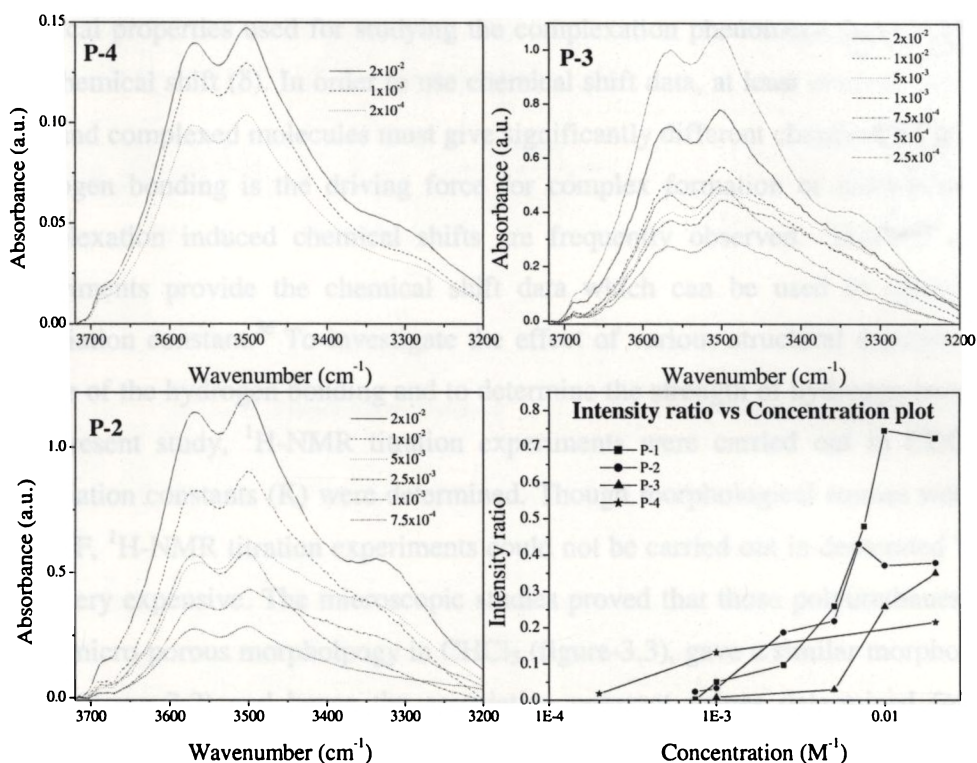
*Figure-3.12: Concentration dependent FTIR for **P-2**, **P-3** and **P-4** in THF at 25 °C and plot of intensity ratio of hydrogen bonded to free N-H in the FT-IR (I_{3329} / I_{3572}) versus the concentration for **P-1** to **P-4***

However, compared to **P-1** and **P-2,** there is a significant difference in the plots for the polyurethanes **P-3** and **P-4** since they have lowest intensity ratio for all concentrations. It confirms that the magnitude of hydrogen bonding is much lower in the partially cycloaliphatic **P-3** and **P-4** compared to that of the fully cycloaliphatic **P-1** and **P-2**. Hence solution FT-IR studies gives direct evidence for the difference in hydrogen bonding based on the difference in the chemical structure of the polyurethane backbones. In order to quantify the extent of hydrogen bonding other spectroscopic tools were used as follows.

3.3.8. Concentration Dependent ^{1}H-NMR Titration Studies

NMR spectroscopy is found to be one of the most useful techniques for investigating supramolecular processes. NMR technique gives the most precise details about the complexes formed through non-covalent secondary interactions. One of the
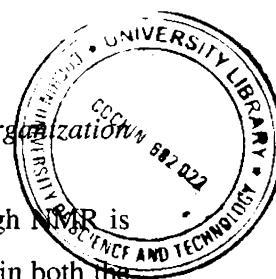
physical properties used for studying the complexation phenomena through NMR is the chemical shift (δ). In order to use chemical shift data, at least one site in both the free and complexed molecules must give significantly different chemical shifts. When hydrogen bonding is the driving force for complex formation or association, then complexation induced chemical shifts are frequently observed. ^{1}H-NMR titration experiments provide the chemical shift data which can be used to calculate the association constant.[56] To investigate the effect of various structural subunits on the nature of the hydrogen bonding and to determine the strength of hydrogen bonding in the present study, ^{1}H-NMR titration experiments were carried out in $CDCl_3$ and association constants (K) were determined. Though morphological studies were done in THF, ^{1}H-NMR titration experiments could not be carried out in deuterated THF as it is very expensive. The microscopic studies proved that those polyurethanes which gave micro-porous morpholpogy in $CHCl_3$ (figure-3.3), gave a similar morphology in THF (figure-3.2) and hence the association constant values determined from ^{1}H-NMR titration studies in $CDCl_3$ would be valid enough to compare the morphological differences in the present study. The best method known for the determination of association constants (K) based on the chemical shift values is Scatchard plot and the Scatchard equation for NMR titration experiment is written as

$$\Delta/[S] = -K\Delta + \Delta_0 K$$

where, $\Delta = \delta_{obs} - \delta_{free}$ and [S] is the concentration of the sample in M and K is the association constant in M^{-1}.[56] The main limitation in applying Scatchard equation for hydrogen bonding interactions in polymer solution is the difficulty in determining the δ_{free} value. For strong complexes ($K=10^4 - 10^8 M^{-1}$), the δ_{free} can be neglected since it is not very significant, whereas for weaker hydrogen bonding interactions ($K = 10$ to 10^3), the δ_{free} is very important.[61] In general, the difficulty in the identification of δ_{free} was the inherent limitation in the calculation of K-values for hydrogen bonding interactions in polymers such as polyamides, polyurethanes and polyureas. In the present investigation the determination of δ_{free} was aided by synthesizing few model compounds whose structure exactly represents the subunits of the polymer chain. Two model compounds (M-1 and M-2) were synthesized by the reaction between isophorone diisocyanate and monoalcohol (TCD-M or Dec) in 1:2 mole ratio. The reaction was performed in toluene in presence of DBTDL as catalyst under nitrogen

atmosphere as shown in scheme-3.6. The structure of the model compounds were confirmed by NMR, FT-IR and FAB-HRMS analysis.
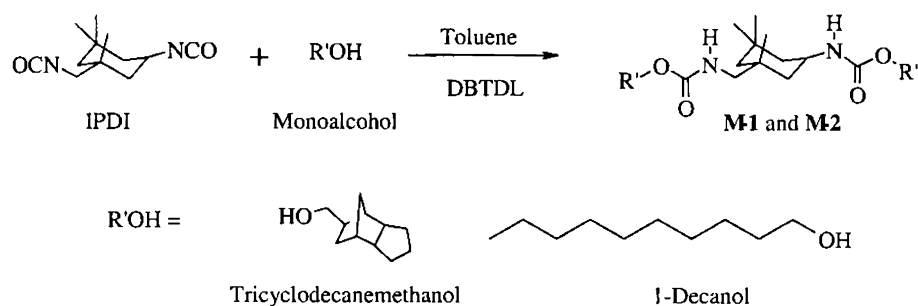
*Scheme-3.6: Synthesis of model compounds **M-1** and **M-2** using isocyanate route*

The model compound **M-3** was obtained by the reaction between DHMD and TCD-M by utilizing the melt transurethane reaction as given in chapter-2. The model compounds **M-1** and **M-2** were synthesized for the purpose of calculating the association constants alone and hence the melt transurethane route was not employed in these two cases. The structure of the model compounds is shown in scheme-3.7.
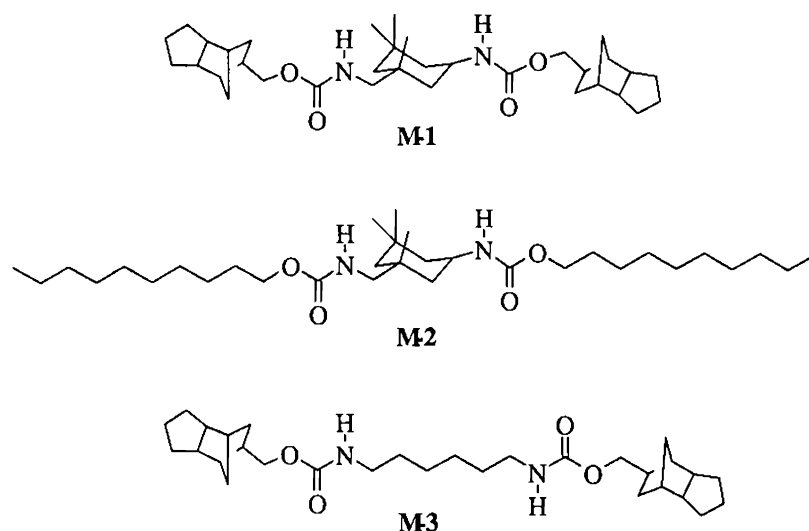
Scheme-3.7: Structure of the Model compounds

The ¹H-NMR titration spectra of few polyurethanes (**P-2** and **P-5**) and their corresponding model compounds (**M-1** and **M-3**) at various concentrations are shown in figure-3.13.
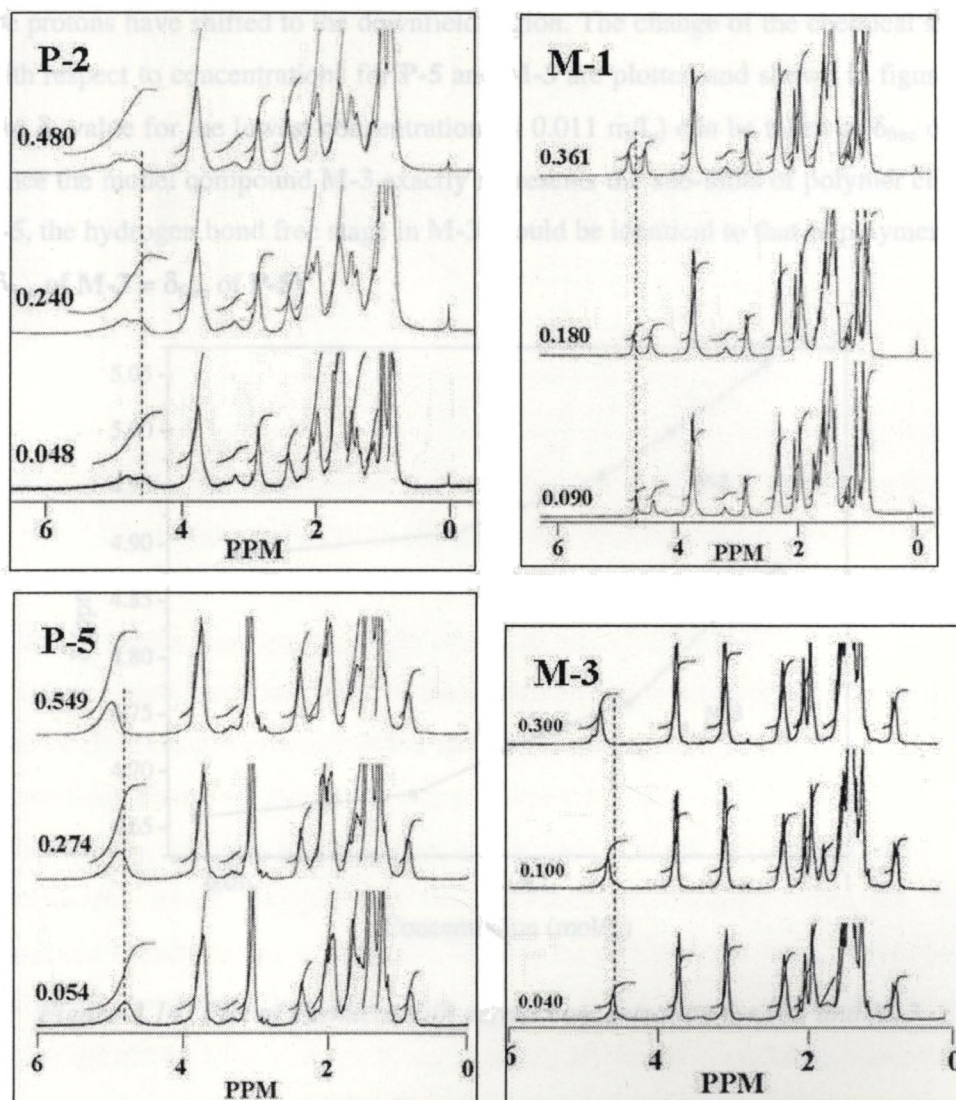
*Figure-3.13: ^1H-NMR titration spectra of **P-2**, **P-5**, **M-1** and **M-3** at various concentrations*

The minimum concentration required for the NMR titration is 2 mg in 0.5 mL of $CDCl_3$ (~ 0.01 m/L). The maximum concentration of the compounds was taken as 125 mg/ in 0.5 mL (~ 0.5 m/L) and higher concentrations could not be tried because of the limited solubility. It is very clear from the figure-3.13 that with the increase in concentration, there is a significant shift in the N-H proton towards the downfield region due to the strong inter or intra chain hydrogen bonding where as all the other ^1H-NMR signals remained intact. In the case of **P-2** and **M-1** (isophorone systems) which contains both primary and secondary urethane linkages, the -NH peak for both

the protons have shifted to the downfield region. The change of the chemical shift (δ) with respect to concentrations for **P-5** and **M-3** are plotted and shown in figure-3.14. The δ- value for the lowest concentration (at 0.011 m/L) can be taken as δ_{free} of **M-3**. Since the model compound **M-3** exactly represents the sub-units of polymer chains in **P-5**, the hydrogen bond free stage in **M-3** should be identical to that of polymer in **P-5** (δ_{free} of **M-3** = δ_{free} of **P-5**).
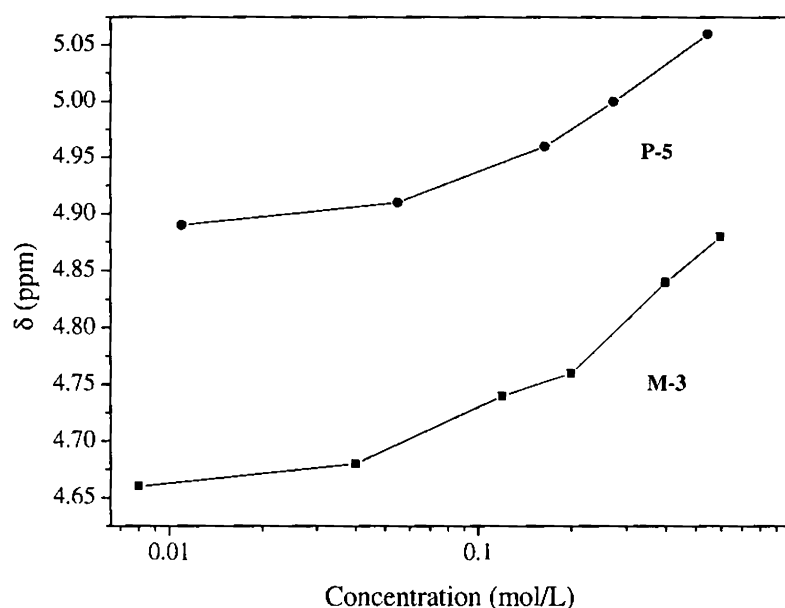

Figure-3.14: Plot of chemical shift versus concentration for P-5 and M-3

In the present investigation for determining the association constant (K) for **P-5**, the δ-value for the free stage of **M-3** is used (δ_{free} at 0.008 m/L). Similarly the δ_{free} value for all other polymers was taken as the δ-value for the free stage of the corresponding structurally similar model compound at the minimum concentration. For **P-1**, δ_{free} value was taken as the corresponding δ-value from structurally similar **M-1** (fully cycloaliphatic). The association constant for the polymers and the model compounds were determined from the slope of the Scatchard plots (Δ/[S] vs Δ). The Scatchard plots for the polyurethanes are shown in figure-3.15 and the values for the association constants for the polymers are model compounds are summarised in table-3.1. In the case of isophorone based polymers and model compounds, both types of N-H protons are shifted and the K-values were calculated for primary urethane linkage.
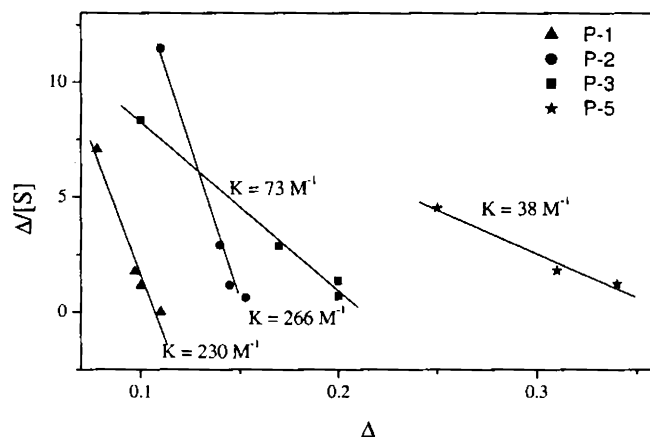
*Figure-3.15: Scatchard plot for polymers **P-1** to **P-3** and **P-5**. The H-bonding association constants (K) are determined from the slopes*

From the values it is clear that fully cycloaliphatic polyurethanes (**P-1** and **P-2**) have K-values almost three times higher than their partially cycloaliphatic counterparts (**P-3** and **P-5**). This also proves that **P-1** and **P-2** are engaged in strong hydrogen bonding interactions in the solution state when compared to **P-3** and **P-5**. The K-values of polyurethanes are 100 to 200 times higher than that of the corresponding model compounds, which suggest that the polymers are strongly hydrogen bonded, compared to their model compounds. Though the difference in the K-values between the model compounds is not so large, there is still a clear distinction, as the fully cycloaliphatic **M-1** has a higher K-value among all the three model compounds which correlated very well to the higher K-value for its corresponding polyurethane.

Table-3.1: ^{1}H-NMR titration experimental data of polyurethanes and model compounds

Sample	Concentration	$\Delta\delta^a$	Association Constant (K)^b
P-1	0.011-0.55	0.22	230
P-2	0.010-0.48	0.17	266
P-3	0.012-0.59	0.13	73
P-5	0.011-0.55	0.20	38
M-1	0.007-0.36	0.12	2.4
M-2	0.011-0.53	0.11	1.2
M-3	0.008-0.40	0.22	0.70

a. (Δ for maximum concentration)-(Δ for minimum concentration)
b. Obtained from the slope of the Scatchard plot.

On comparing the T_g values of the polyurethanes it is clear that the T_g of **P-1** and **P-2** (91 and 118 °C, respectively) are much higher than the other three polymers (**P-3**, **P-4** and **P-5**: 78, 27 and 59 °C, respectively) which gives direct evidence for the existence of strong hydrogen bonding in **P-1** and **P-2** compared to **P-3** to **P-5**. The hydrogen bonding association constants (K) also match well with their T_g: higher K-values corresponds to high T_g polymers. Hence the T_g trend as well as the K-value trend for the polyurethanes are in the order **P-2** > **P-1** > **P-3** > **P-5**. This clearly indicates that fully cycloaliphatic polyurethanes have high rigidity and hence greater hydrogen bonding as revealed by their T_g and K-values. On replacing one of the cycloaliphatic units with a linear aliphatic chain the hydrogen bonding is weakened. In general, cycloaliphatic structures are expected to disturb the close packing of polymer chains due to the conformational strain in the cyclohexyl ring. However, the opposite trend is observed in the T_g's and K-values (more linear polymer **P-3** and **P-5** has low values). It suggests that the cycloaliphatic polyurethanes have strong hydrogen bonding interactions which overcome the conformational strain to produce higher T_g compared to their linear counterparts.

Hence FT-IR along with ^{1}H-NMR titration experiments coupled with the T_g data proved that polyurethanes **P-1** and **P-2** are involved in strong hydrogen bonding interactions in the solution state and these inter-chain interactions induce strong phase separation in the polyurethane chains, which leads to the formation of porous membrane morphology. The porous structures behave as a seed for growing higher ordered polymeric hexagons and spheres. The partially cycloaliphatic structures have weak hydrogen bonding ability and fail to produce any significant morphology during the solvent evaporation.

3.3.9. Energy Minimised AM1 Calculations

One of the ways to directly confirm the chain packing ability of these different polyurethanes is studying the single crystal packing of structurally similar model compounds. Though structurally similar model compounds were prepared, the cyclic compounds were found sluggish to crystalline and failed to grow good crystals. Therefore, to understand the polymer chain orientation, the repeating unit structures of few of the polymers (**P-1** to **P-3**) were energy minimized by AM1 calculations and the theoretical structure of the units are shown in figure-3.16.
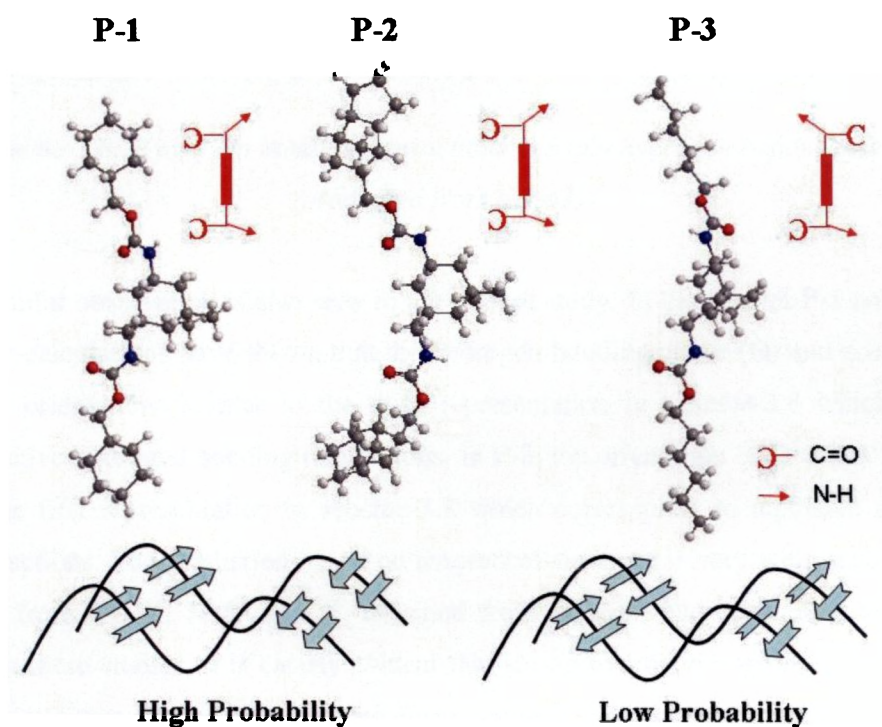
Figure-3.16: AM1 Energy minimized structures of polyurethane repeating units and the representation of hydrogen bonding in the two different systems

The C=O and N-H bonds present in the carbamate units are depicted using 'C' and '→', which indicate the hydrogen bond acceptor and donor groups. From the structures, it is clear that the two adjacent carbamate linkage in **P-1** and **P-2** have same side orientation of hydrogen bonding vectors whereas they were opposite in **P-3**. During the solvent evaporation process, the polymer chains comes together to form strong hydrogen bonding, and therefore, the donor and acceptor orientation in the polymer chain significantly influence the extent of the hydrogen bonding. From the AM1 structures, it is clear that the same side orientation in **P-1** and **P-2** gives more probabilities for the polymer chains to involve in greater magnitudes of hydrogen bonding compared to that of the opposite alignment of C=O and N-H groups as in **P-3**. Jorgenson and coworkers have studied the association of linear arrays of three hydrogen bonding sites (scheme-3.8) and they suggested that diagonally opposed sites repel each other electrostatically when they are of the same kind where as dissimilar sites attract each other.[62]

D ········· A   D ········· A   A ········· D   ✎ = attractive secondary interaction
A ↗ ↘ D   A ↗ ↘ D   A ↗ ↘ D   ✎ = repulsive secondary interaction
D ········· A   A ········· D   A ········· D   D = donor A = acceptor

Scheme-3.8: Hydrogen bonding interactions in triply hydrogen bonded systems

(adapted from ref. 62)

A similar observation is also seen in the present study. In the case of **P-1** and **P-2** the AM1 calculations have shown that the hydrogen bonding donor (D) and acceptor (A) have orientations similar to the third representation in scheme-3.8 which favours attractive hydrogen bonding interactions. In **P-3**, the orientation of D and A is similar to the first representation in scheme-3.8 which corresponds to repulsive secondary interactions. The prediction based on theoretical structure is very well matching with data from FT-IR, NMR and T_g obtained from solution and solid state techniques. From these studies, it is clearly evident that strong hydrogen bonding interactions in polyurethanes are the main driving force for their selective self-organization, which leads to various morphologies such as pores, polymeric hexagons and spheres during the slow evaporation process. The chemical structure of the polyurethane backbone is a very crucial factor for better self-organization in solvent and in the present case fully cycloaliphatic rings favours the morphology development.

3.4. Conclusion

The present investigation has successfully demonstrated that the chemical structure of the polymer, more particularly; the polyurethanes play a major role in the formation of micro and nano meter size pores, hexagon and spheres. The approach demonstrated here have many unique features and advantages: (i) fully and partially cycloaliphatic polyurethanes were subjected to solvent induced self-organization under atmospheric conditions for the formation of polymeric hexagons and spheres, (ii) the chemical structure of the polyurethane backbone plays a major role in the self-organization process and only fully cycloaliphatic structures produced micro-porous templates, which further seeds for higher ordered hexagons and spheres in large amount of water content in the solvent mixture, (iii) by controlling the concentration of polymer samples and THF/water ratio in the solvent mixture, the size and shape of the polymeric architectures could be precisely controlled from micron to nano-meter level, (iv) concentration dependant solution FT-IR studies revealed that fully cycloaliphatic rings have strong hydrogen bonding interactions compared to their partially cyclic counterparts, which is the main driving force for the phase separation process for producing various morphologies, (v) hydrogen bonding association constant (K) determined by the ^{1}H-NMR studies revealed that fully cycloaliphatic structures have three times stronger hydrogen bonding compared to partially cyclic systems and supports the solvent induced self-organization mechanism, (vi) T_g data supported the strong hydrogen bonding in fully cycloaliphatic structures and correlates the self-organization process for morphological evolution, (vii) AM1 calculation for the polymeric repeating units helped in elucidating the orientation of hydrogen bonding vectors and its influence on the self-organization. The micro-porous templates, polymeric micro or nano-hexagons and spheres can be utilized as support for nano-materials synthesis in opto-electronic devices or vehicles for drug delivery. Hence, solvent induced self organization process was utilized for the first time to make various morphologies of polyurethanes such as micro-porous templates, polymeric hexagons of single, 2, 3,...12 fused structures and spheres and the hydrogen bonding interactions were analyzed by various analytical techniques for understanding the mechanistic aspects.

3.5. References

1. Lee, M.; Cho, B-K.; Zin, W-C. *Chem. Rev.* **2001**, *101*, 3869.

2. Govor, L. V.; Bashmakov, I. A.; Kiebooms, R.; Dyakonov, V.; Parisi, J. *Adv. Mater.* **2001**, *13*, 588.

3. Bolognesi, A.; Mercogliano, C.; Yunus, S.; Civardi, M.; Comoretto, D.; Turturro, A. *Langmuir* **2005**, *21*, 3480.

4. Ruotsalainen, T.; Turku, J.; Heikkila, P.; Ruokolainen, J.; Nykanen, A.; Laitinen, T.; Torkkeli, M.; Serimaa, R.; Brinke, G. T.; Harlin, A.; Ikkala, O. *Adv. Mater.* **2005**, *17*, 1048.

5. Li, Z.; Zhao, W.; Liu, Y.; Rafailovich, M. H.; Sokolov, J.; Khougaz, K.; Eisenberg, A.; Lennox, R. B.; Krausch, G. *J. Am. Chem. Soc.* **1996**, *118*, 10892.

6. Zubarev, E. R.; Pralle, M. U.; Sone, E. D.; Stupp, S. I. *J. Am. Chem. Soc.* **2001**, *123*, 4105.

7. (a) Kato, T.; Mizoshita, N.; Kishimoto, K. *Angew. Chem. Int. Ed.* **2006**, *45*, 38. (b) Kato, T.; Mizoshita, N.; Kanie, K. *Macromol. Rapid Commun.* **2001**, *22*, 797.

8. Brunsveld. L.; Folmer, B. J. B.; Meijer, E. W.; Sijbesma, R. P. *Chem. Rev.* **2001**, *101*, 4071.

9. Kato, T.; Frechet, J. M. J. *Macromolecules* **1989**, 22, 3818.

10. Porrata, P.; Goun, E.; Matsui, H. *Chem. Mater.* **2002**, *14*, 4378.

11. Martin, C. R. *Chem. Mater.* **1996**, *8*, 1739.

12. Parthasarathy, R. V.; Martin, C. R. *Chem. Mater.* **1994**, *6*, 1627.

13. Slomkowski, S.; Basinska, T.; Miksa, B. *Polym. Adv. Technol.* **2002**, *13*, 906.

14. Hoa, M. L. K.; Lu, M.; Zhang, Y. *Adv. Colloid Interface Sci.* **2006**, *121*, 9.

15. Batra, D.; Vogt, S.; Laible, P. D.; Firestone, M. A. *Langmuir* **2005**, *21*, 10301.

16. Ma, Z.; Guan, Y.; Liu, X.; Liu, H. *Polym. Adv. Technol.* **2005**, *16*, 554.

17. Bognitzki, M.; Czado, W.; Frese, T.; Schaper, A.; Hellweg, M.; Steinhart, M.; Greiner, A. Wendorff, J. H. *Adv. Mater.* **2001**, *13*, 70.

18. Bognitzki, M.; Frese, T.; Steinhart, M.; Greiner, A.; Wendorff, J. H.; Schaper, A.; Hellweg, M. *Polym. Eng. Sci.* **2001**, *41*, 982.

19. Megelski, S.; Stephens, J. S.; Chase, D. B.; Rabolt, J. F. *Macromolecules* **2002**, *35*, 8456.

20. Matsuyama H.; Yano, H.; Maki, T.; Teramoto, M.; Mishima, K.; Matsuyama, K. *J. Membr. Sci.* **2001**, *194*, 157.

21. Chandavasu, C.; Xanthos, M.; Sirkar, K. K.; Gogos C. G. *J. Membr. Sci.* **2003**, *211*, 167.

22. a) Cui, L.; Han, Y. *Langmuir* **2005**, *21*, 11085. b) Meier-Haack, J.; Valko, M.; Lunkwitz, K.; Bleha, M. *Desalination* **2004**, *163*, 215.

23. Maekawa, H.; Esquena, J.; Bishop, S.; Solans, C.; Chmelka, B. F. *Adv. Mater.* **2003**, *15*, 591.

24. Cheng, L. P.; Young, T. H.; Fang, L.; Gau, J. J. *Polymer* **1999**, *40*, 2395.

25. Yang, Q.; Xu, Z. K.; Dai, Z. W.; Wang, J. L.; Ulbricht, M. *Chem. Mater.* **2005**, *17*, 3050.

26. Kou, R. Q.; Xu, Z. K.; Deng, H. T.; Liu, Z. M.; Seta, P.; Xu, Y. *Langmuir* **2003**, *19*, 6869.

27. Liu, X.; Neoh K. G.; Kang, E. T. *Macromolecules* **2003**, *36*, 8361.

28. (a) Tzanetos, N. P.; Dracopoulos, V.; Kallitsis, J. K.; Deimede, V. A. *Langmuir* **2005**, *21*, 9339. (b) Lin, C-L.; Tung, P-H.; Chang, F-C. *Polymer* **2005**, *46*, 9304.

29. Jenekhe, S. A.; Chen, X. L. *Science* **1999**, *283*, 372.

30. Widawski, G.; Rawiso, M.; Francois, B. *Nature* **1994**, *369*, 387.

31. Srinivasarao, M.; Collings, D.; Philips, A.; Patel, S. *Science* **2001**, *292*, 79.

32. Chen, D.; Jiang, M. *Acc. Chem. Res.* **2005**, *38*, 494.

33. Park, M. S.; Kim, J. K. *Langmuir* **2004**, *20*, 5347.

34. Kuang, M.; Duan, H.; Wang, J.; Jiang, M. *J. Phys. Chem. B* **2004**, *108*, 16023.

35. Lee, M.; Cho, B-K.; Ihn, K. J.; Lee, W-K.; Oh, N-K.; Zin, W-C. *J. Am. Chem. Soc.* **2001**, *123*, 4647.

36. de Boer, B.; Stalmach, U.; Nijland, H.; Hadziioannou, G. *Adv. Mater.* **2000**, *12*, 1581.

37. a) Duan, H.; Kuang, M.; Wang, J.; Chen, D.; Jiang, M. *J. Phys. Chem. B* **2004**, *108*, 550. b) Nishikawa, T.; Ookura, R.; Nishida, J.; Sawadaishi, T.; Shimomura, M. *RIKEN Review* **2001**, *37*, 43. c) Hayakawa, T.; Horiuchi, S. *Angew. Chem. Int. Ed.* **2003**, *42*, 2285.

38. Cheng, C. X.; Tian, Y.; Shi, Y. Q.; Tang, R. P.; Xi, F. *Langmuir* **2005**, *21*, 6576.

39. a) Yin, Y.; Li, Z-Y.; Xia, Y. *Langmuir* **2003**, *19*, 622. b) Park, S. H.; Xia, Y. *Chem. Mater.* **1998**, *10*, 1745.

40. a) Bormashenko, E.; Pogreb, R.; Musin, A.; Stanevsky, O.; Bormashenko, Y.; Whyman, G.; Barkay, Z. J. *Colloid and Interface Sci.* **2006**, *300*, 293. b) Bormashenko, E.; Pogreb, R.; Stanevsky, O.; Bormashenko, Y.; Tamir, S.; Cohen, R.; Nunberg, M.; Gaisin, V-Z.; Gorelik, M.; Gendelman, O. V. *Mater. Lett.* **2005**, *59*, 2461.

41. a) Cui, L.; Xuan, Y.; Li, X.; Ding, Y. ; Li, B. ; Han, Y. *Langmuir* **2005**, *21*, 11696. b) Song, J-S.; Winnik, M. A. *Macromolecules* **2006**, *39*, 8318.

42. Karthaus, O.; Maruyama, N.; Cieren, X.; Shimomura, M.; Hasegawa, H.; Hashimoto, T. *Langmuir* **2000**, *16*, 6071.

43. Wang, Y.; Liu, Z.; Huang, Y.; Han, B.; Yang, G. *Langmuir* **2006**, *22*, 1928.

44. a) Sivakumar, M.; Rao, K. P. *J. Appl. Polym. Sci.* **2002**, *83*, 3045. b) Ni, H.; Kawaguchi, H. *J. Polym. Sci. Part A: Polym. Chem.* **2004**, *42*, 2833. c) Dong, A.; An, Y.; Feng, S.; Sun, D. J .*Colloid Interface Sci.* **1999**, *214*, 118.

45. (a) Park, M. S.; Kim, J. K. *Langmuir* **2005**, *21*, 11404. (b) Park, M. S.; Joo, W.; Kim, J. K. *Langmuir* **2006**, *22*, 4594.

46. Stenzel-Rosenbaum, M. H.; Davis, T. P.; Fane, A. G.; Chen, V. *Angew. Chem. Int. Ed.* **2001**, *40*, 3428.

47. Deepak, V. D.; Asha, S. K. *J. Phys. Chem. B* **2006**, *110*, 21450.

48. Park, S. H.; Xia, Y. *Adv. Mater.* **1998**, *10*, 1045.

49. Hirose, M.; Zhou, J.; Kadowaki, F. *Colloids Surf. A* **1999**, *153*, 481.

50. Dong, A.; An, Y.; Feng, S.; Sun, D. J. *Colloid Interface Sci.* **1999**, *214*, 118.

51. Chen, S.; Tian, Y.; Chen, L.; Hu, T. *Chem. Mater.* **2006**, *18*, 2159.

52. Thandavamoorthy, S.; Gopinath, N.; Ramkumar, S. S. *J. Appl. Polym. Sci.* **2006**, *101*, 3121.

53. Frere, Y.; Danicher, L.; Gramain, P. *Eur. Polym. J.* **1998**, *34*, 193.

54. Wang, J.; Cormack, P. A. G.; Sherrington, D. C.; Khoshdel, E. *Angew. Chem. Int. Ed.* **2003**, *42*, 5336.

55. Jabbari, E.; Khakpour, M. *Biomaterials* **2000**, *21*, 2073.

56. Tsukube, H.; Furuta, H.; Odani, A.; Takeda, Y.; Inoue, Y.; Liu, Y.; Sakamoto, H.; Kimura, K. *Comprehensive Supramolecular Chemistry*, Vol. 8; Davis, J. E. D.; Ripemeester, J. A., Eds.; Pergamon: Oxford, **1996**.

57. Anilkumar, P.; Jayakannan, M. *Langmuir* **2006**, *22*, 5952.

58. Wang, M.; Zhang, G.; Chen, D.; Jiang, M.; Liu, S. *Macromolecules* **2001**, *34*, 7172.

59. Ding, J.; Liu, G. *Chem. Mater.* **1998**, *10*, 537.

60. Syamakumari, A.; Schenning, A. P. H. J.; Meijer, E. W. *Chem. Eur. J.* **2002**, *8*, 3353.

61. Jayakannan, M.; Ramakrishnan, S. *J. Polym Sci. Part A: Polym Chem.* **2000**, *38*, 2625.

62. (a) Jorgenson, W. L.; Pranata, J. *J. Am. Chem. Soc.* **1990**, *112*, 2008. (b) Pranata, J.; Wierschke, S. G.; Jorgenson, W. L. *J. Am. Chem. Soc.* **1991**, *113*, 2810.

Chapter-4

Polyurethane-Oligophenylenevinylene Random Block Copolymers: Morphology and Photophysical Properties

4.1. Introduction

Polymeric assembled materials with well-defined structure on sub-micrometer and nanometer scales have fascinated researchers due to their broad potential applications in micro-and nanotechnology.[1-6] Supramolecular architectures have been assembled by non-covalent secondary interactions of appropriate tectons through hydrogen bonding,[5,7-9] electrostatic,[10-11] aromatic π-π stacking,[12-13] metal-ligand,[14-15] van der Waals forces[16] and charge transfer interactions,[17]etc. Wurthner et al. have developed mesoscopic superstructures by complexing perylene bisimide derivatives with a ditopic melamine unit. In these structures, multiple orthogonal intermolecular interactions such as hydrogen bonding, π-π stacking and vander Waals interaction along with solvent polarity play major roles in obtaining cylindrical strands (scheme-4.1).[18]
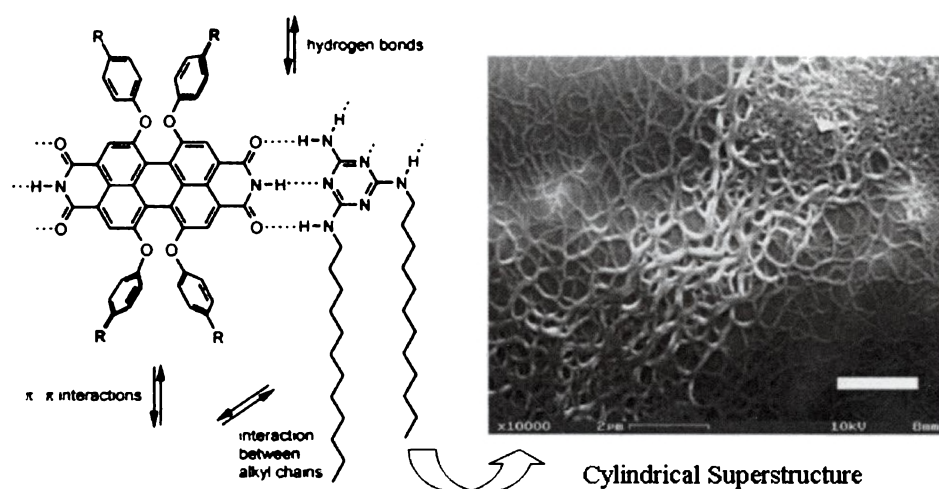
Scheme-4.1: Self-organization in complexes of perylene bisimide with melamine units (adapted from ref. 18)

Among these secondary interactions a great deal of effort has been made to self-organize molecules using π-stacking for use in molecular electronics such as field effect transistors, light emitting diodes and photovoltaic cells, etc.[19] Mesoscopic ordering in π conjugated systems for their successful use in such devices depends greatly on their supramolecular organization brought about by controlling their chemical structure or by various processing methodologies.[20] Recently, solvent induced self-organization of polymeric chains in the molecular level has been

explored to produce a variety of supramolecular architectures such as honeycomb patterns,[21]micelles[22] and vesicles[23]. Xie et al. have recently reported on the formation of mixed polymeric micellar clusters through the hydrogen bonding interaction between the PAA blocks in a PS-b-PAA (polystyrene-b-poly(acrylic acid)) copolymer with the PEO blocks in a PS-B-PEO (polystyrene-b-poly(ethylene oxide)) copolymer.[22] Bang and coworkers studied the aggregation of asymmetric poly(styrene-b-isoprene) in organic solvent such as dialkyl phthalates in various combinations. They observed the formation of spheres, cylinders or vesicles depending upon the solvent combinations employed, suggesting the importance of solvent towards the formation of various self-organized structures (scheme-4.2).[23]
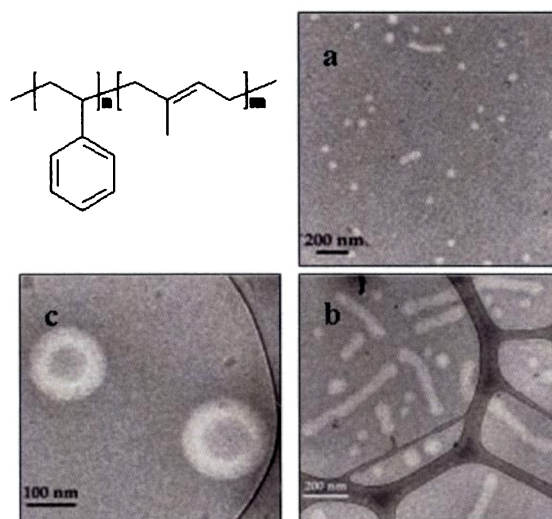
Scheme-4.2: Cryo-TEM images of poly(styrene-b-isoprene) showing varied morphologies such as spheres(a), cylinders (b) and vesicles (c) in different combinations of dialkyl phthalates as solvent (adapted from ref. 23)

Various types of polymeric architectures such as star polymers,[24] and block copolymers of amphiphilic, [25] rod-coil diblock [26-30] and triblock [31-32] and dendronized block copolymers, [33] polyacrylates,[34] and cellulose acetate butyrate,[35] etc. have been reported for forming regular micron to nano-sized patterns in films. Among them polystyrene-conducting block copolymers showing high degree of ordering and strong periodicity have been studied because of their applications in various opto-electronic devices. de Boer et al. synthesized a rod-coil copolymer consisting of poly(2,5-dioctyloxy-p-phenylenevinylene) as the rod block and polystyrene as the coil. The

films of these polymers prepared from carbon disulfide were found to exhibit uniform honey-comb morphology as shown in scheme-4.3.[36]
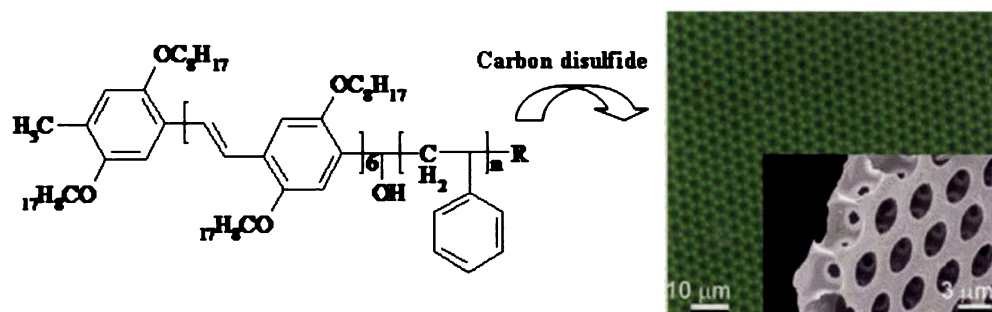
Scheme-4.3: Formation of honey-comb morphology in a rod-coil copolymer (adapted from ref. 36)

Another attempt was made by Jenekhe et al. for the self-organization of rod-coil copolymer consisting of polystyrene coil block and poly(phenylquinoline) rod block in carbon disulfide. They observed discrete micellar aggregates in the form of soft hollow spheres as shown in scheme-4.4 (a and b). With the increase in concentration of the polymer solution stacks of one to eight layers of hexagonally close packed two dimensional lattices of spherical air holes in a polymeric matrix was observed (scheme-4.4c).[27]
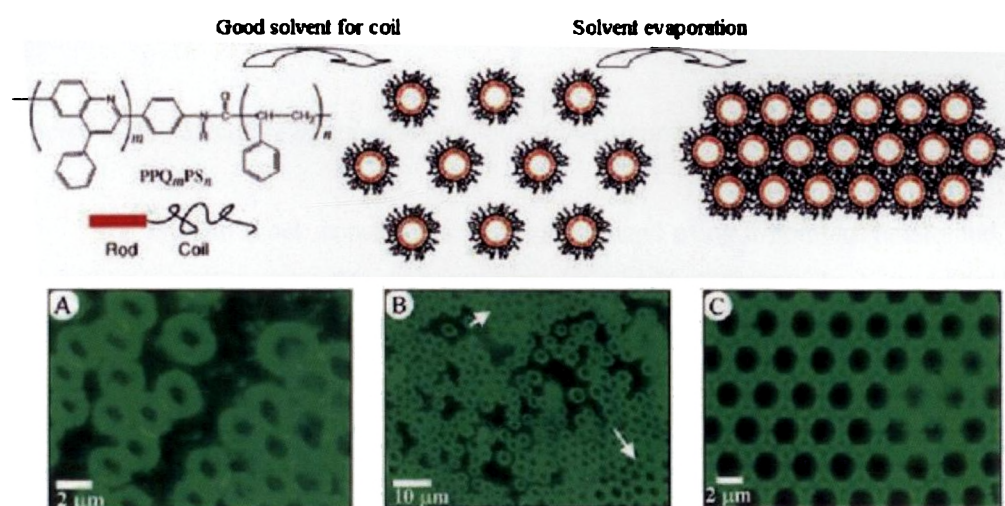
Scheme-4.4: Self-organization of PPQ_mPS_n block copolymers in CS_2 at concentrations such as 0.005 wt % (a), 0.01 wt % (b) and 0.5 wt % (c) (adapted from ref. 27)

Polyurethanes belong to the class of engineering thermoplastics bearing elastomeric properties due to the presence of reversible hydrogen bonds via hard-soft block self assembly. Recently, polymers containing π-conjugated oligomer: oligo-phenylenevinylene (OPV) with carbamate (urethane) linkages have been synthesized to study the performance of these polymers for opto-electronic devices, mechanochromic properties and as light emitting electrochemical cells, etc.[37-40] However, there are no reports in the literature to utilize the potential of reversible hydrogen bonding in polyurethane (or polyurea) to induce various types of morphological evolution in π-conjugated polymers.

This chapter aims at synthesizing a new series of polyurethane-oligo (phenylenevinylene) random block copolymers and to utilize these copolymers to study the morphological evolution via solvent induced self-organization process in a π-conjugated backbone. The random block copolymer (scheme-4.5) has two types of secondary interaction modes namely hydrogen bonding (via hydrophilic urethane linkage) and π-stacking (via hydrophobic aromatic OPV units), and therefore, it opens up a new opportunity to trace the solvent induced self-organization by both microscopic and various spectroscopic tools.
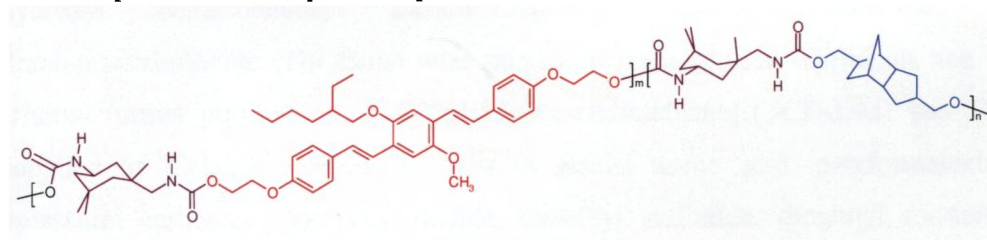
Scheme-4.5: Structure of polyurethane-oligo(phenylenevinylene) block copolymer

The random block copolymers were synthesized using a non-isocyanate and solvent free melt transurethane process as described in chapter-2. A hydroxyl terminated oligo(phenylenevinylene) (OPV) was synthesized and polycondensed with isophorone diurethane monomer (DIPD) and 1,8-tricyclodecanedimethanol (TCD-DM) under melt transurethane process to prepare the random copolymers. The amount of OPV was varied up to 50 mol % in the feed to incorporate various amounts of π-conjugated segments in the chain backbone. The selection of isophorone-ring and TCD-DM was based on the results in chapter-3 as these fully cycloaliphatic polyurethanes were novel in their structure and they demonstrated excellence in terms

of solubility, thermal stability and tendency for good morphology. The structures of the polymers were confirmed by NMR, FT-IR and the molecular weights were determined by GPC. The polyurethane-OPV block copolymers were found to produce variety of morphologies ranging from micron to nano-meter range porous membranes, hexagons, spheres (also luminescent nano-spheres) and vesicles depending upon the chemical structure of the polymer chain backbone or the nature of the solvent employed for the self-organization processes. The different types of morphologies were analyzed by techniques such as SEM, TEM and fluorescence microscopy. The role of hydrogen bonding and π-π stacking secondary interaction on the morphological evolutions were analyzed by solution FT-IR spectroscopy, absorption, emission, excitation and time resolved fluorescence decay techniques in both solution as well as solid state.

4.2. Experimental Methods

4.2.1. Materials: 4-Methoxyphenol, 2-ethylhexylbromide, triethylphosphite, 4-hydroxy benzaldehyde, 2-chloroethanol, potassium-*tert*-butoxide, and titaniumtetrabutoxide (Ti(OBu)$_4$) were purchased from Aldrich Chemicals and used without further purification. 1, 8-Tricyclodecanedimethanol (TCD-DM) was kindly supplied by Celanese Chemicals. HBr in glacial acetic acid, paraformaldehyde, potassium carbonate, potassium iodide, dimethyl sulfoxide, dimethyl formamide, tetrahydrofuran (THF) and all other solvents were purchased locally and purified using standard procedures.

4.2.2. Measurements: ^{1}H, ^{13}C-NMR and FT-IR spectra of the monomers and polymers were recorded as explained in chapter-2. The solution FT-IR spectra of the samples were recorded by dissolving appropriate amounts of the sample in THF and proceeded as given in chapter-3. The purity of the monomers was determined by JEOL JSM600 fast atom bombardment (FAB) high-resolution mass spectrometry. The compound was dissolved in CHCl$_3$ and suspended in 3-nitrobenzylalcohol as a matrix for FAB-Mass measurements. The molecular weights of the polymers were determined by gel permeation chromatography (GPC) in tetrahydrofuran (THF) using polystyrene as standards. The chromatograms were recorded using Waters 510 pump

and Waters 410 differential RI and Waters 2487 UV-Vis detectors. The absorption and emission studies were performed using a Perkin-Elmer Lambda 35 UV-Vis spectrophotometer and Spex-Fluorolog DM3000F spectrofluorometer with a double grating 0.22 m Spex 1680 monochromator and a 450 W Xe lamp as the excitation source using the front-face mode. The fluorescence lifetime was measured using an IBH FluoroCube Time-correlated picosecond single photon counting system (TCSPC). Solutions were excited with a pulsed diode laser 401 nm < 100 ps pulse duration with a repetition rate of 1 MHz. The detection system consists of a microchannel plate photomultiplier (5000U-09B, Hamamatsu) with a 38.6 ps response time coupled to a monochromator (5000M) and TCSPC electronics (DataStation Hub including Hub-NL, NanoLED controller and preinstalled Fluorescence Measurement and Analysis Studio (FMAS) software). The fluorescence lifetime values were determined by deconvoluting the data with exponential decay using DAS6 decay analysis software. The quality of the fit has been judged by the fitting parameters such as $R^2 < 1$ as well as the visual inspection of the residuals. Scanning electron microscopy (SEM) measurements were done on a JEOL JSM-5600 LV scanning electron microscope. Transmission electron microscopy (TEM) was performed on FEI, TEC NAI 30 G2 S-TWIN microscope with an accelerating voltage of 100 kV. Fluorescence microscopy was done on a NIKON ECLIPSE TE-2000-E using excitation filter FF01-377/50-25, emission filter FF01-447/60-25 and dichromatic mirror FF409-DiO2 25x36. Thermal analysis of the polyurethanes was performed as explained in chapter-2.

4.2.3. Synthesis of Monomers

4.2.3.1. Synthesis of 1-methoxy-4-(2-ethylhexyloxy)benzene (1): 4- Methoxyphenol (10g, 0.08 mol) and powdered KOH (18.4 g, 0.33 mol) were taken in a 250 mL flask containing 40 mL of dry DMSO and refluxed under nitrogen atmosphere for 0.5 h. 2-Ethylhexylbromide (17.3 g, 16 mL, 0.09 mol) was added and the reaction was continued by refluxing for 36 h under nitrogen atmosphere. It was cooled, poured into water and extracted with dichloromethane. The organic layer was washed with 10 % NaOH solution followed by brine solution and dried using anhydrous Na_2SO_4 and the solvent was evaporated. The crude product was further purified by passing through a

silica gel column using 35% CH$_2$Cl$_2$ in petroleum ether as the eluent to obtain the product as a light yellow liquid. Yield = 10.1 g (52 %). ^{1}H NMR (300 MHz, CDCl$_3$) δ: 6.85 ppm (s, 4H, Ar-H), 3.78 ppm (m, 5H, -OCH$_3$ and –OCH$_2$), 1.71-0.89 ppm (m, 15H, others). ^{13}C NMR (75 MHz, CDCl$_3$) δ: 115.6 (Ar-C), 71.4 (Ar-OCH$_2$), 55.8, 39.7, 30.7, 29.3, 24.0, 23.3, 14.3, 11.3 ppm. FT-IR (cm^{-1}): ν = 3045, 2958, 2930, 2873, 1591, 1508, 1465, 1442, 1380, 1288, 1231, 1180, 1105, 1043. HRMS (FAB): calcd for C$_{15}$H$_{24}$O$_2$ [M$^+$]: 236.36: found: 236.51

4.2.3.2. Synthesis of 1, 4-bis(bromomethyl)-2-methoxy-5-(2-ethylhexyloxy)benzene (2): Compound **1** (6 g, 0.02 mol) and paraformaldehyde (4.57 g, 0.15 mol) in 30 mL glacial acetic acid were taken in a 250 mL flask. HBr in glacial acetic acid (6 g, 22.1 mL, 132 wt %) was added dropwise to the above solution at 25 °C and stirred for 0.5 h under nitrogen atmosphere. It was gradually heated to 80 °C and stirred for an additional 5 h. The light brown coloured reaction mixture was poured into ice and washed with water until the filtrate was neutral. The solid was dissolved in 150 mL chloroform, washed with NaHCO$_3$ solution and saturated brine solution. The organic layer was separated and dried over anhydrous Na$_2$SO$_4$, and the solvent was evaporated to obtain a solid product which was purified by recrystallization from hot hexane. Yield = 7.02 g, (65 %) M.P. = 99 °C. ^{1}H NMR (300 MHz, CDCl$_3$) δ: 6.86 ppm (s, 2H, Ar-H), 4.53 ppm (s, 4H, ArCH$_2$-), 3.89 ppm (d, 5H, ArOCH$_3$+ ArOCH$_2$-), 1.75 - 0.88 ppm (m, 15H, aliphatic). ^{13}C NMR (75 MHz, CDCl$_3$) δ: 151.2, 127.7, 114.5 (Ar-C), 71.2 (Ar-OCH$_2$), 56.4, 39.8, 30.8 (Ar-CH$_2$Br), 29.3, 24.2, 14.3, 11.4 ppm. FT-IR (cm^{-1}): ν =2950, 2928, 2862, 1507, 1459, 1407, 1316, 1251, 1225, 1207, 1037, 772. HRMS (FAB): calcd for C$_{17}$H$_{26}$Br$_2$O$_2$ [M$^+$]: 422.20: found: 422.60

4.2.3.3. Synthesis of 4-(diethoxy-phosphoryl methyl)-2-methoxy-5-(2-ethylhexyloxy)-benzyl phosphonic acid diethylester (3): Bis-bromomethylated compound **2** (6 g, 0.01 mol) and triethylphosphite (4.72 g, 4.87 mL, 0.02 mol) were taken in a 100 mL flask and was heated at 150 °C for 15 h under nitrogen atmosphere. Excess triethylphosphite was removed by vacuum distillation to obtain the ylide (**3**) as a brown viscous liquid. Yield = 7.36 g, (96 %) ^{1}H NMR (300 MHz, CDCl$_3$) δ: 6.87 ppm (s, 2H, Ar-H), 3.97 ppm (m, 8H, -POOCH$_2$-), 3.74 ppm (d, 5H, ArOCH$_3$+

ArOCH$_2$-), 3.19 ppm (d, 4H, ArCH$_2$-), 1.75-0.83 ppm (m, 15H, aliphatic). FT-IR (cm$^-$^{1}): ν = 2960, 2930, 1509, 1465, 1413, 1390, 1250, 1215, 1163, 1097, 1029, 962. HRMS (FAB): calcd for C$_{25}$H$_{46}$O$_8$P$_2$ [M$^+$]: 536.59: found: 537.80

4.2.3.4. Synthesis of 4-(2-hydroxyethoxy) benzaldehyde (4): K$_2$CO$_3$ (16.9 g, 0.12 mol) and dry DMF (40 mL) were taken in a 250 mL flask and heated at 80 °C for 10 min. 4-hydroxy benzaldehyde (10 g, 0.08 mol) was added and was heated at 80 °C for 1 h. 2-chloroethanol (8.4 g, 7 mL, 0.10 mol) was added followed by adding a pinch of KI in DMF (1 mL) and heated at 85 °C for 48 h. Excess DMF was removed by vacuum distillation and the contents were cooled and poured into water to obtain a yellowish brown solution. It was extracted with chloroform, washed with 10 % NaOH solution, brine and dried using anhydrous Na$_2$SO$_4$. The solvent was evaporated to obtain the product as yellow liquid. It was purified by passing through a silica gel column using dichloromethane as eluent. Yield = 6.5 g (48 %). ^{1}H NMR (300 MHz, CDCl$_3$) δ: 9.76 ppm (s, 1H, -CHO), 7.73 ppm (d, 2H, aromatic), 6.93 ppm (d, 2H, Ar-H), 4.09 ppm (t, 2H, ArOCH$_2$-), 3.94 ppm (t, 2H, -CH$_2$OH), 3.30 ppm (s, 1H, -OH). FT-IR (cm^{-1}): ν = 3447, 2931, 2868, 2741, 1684, 1601, 1577, 1508, 1453, 1427, 1313, 1259, 1217, 1162, 1078, 1041, 914, 832. HRMS (FAB): calcd for C$_9$H$_{10}$O$_3$ [M$^+$]: 166.18: found: 167.34

4.2.3.5. Synthesis of hydroxyl functionalized oligo(phenylenevinylene) (OPV): The crude ylide (3) (1.04 g, 0.002 mol) was treated with 15 mL dry THF, compound **4** (0.71 g, 0.004 mol) and potassium-*tert*-butoxide (12 mL, 0.002 mol) and the contents were stirred under nitrogen for 24 h at 30 °C. The contents were cooled and poured into water to obtain a yellow powder which was dissolved in chloroform, washed with water, brine and dried using anhydrous Na$_2$SO$_4$. The red sticky solid was further purified by passing through a silica gel column using ethyl acetate and hexane (1: 20 v/v) as eluent. Yield = 0.67 g (61 %). ^{1}H NMR (300 MHz, CDCl$_3$) δ: 7.48 - 6.93 ppm (3xm, 14H, Ar-H and vinylic H), 4.12-3.86 ppm (m, 10H, ArOCH$_2$-), 3.75 ppm (s, 3H, ArOCH$_3$), 1.86-0.92 ppm (3xm, 15H, aliphatic). FT-IR (cm^{-1}): ν = 3567, 3324, 3032, 2928, 2862, 1603, 1508, 1459, 1412, 1250, 1204, 1171, 1038, 965(CH=CH$_{trans}$), 913, 770. HRMS (FAB): calcd for C$_{35}$H$_{44}$O$_6$ [M$^+$]: 560.74: found: 560.00

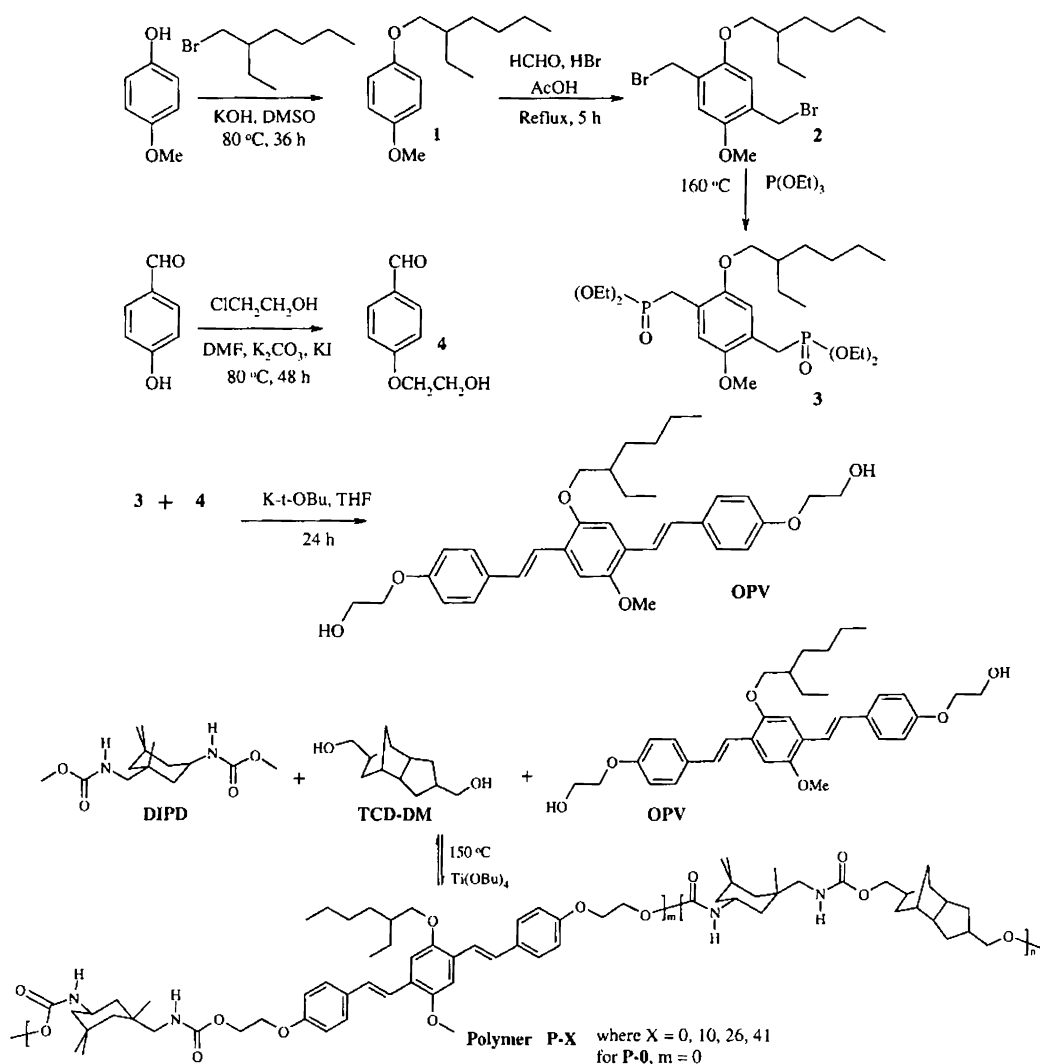**4.2.4. Synthesis of Polymers**

4.2.4.1. Synthesis of Polyurethane-oligophenylenevinylene random block copolymers (P-X): 1, 8-Tricyclodecanedimethanol (TCD-DM) (0.50 g, 2.56 mmol), di-urethane monomer **DIPD** (0.77g, 2.71 mmol) and **OPV** (0.08 g, 0.15 mmol) (for **P-10**) were taken in a test tube shaped polymerization apparatus and melted by placing in an oil bath at 100 °C with constant stirring. It was cooled and 3 drops of Ti(OBu)$_4$ (40 mg, 0.1 mmol) was added as catalyst and the polycondensation apparatus was made oxygen and moisture free by nitrogen purge followed by vacuum. The polymerization tube was then immersed in the oil bath at 150 °C and the polymerization was carried out along with nitrogen purge for 4 h. The resultant viscous mass was further condensed by applying high vacuum (0.01 mm of Hg) at 150 °C for 2h. At the end of the polymerization, the polyurethane was obtained as a red solid mass. The polymer was purified by dissolving in minimum amount of glacial acetic acid and precipitating into methanol. Yield = 0.98 g (77 %). ^{1}H NMR (300 MHz, CDCl$_3$) δ: 7.46-6.91 ppm (3xm, 14H, Ar-H and vinylic-H), 4.81 ppm (s, 1H, -CH$_2$NH), 4.58 ppm (s, 1H, cy-CHNH), 4.42 ppm (s, 4H, Ar-OCH$_2$), 4,18 ppm (s, 4H, ArOCH$_2$CH$_2$OCONH), 3.90-3.66 ppm (m, 11H, -COOCH$_2$ + cy-CH-NH + Ar-OCH$_3$ + Ar-OCH$_2$), 3.26, 2.92 ppm (s, 4H, -CH$_2$NH), 2.46-0.88 ppm (56H, cy-**H**, others). FT-IR (cm^{-1}): ν = 3325 (-NH $_H$ $_{bond}$), 2976, 2860 (-CH$_2$), 2686, 1964, 1807, 1724 (C=O $_H$ $_{bond}$), 1458, 1358, 1192, 1068, 910, 653.

4.3. Results and Discussion

4.3.1. Synthesis of Monomers

The hydroxyl functionalized **OPV** was synthesized through a series of steps as shown in scheme-4.6. Williamson's synthesis was performed on 4-Methoxy phenol to convert it into 1-methoxy-4-(2-ethylhexyloxy) benzene (**1**) using 2-ethylhexylbromide in KOH/DMSO. **1** was bisbromomethylated using paraformaldehyde and HBr in glacial acetic acid to give the bisbromomethylated compound: 1, 4-bis(bromomethyl)-2-methoxy-5-(2-ethylhexyloxy)benzene (**2**). This compound was subsequently subjected to phosphorylation in presence of triethylphosphite to give the corresponding bis-ylide, 4-(diethoxy-phosphoryl methyl)-2-methoxy-5-(2-

ethylhexyloxy)-benzyl phosphonic acid diethylester (**3**). 4-Hydroxy benzaldehyde was coupled with 2-chloroethanol to give 4-(2-hydroxylethyloxy)benzaldehyde (**4**). **3** was reacted with **4** under the Wittig- Horner reaction conditions to give the hydroxyl functionalized oligo-phenylenevinylene (**OPV**).[41-42] The diurethane monomer (**DIPD**) was synthesized by reacting isophorone diamine with dimethyl carbonate in presence of freshly prepared sodium methoxide as the base as described in chapter-2.

Scheme-4.6: Synthesis of monomers and polyurethane-oligo (phenylenevinylene) random block copolymers

The structure of the monomers was confirmed by ^{1}H and ^{13}C-NMR, FTIR and FAB-Mass analysis. The ^{1}H-NMR spectra of the monomers used for the synthesis of **OPV** are shown in figure-4.1. The peaks corresponding to different types of protons in the monomers are assigned alphabetically. Figure-4.1a represents the NMR spectrum of the monomer **1**. The aromatic peak for the compound appears at 6.85 ppm (a), the ArOCH$_3$ and ArOCH$_2$ appeared together as a multiplet at 3.78 ppm (b+c) and the remaining aliphatic protons appeared between 1.71 and 0.89 ppm. For the bis-bromomethylated compound **2** (figure-4.1b), the aromatic peak appeared at 6.86 ppm (a), the ArCH$_2$Br peak appeared at 4.53 ppm (b), and the ArOCH$_3$ and ArOCH$_2$ appeared together as a multiplet at 3.89 ppm (c+d) which was downfield compared to the similar protons in **2** due to the presence of the -CH$_2$Br unit along the aromatic ring.
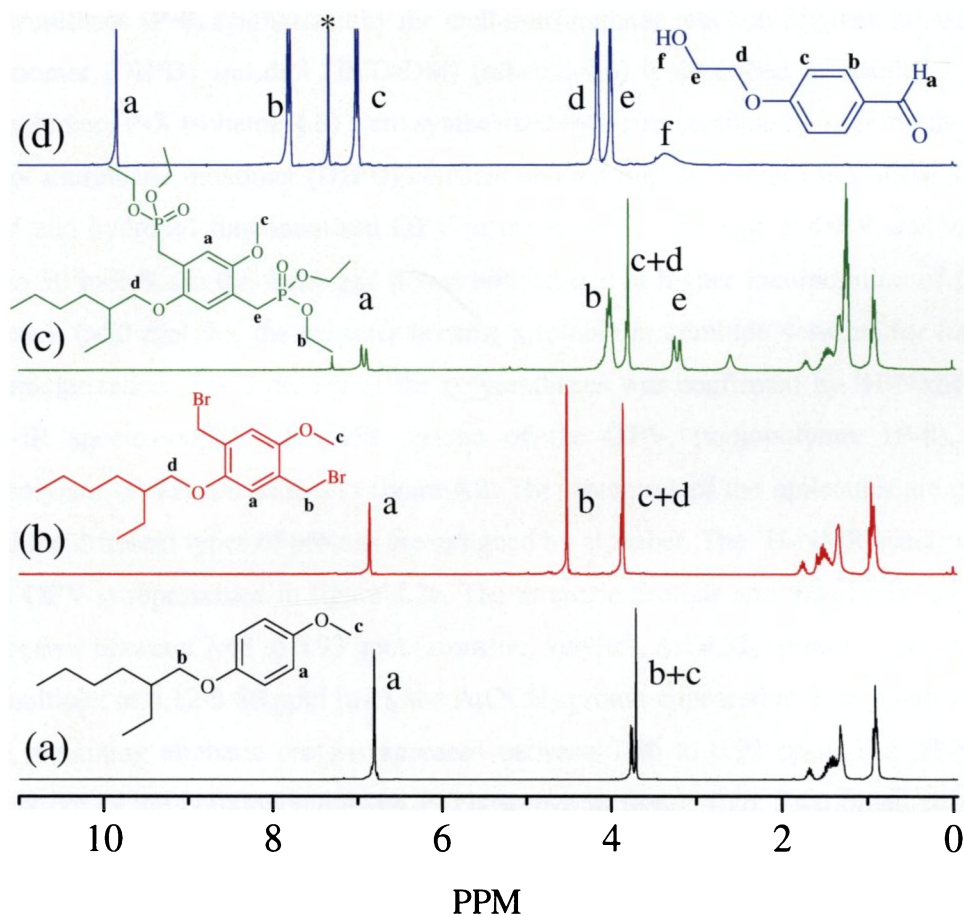

Figure-4.1: [1]*H-NMR spectra of monomers **1** (a), **2** (b), **3** (c) and **4** (d). The peak at the asterisk corresponds to the solvent peak.*

The NMR spectrum of the crude ylide **3** is shown in figure-4.1c. The aromatic peak for the compound appeared at 6.87 ppm (a), the -POOCH$_2$- appeared at 3.97 ppm (b), the ArOCH$_3$ and ArOCH$_2$ appeared together as a multiplet at 3.74 ppm (c+d) and the ArCH$_2$- protons appeared at 3.19 ppm (e). The NMR spectrum of the monomer **4** is represented in figure-4.1d. The aldehydic proton appeared downfield at 9.76 ppm (a), the aromatic protons appeared as two peaks, one at 7.73 ppm (b), and the other at 6.93 ppm (c), the ArOCH$_2$- proton appeared at 4.09 ppm (d), the -CH$_2$OH proton appeared at 3.94 ppm (e) and a small broad peak at 3.30 ppm corresponds to the -OH proton (f).

4.3.2. Synthesis of Polymers

The polyurethanes were synthesized by the solvent free and non-isocyanate melt transurethane polymerization route using Ti(BuO)$_4$ as a catalyst. The homo-polyurethane (**P-0**) synthesized by the melt transurethane reaction between diurethane monomer (**DIPD**) and diol (**TCD-DM**) (scheme-4.6) is described in chapter-2. The copolymers **P-X** (scheme-4.6) were synthesized by a similar route by keeping the mol % of diurethane monomer (**DIPD**) constant and varying the molar ratio of the TCD-DM and hydroxyl functionalized **OPV** in the feed. The amount of **OPV** was varied upto 50 mol % (in the feed) and it was noticed that at higher incorporation of **OPV** content (>50 mol %), the polymer became insoluble in common solvents for further characterization. The structure of the polyurethanes was confirmed by ^{1}H-NMR and FT-IR spectroscopies. ^{1}H-NMR spectra of the **OPV**, homopolymer (**P-0**), and copolymer (**P-41**) are shown in figure-4.2. The structures of the molecules are given and the different types of protons are assigned by alphabet. The ^{1}H-NMR spectrum of the **OPV** is represented in figure-4.2a. The aromatic protons and the vinylic protons appeared between 7.48 to 6.93 ppm (aromatic, vinylic), ArOCH$_2$- protons appeared as a multiplet at 4.12-3.86 ppm (a-c), the ArOCH$_3$ proton appeared at 3.75 ppm (d) and the remaining aliphatic protons appeared between 1.86 to 0.92 ppm. The ^{1}H-NMR spectrum of the homopolyurethane **P-0** is shown in figure-4.2b. Two broad peaks at 4.85 ppm and 4.60 ppm corresponds to the –NH protons (e and e', respectively), the -COOCH$_2$ and cy-CH-NH appeared together at 3.79 ppm (f and g), the -CH$_2$NH proton appeared as two separate peaks at 3.24 and 2.89 ppm (h), the bridge headed proton on the tricyclic ring appeared at 2.46 ppm (i). The protons from the OPV block as well as the homopolyurethane block were observed in the copolymer as shown in

figure-4.2c. In order to determine the mol % incorporation of the **OPV** unit into the copolymer backbone, ¹H-NMR peak corresponding to the **OPV** unit ('b' proton, see figure-4.2a) was compared with that of the TCD-DM unit ('i' proton, see figure-4.2b). From ¹H-NMR spectra the mol % of **OPV** incorporated in the polyurethane copolymers were determined as 10, 26 and 41 mole % for their incorporation of 5, 20 and 45 mole % in the feed, respectively.
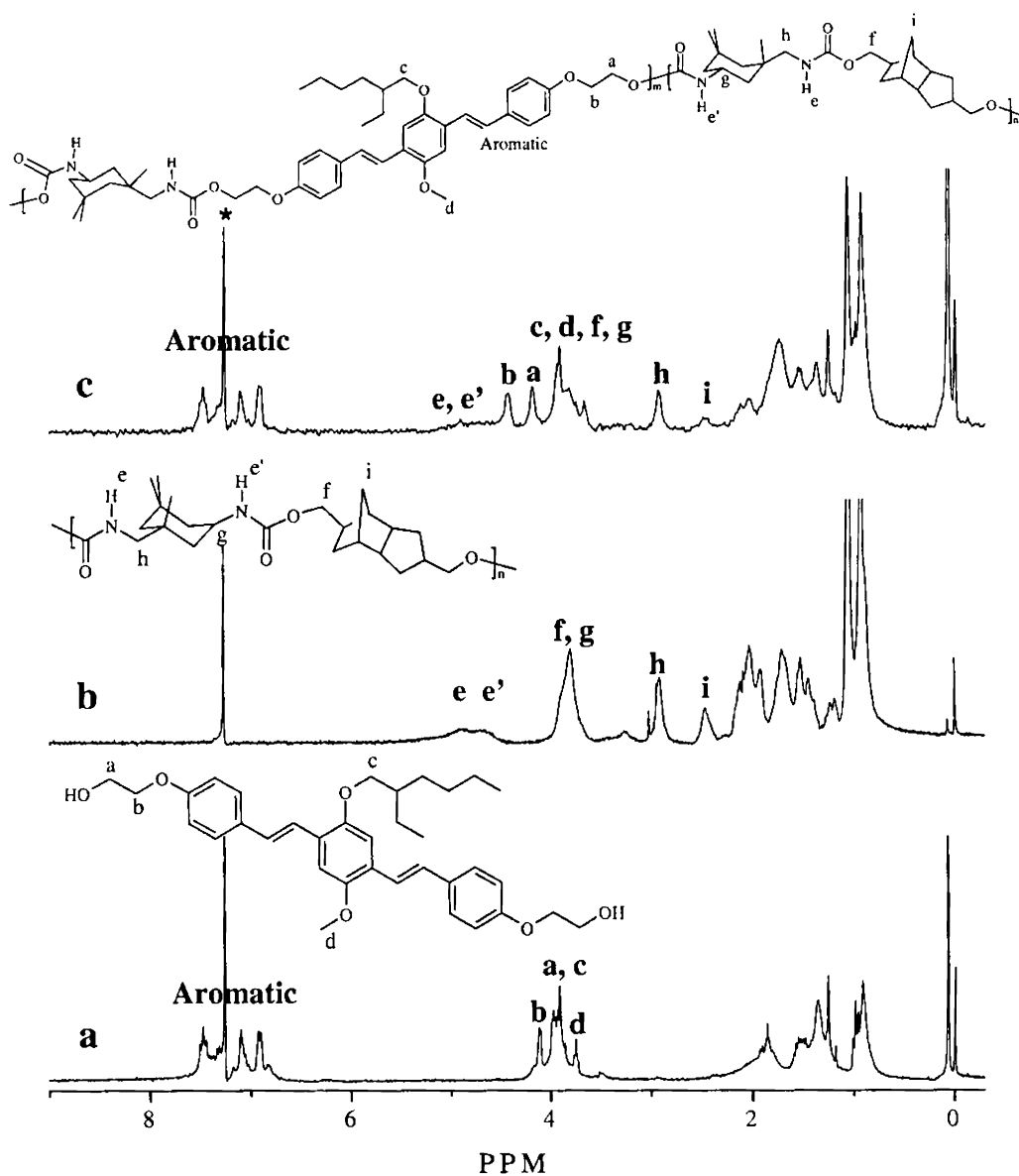

Figure-4.2: ¹H-NMR spectra of OPV (a), homopolymer, P-0 (b) and copolymer, P-41 (c). The peak at asterisk corresponds to the solvent peak

The polymers were named as **P-X,** where **X**-represents (X= 0, 10, 26 and 41), the amount of **OPV** content in the copolymers (table-4.1). All the polyurethanes were devoid of any gels (or insoluble mass) and they were soluble in common organic solvents such as chloroform and tetrahydrofuran for further characterization and morphological studies. The molecular weights of all the polyurethanes were determined by GPC in THF and the GPC molecular weights are given in table-4.1.

Table-4.1: Mole % of OPV in the copolymer, molecular weights and thermal data of polymers

Polymer	mol % of OPV (in mole %)		M_w^b	PDI^c	T_g $(^oC)^d$	T_D $(^oC)^e$
	Feed	Copolymer^a				
P-0	0	0	7, 800	2.4	118	270
P-10	5	10	10,000	1.5	120	286
P-26	20	26	12,000	2.0	108	270
P-41	45	41	15,400	3.6	103	278

a. Determined from ^{1}H-NMR spectra.
b. Molecular weights as determined by gel permeation chromatography in THF at 30 °C using polystyrene standards for calibration.
c. Values indicate polydispersities as determined by gel permeation chromatography.
d. Measured for the quenched sample in the second heating cycle at 10 °/min.
e. Temperature represents 10 % weight loss in TGA measurements under nitrogen.

The GPC chromatograms of the polyurethanes are shown in figure-4.3 and the chromatograms represents a mono-modal distribution of the molecular weights.
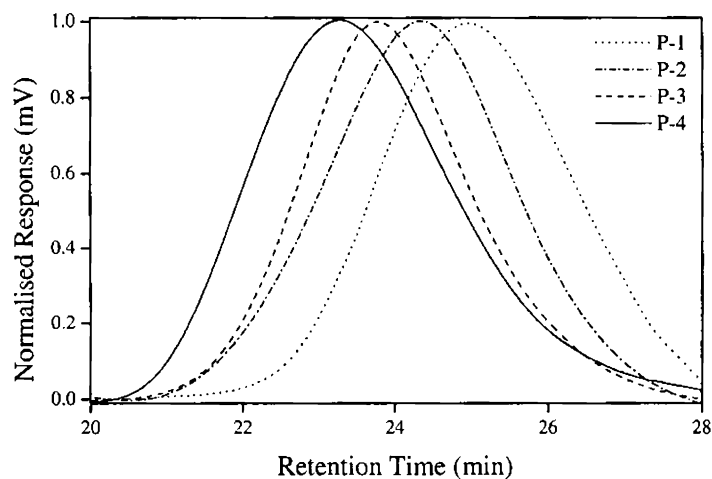

Figure-4.3: GPC chromatograms of Polymers

The values for the weight average molecular weight; M_w ranges from 7800-15,400 with polydispersities in the range of 2.0-3.6. On comparing the value of the molecular weights of the polyurethanes, it was found that the homopolymer, **P-0** had the lowest molecular weight and with the incorporation of the **OPV** units into the polymer backbone the molecular weights were found to increase. The TGA analysis (figure-4.4) confirmed that all the polymers were thermally stable from 270-286 °C (table-4.1) and so they could be used for various high temperature applications.
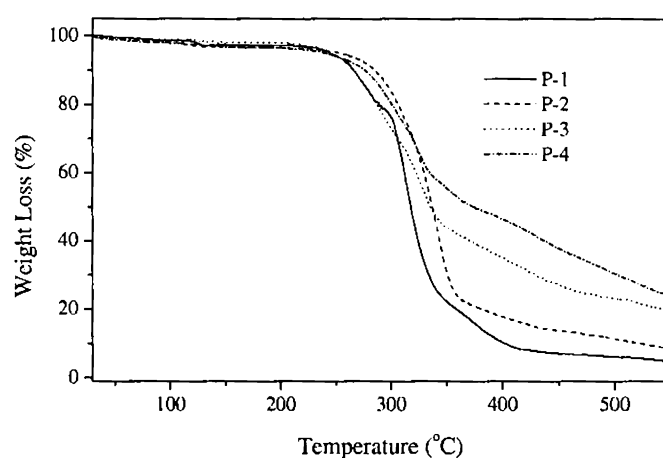

Figure-4.4: TGA plots of Polyurethanes

The thermal analysis by DSC (figure-4.5) proved that all the polyurethanes were sluggish to crystallise and they showed only T_g (table-4.1).
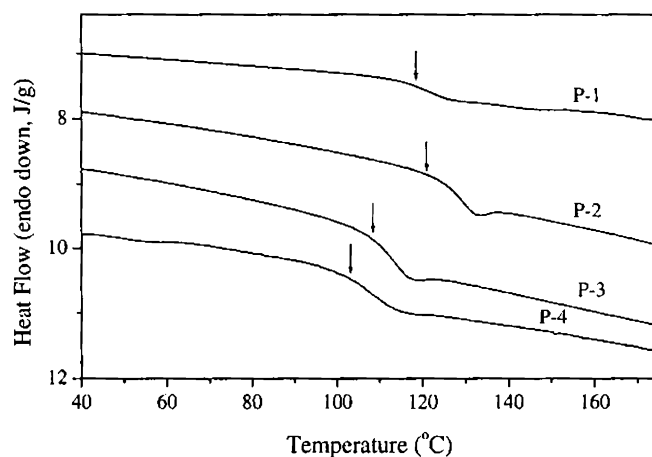

Figure-4.5: DSC thermograms of quenched samples of Polyurethanes at 10 °C/min

The DSC plot indicates a single T_g for all the copolymers and a comparison of the T_g values of the copolymers with that of the homopolymer showed a decreasing trend with the increase in the **OPV** content in the polymer backbone. The lowering of T_g points to the fact that with the increase in the amount of **OPV** in the copolymer, the polymer backbone becomes less rigid.

4.3.3. Scanning Electron Microscopy (SEM) Analysis

Solvent induced self-organization of random block copolymers were studied by dissolving the polymer (5 wt % solution) in dry THF or THF: water - 90:10 (v/v), filtered and drop cast on a glass substrate. All the polymer films were subjected to slow evaporation for 24 h under ambient conditions in air.[43-45] SEM pictures of polymer films of homopolymer **P-0** and the copolymers **P-10** to **P-41** in THF and THF + water are shown in figure-4.6. It is very clear from the SEM pictures that all the polymers produce a typical micro-porous membrane type morphology for the films prepared from THF (image a, c and e in figure-4.6). The average pore size and the distance between each pore were calculated from the SEM-images and reported for the polymers in table-4.2. In all the cases the size of the pores were found to be uniform and they were straight through pores and no traces of 3D-honey-comb pattern could be noticed along the entire polymer films (figure-4.7).

Table-4.2: Morphology data of Polyurethanes

Polymer	SEM Data of Films		TEM Data
	THF alone	THF+H$_2$O	
P-0	500 nm ± 40 nm[a] 1.28 µm ± 100 nm[b]	1.48 µm ± 80 nm[c]	-
P-10	0.92 µm ± 10 nm 360 nm ± 50 nm	400 nm ± 50 nm	1.7 µm ± 100 nm[d] 60 nm ± 130 nm[e] 110 nm ± 30 nm[f]
P-26	680 nm ± 60 nm 1.14 µm ± 160 nm	1.97 µm ± 30 nm	-
P-41	790 nm ± 60 nm 1.88 µm ± 170 nm	2.07 µm ± 440 nm	250 nm ± 40 nm[f]

a.   Values indicate the size of the pores calculated from figure-4.6.
b.   Values indicate the pore distance calculated from figure-4.6.
c.   Values indicate the size of spheres calculated from figure-4.6.
d.   Value indicates the size of vesicle calculated from figure-4.10.
e.   Value indicates the wall thickness of vesicle calculated from figure-4.10.
f.   Values indicate the size of spheres calculated from figure-4.10
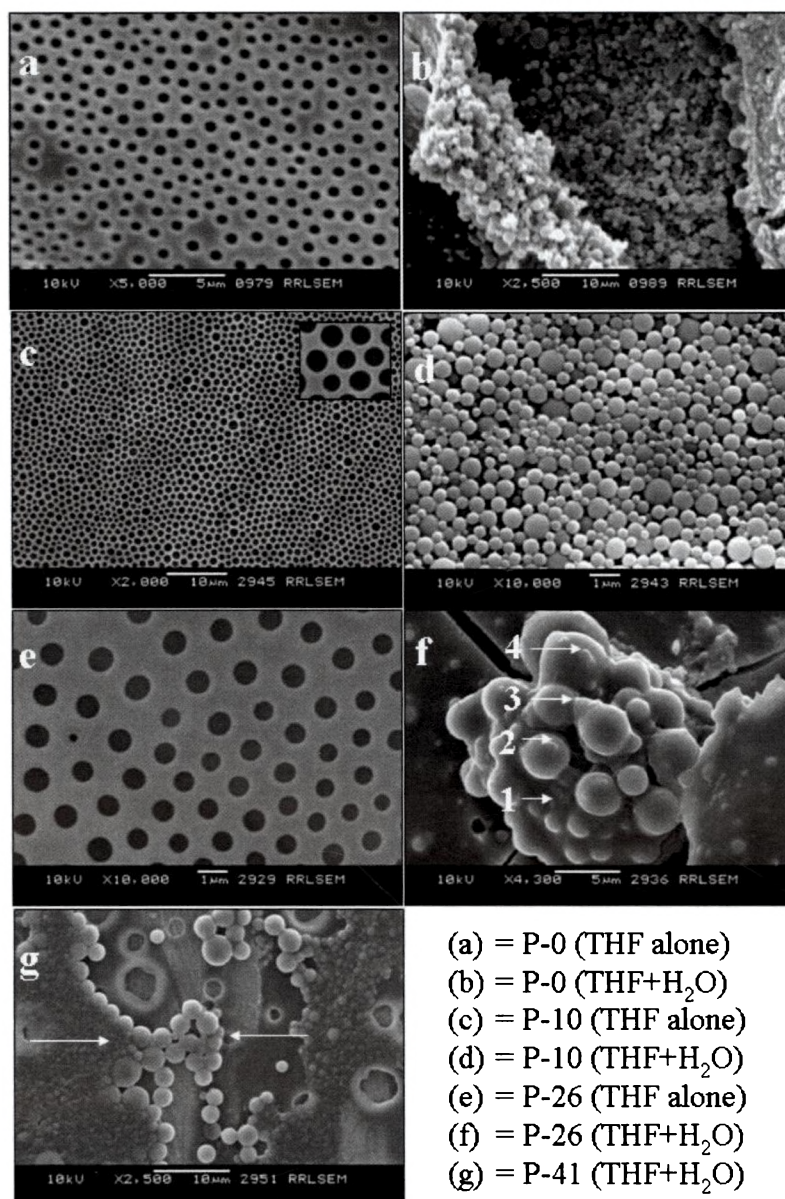
(a) = P-0 (THF alone)
(b) = P-0 (THF+H$_2$O)
(c) = P-10 (THF alone)
(d) = P-10 (THF+H$_2$O)
(e) = P-26 (THF alone)
(f) = P-26 (THF+H$_2$O)
(g) = P-41 (THF+H$_2$O)

Figure-4.6: SEM images of polyurethanes in THF alone and THF: water-90:10

P-0 has pore sizes in the range of 500 nm ± 40 nm and they were separated by 1.28 μm ± 100 nm. **P-10** has much bigger pores (0.92 μm ± 10 nm) but the pores are more closely packed (360 nm ± 50 nm) compared to **P-0**. In the case of **P-26** the pore size was bigger than **P-0** but smaller than **P-10** (680 nm ± 60 nm) with a much bigger pore distance of 1.14 μm ± 160 nm.
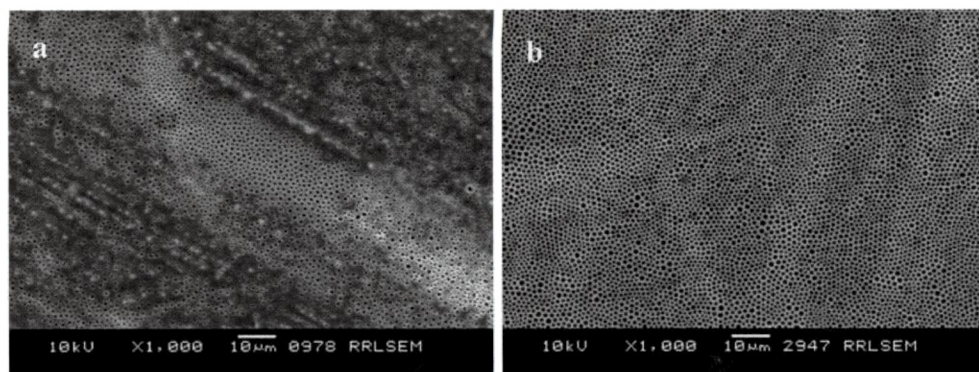
Figure-4.7: Expanded SEM images of P-0 (a) and P-10 (b) in THF alone

The porous morphology is not confined to small domains or edges and it appeared throughout the sample for more than 100 micron square meters as shown in the lower magnification SEM images in figure-4.7. It is often noticed in the literature that the amount of water in the solvent combinations plays a crucial role in the self-assembly and morphological changes in the block copolymers.[46] With the increase in the amount of water in the THF + water combinations, the pores (in THF alone) disappeared and the formation of micron to nano-meter sized spheres were noticed (THF: water-90:10, images b, d, f and g in figure-4.6). The size of the spheres (diameter) in the random copolymers were found to vary in the order **P-10** (400 nm) < **P-26** (1.97 μm) < **P-41** (2.07 μm). This suggests that, with the increase in the amount of **OPV** content in the polymer backbone, the size of the spheres is found to increase (except for **P-0**, without **OPV** units) from nano-meter to micron size. The SEM pictures gave clear evidence for the appearance of spheres in a vertical direction in **P-26** (bottom to top, see figure-4.6f)) and laterally arranged in a single layer in **P-41** (figure-4.6g). To investigate the effect of large amount of water on the morphology of polymers, **P-10** was subjected to solvent induced self-organization with up to 50:50 of water/THF (figure-4.8). On increasing the amount of water (THF: water-70:30) the spheres are distributed in random along the substrate and the number of spheres have decreased to a very great extent as seen in figure-4.8c. For THF: water-50:50, the aggregation becomes uncontrollable resulting in the vanishing of the polymeric spheres and the successive formation of polymeric flakes as evident in figure-4.8d.[47]
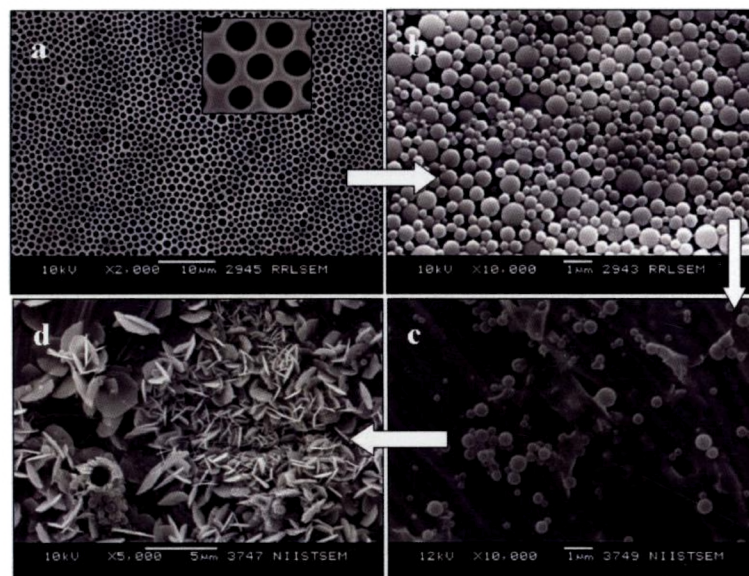
Figure-4.8: SEM images of P-10 in THF alone (a), THF: water-90:10 (b), THF: water-70:30 (c) and THF: water-50:50 (d)

It is also important to mention that the polymer solutions were clear up to 30 % of water in THF, however, large amounts of water (50 % and more) rendered the polymer solutions hazy. Therefore, the amount of water in THF + water is very crucial in obtaining a good morphology of polymers via solvent induced evaporation process. The variation of water content in **P-26** interestingly showed the appearance of polymer hexagons (figure-4.9) for THF: water- 95:5.
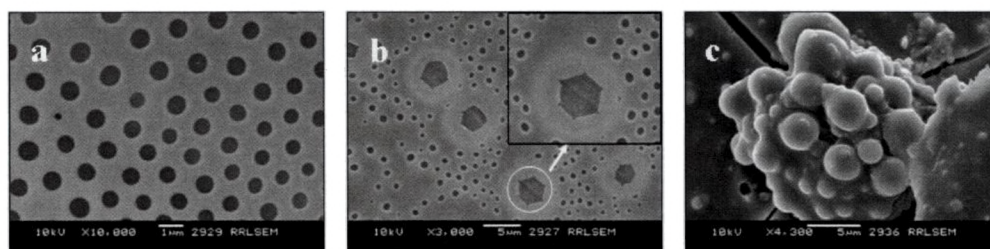

Figure-4.9: SEM images of P-26 in THF alone (a), THF: water-95:5 (b) and THF: water-90:10 (c)

A closer look at the polymeric hexagon indicates that the hexagonal edges are perfect and the hexagonal faces are slowly transforming into curved surfaces which gives a

clear indication for the formation of spheres from these hexagons. This observation was in accordance with the results in chapter-3 that the homo polyurethane, **P-0** (**P-2** of chapter-3 and also another polyurethane having 1,4-cyclohexanedimethanol instead of TCD-DM in the backbone, **P-1** of chapter-3) showed the appearance of perfect edged polymer hexagons in the film obtained in the presence of trace amount of water (THF: water- 95:5). The observation of hexagons in the present investigation strongly supports the possibilities for the existence of polymeric hexagons in the morphological development of solvent evaporated self-organization process. However, attempts to obtain hexagons in the other two polymers **P-10** and **P-41** was not successful. Since, the hexagons were not observed in all polymer samples, it can be assumed that the formation of hexagons is an intermediate stage between pores to spheres and they are not the stable final products of the solvent evaporation process.

4.3.4. Transmission Electron Microscopy (TEM) Analysis

The polymer samples were also subjected to transmission electron microscopic (TEM) analysis. The TEM images of 1 wt % polymer solution were recorded for **P-10** and **P-41** in films obtained from THF alone or THF: water-90:10 (see figure-4.10).
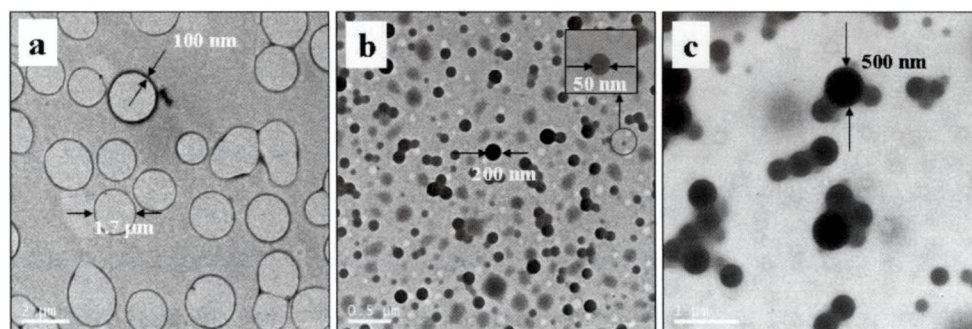

Figure-4.10: TEM images of P-10 in THF alone (a), P-10 in THF: water-90: 10 (b) and P-41 in THF: water-90:10 (c)

The polymer films were prepared by drop casting the above solution on the top of Formvar coated copper grid at ambient conditions. The TEM image of **P-10** (films obtained from THF, figure-4.10a) showed the existence of vesicles as there is an obvious contrast between the contour and the centre of the aggregates.[48] These

vesicles varied in sizes ranging from 1.2-1.7 µm with a wall thickness of around 100 nm (table-4.2). The comparison of TEM and SEM images of **P-10** films prepared from THF alone showed the appearance of two different types of morphology: for instance pores in SEM and vesicles in TEM. The difference in this trend is correlated to the variation in the concentration of polymer solutions in sample preparations (for TEM 1 wt % and SEM 5 wt %). Deepak et al. and Tung et al. have recently reported that polymers like polyacrylics and poly(vinyl phenol)-block-polystyrene diblock copolymers also showed similar dissimilarities in the TEM and SEM images.[49,30] For example, the PVP-b-PS diblock copolymers showed 3D- honey-comb morphology in SEM whereas vesicles were observed in TEM images. It was postulated that with the increase in the concentration of solutions, the vesicles transform into honey-comb morphology.[30] In the present investigation also, a similar concentration range was employed for the analysis, and therefore, the formation of vesicle in TEM images may be due to the concentration effect. In the presence of water, (for THF: water-90: 10 solvent combinations, figure-4.10b and 4.10c), the morphology of **P-10** and **P-41** were observed as solid spheres, which are in accordance with that of SEM images. For **P-10** the size of the spheres ranges from 50 nm to 200 nm (figure-4.10b) whereas in the case of **P-41** the size of the spheres ranges from 250 nm to 500 nm (figure-4.10c).

4.3.5. Fluorescence Microscopic Analysis

The random block copolymers contain fluorescent OPV units in the polymer backbone, and therefore, shining of light on the nano-spheres is expected to transform these solid spheres into luminescent balls (under fluorescence microscope). The polymer solutions (5 wt % in THF alone or THF: water-90:10) were drop cast on a glass slide and the dry film was observed under the fluorescence microscope with an excitation at 377 nm (the absorbance maxima of OPV = 370 nm). Figure-4.11a represents the fluorescence microscopic images of **P-10** (films obtained from THF) and the image shows the presence of very faint blue fluorescent spheres. The films obtained from THF + water mixture showed large number of highly luminescent fluorescent solid spheres (figure-4.11b), which is in accordance with SEM and TEM images. In the case of **P-41** (in THF: water-90:10, figure-4.11c) the number and size

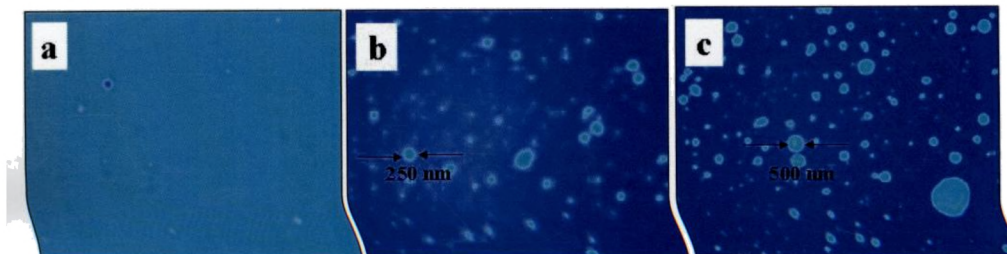of the spheres are found to increase and in some areas these spheres are seen to coexist with each other.

*Figure-4.11: Fluorescence microscopy images of **P-10** in THF alone (a), **P-10** in THF: water-90: 10 (b) and **P-41** in THF: water-90:10 (c)*

The luminescent behaviour of the spheres is uniform in all parts, which suggest that the OPV segments in the copolymer are homogeneously distributed throughout the entire polymer chain during the sphere formation.[36,50] Though there is a variation in each microscopic technique such as SEM, TEM and fluorescence microscopy, in the present investigation micron or nano-sized materials were created in good reproducibility via solvent induced self-organization process. It is evident from the above morphological analysis that the polymer films showed porous morphology when cast from THF (or vesicles at low concentration inferred from TEM) and increasing the amount of water in the polymer solution induce the formation of spheres. Further, depending upon the amount of **OPV** present in the copolymers, they either appeared as isolated (also small) or aggregated (bigger in size) spheres. It is very important to add here that this is for the first time that such a variety of morphologies- porous membranes, spheres (luminescent), vesicles and hexagons were observed for any type of π-conjugated polymers or π-conjugated-block copolymers in the literature. Therefore, both the solvent combination as well as the chemical composition of copolymer backbone (i.e. the amount of **OPV** units) play major role in determining the morphology of the solvent evaporated films.

4.3.6. Solution FT-IR Spectroscopy

In the present case, the self-organization during solvent evaporation may arise via two non-covalent interactions: (i) hydrogen bonding through urethane linkage and (ii) π-π stacking of **OPV** aromatic core. In order to study the effect of hydrogen

bonding in the polyurethane segments, the polymers were subjected to solution FTIR studies in THF. The expanded region of the N-H stretching vibration of FT-IR spectra of **P-0** to **P-41** for 2×10^{-2} M^{-1} in THF are shown in figure-4.12.
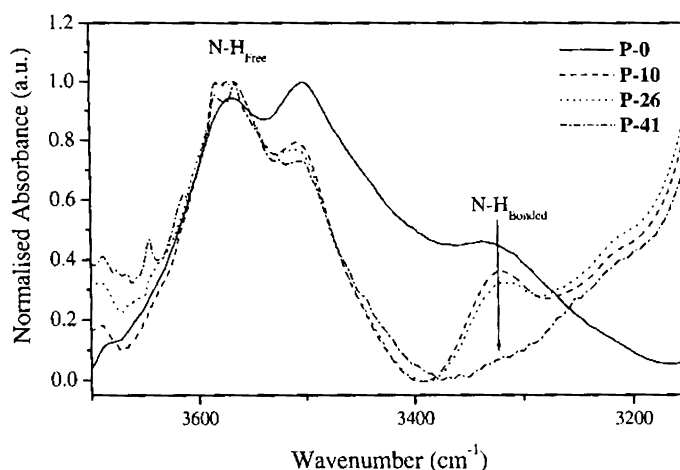

Figure-4.12: FT-IR spectra of Polyurethanes in THF alone

The two peaks at higher wave numbers (3572 and 3500 cm^{-1}) are corresponding to the free anti-symmetric and symmetric stretching vibrations of the N-H group in the urethane linkage, respectively.[51] The peak at lower wavenumber (3329 cm^{-1}) is corresponding to the hydrogen-bonded N-H stretching vibration. The hydrogen bonded peaks are more intense in **P-0**, **P-10** and **P-26** and they are almost absent in **P-41**. It suggests that with the increase in the amount of **OPV** in the polyurethane backbone, the extent of hydrogen bonding is disrupted. This observation was well supported by the T_g values of the polymers (table-4.1). The more hydrogen bonded polymer possesses higher rigidity and so the glass transition temperature is expected to be higher than that of weakly hydrogen bonded polymers. Hence the driving force for aggregation for copolymers with lower **OPV** content is mainly due to hydrogen bonding whereas this may be a weak force for higher **OPV** content polymer.

4.3.7. Photophysical Studies of Polyurethane Copolymers

To trace the π-π stacking of **OPV** aromatic core and photophysical properties of conjugated segments, the copolymers were subjected to absorption and emission studies in both solution and solid state (table-4.3).

Table-4.3: Photophysical properties of the polyurethane-oligo phenylenevinylene random block copolymers

Polymer	Solvent THF:H$_2$O	In solution			In film		
		λ_{max}(abs) (nm)	λ_{max}(em)[a] (nm)	ϕ_{FL}[b]	λ_{max}(abs) (nm)	λ_{max}(em)[c] (nm)	PL$_{Intensity}$[d]
P-10	100:0	396	441	0.38	401	510	8×10^6
	90:10	396	441	0.43	434	526	1.5×10^7
	50:50	396	490	0.35	-	-	-
	10:90	396	517	0.20	-	-	-
P-26	100:0	396	441	0.33	397	518	4.7×10^6
	90:10	396	441	0.41	407	524	7.1×10^6
	50:50	398	441	0.33	-	-	-
	10:90	407	522	0.02	-	-	-
P-41	100:0	396	441	0.38	401	510	9.3×10^6
	90:10	396	441	0.44	432	529	1.1×10^7
	50:50	399	441	0.36	-	-	-
	10:90	405	528	0.13	-	-	-

a. Excitation wavelength used is 396 nm
b. Calculated using Quinine sulphate as standard and excited at 396 nm; the absorbance of solutions was maintained as 0.1 at 396 nm.
c. Excitation wavelength is the absorbance maximum.
d. The emission intensity of the polymers at the emission maxima.

The absorbance and emission spectra of the copolymers **P-10** and **P-41** were recorded in THF: water (from 0-100 %, v/v) solvent combinations and shown in figure-4.13. The absorbance peaks over 390-520 nm can be attributed to the π-π* electron transition for **OPV** in polymer backbones.[52] In both **P-10** and **P-41** (in THF), there is a strong absorption at 396 nm and a shoulder at 467 nm which increased in intensity with the addition of water (figure-4.13a and 4.13c). This red shift in the peak maxima may be caused by the inter-chain interactions resulting from aggregation upon adding a non-solvent such as water into the polymer solution in THF.[53] The ratio of the absorbance intensities (I$_{467}$/I$_{396}$) were plotted against the volume % of water in the polymer solution for **P-10** and **P-41** and shown in figure-4.13e. The plot shows a sigmoidal nature with the existence of two types of species with a break point at around 40-60 volume % of water where there is a sudden jump in the intensity at 467 nm. The plot also indicates that the increase in intensity of peak at 467 nm is more in the case of **P-41** when compared to **P-10**. It suggest that the polymer with more

number of **OPV** units (**P-41**) experience strong π-π stacking compared to that of polymer with few **OPV** units (**P-10**).
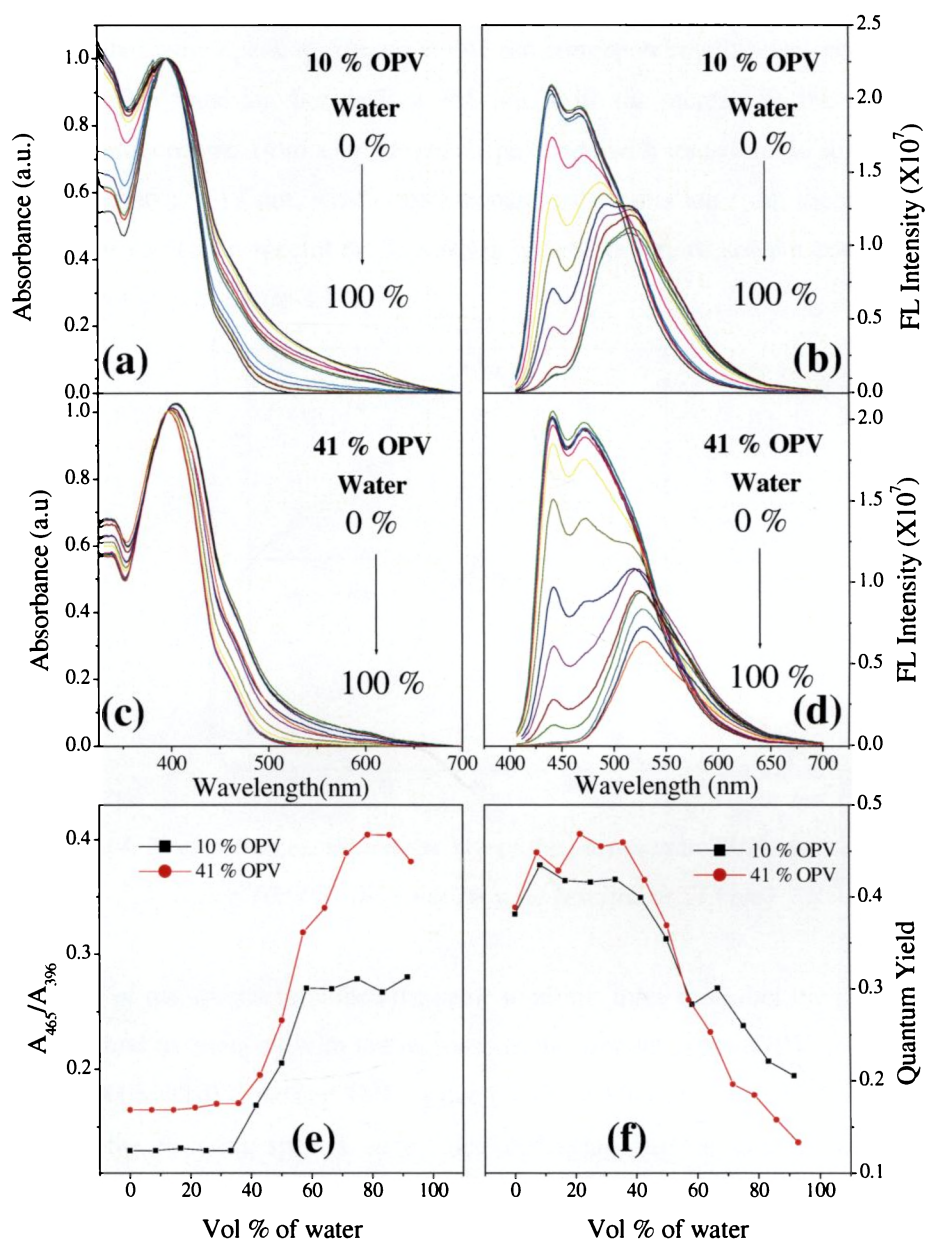

*Figure-4.13: UV-visible absorption and Fluorescence emission spectra of **P-10** (a, b) and **P-41** (c, d) in THF and THF/water solvent combinations and the plot of absorbance intensity versus volume % of water for **P-10** and **P-41** (e) and quantum yield versus volume % of water for **P-10** and **P-41** (f). Emission spectra were obtained at 396 nm.*

The emission spectra of the above solutions (0.1 O. D.) were obtained by exciting at the absorption maximum (figure-4.13b and 4.13d). The solution emission spectra are fine structured with a peak maximum at 441 nm corresponding to blue light emission upon excitation[32] and another peak at 468 nm. With the increase in the amount of water the peak changes from a structured shape to one with less vibronic structure and a peak emerges at 517 nm, which corresponds to the emission from the aggregated species. The excitation spectra of the three polymers in various solvent combinations were also compared (figure-4.14).
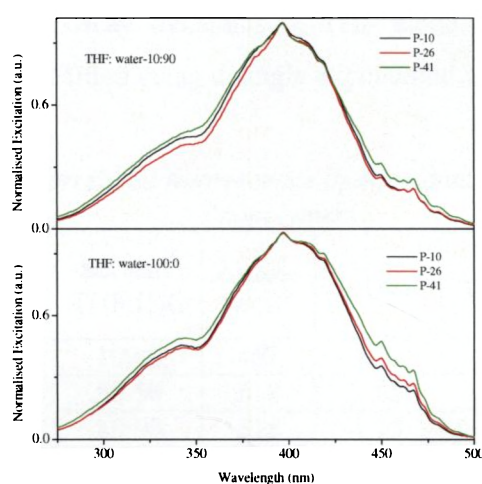

Figure-4.14: Normalised excitation spectra of the polymers in THF alone and THF: water-10:90 in the solution state (excited at 515 nm)

The nature of the spectra remained the same in all the three cases but the peak at 465 nm was found to intensify with the increase in the amount of the **OPV** content from **P-10** to **P-41** in THF alone and THF: water-10:90 solvent combinations. The quantum yields for the emission spectra were calculated using quinine sulphate as standard following the equation $\phi_s = \phi_r (F_s A_r / F_r A_s)(n_r/n_s)^2$, where ϕ is the fluorescent quantum yield, F is the area of the emission, n is the refractive index of the solvent and A is the absorbance of the solution at the exciting wavelength.[54] The subscripts r and s denote the reference and sample, respectively. A plot of quantum yield versus the volume % of water in the polymer solution for **P-10** and **P-41** are shown in figure-4.13f. The plot shows a decrease in the ϕ_s with the increase in the amount of water and as seen in figure-4.13e, the plot is sigmoidal with a breakpoint at 40-60 volume % of water. The

decrease in the fluorescence quantum yield denotes a quenching of fluorescence through a non-radiative decay arising from the strong π-stacking interaction.[55] It should also be noted that the quenching of fluorescence is more in the case of **P-41** when compared to **P-10**, as this could be due to greater aggregation in **P-41** via aromatic π-stacking.

4.3.8. Time-resolved Photoluminescence Decay Studies

The time-resolved photoluminescence decay dynamics were carried out for the copolymers at an excitation wavelength of 401 nm to understand the nature of their excited state. The PL decay dynamics in THF alone and in THF/water solvent combinations were best fitted using a single exponential and bi-exponential function, respectively (table-4.4).

Table-4.4: Time correlated fluorescence lifetime data of Polyurethane block copolymers

Polymer	Solvent[a] THF:H$_2$O	$\lambda_{monitor}$ (nm)[b]	τ_1 (ns)[c]	τ_2 (ns)[c]	R^2 [d]
P-10	100:0	467	1.52	-	0.999
	50:50	518	1.85	1.34	0.998
	10:90	518	1.15	0.95	0.999
P-26	100:0	467	1.51	-	0.999
	50:50	518	1.50	0.71	0.999
	10:90	518	0.73	0.55	0.986
P-41	100:0	467	1.48	-	0.999
	50:50	518	1.25	0.63	0.999
	10:90	518	0.66	0.66	0.998

a. The optical density of the solutions was maintained at ~0.1 for the life time measurements.
b. Emission wavelengths for which the decay was monitored (λ_{exc} = 401 nm).
c. Lifetimes obtained from the exponential decay fitting.
d. Values indicate the fitting parameter obtained from the exponential decay fitting.

The PL decay curves for **P-10**, **P-26** and **P-41** in THF alone and in THF: water-50:50 and THF: water-10:90 solvent combinations are shown in figure-4.15. For all the three copolymers the decay is very rapid with increasing amount of water indicating the enhancement of aggregated luminescent quenching. A single exponential fit in THF alone suggested the existence of a single luminescent species.

Two decay components in THF/water solvent combinations confirm the existence of two types of luminescent species corresponding to the aggregated and isolate chains.
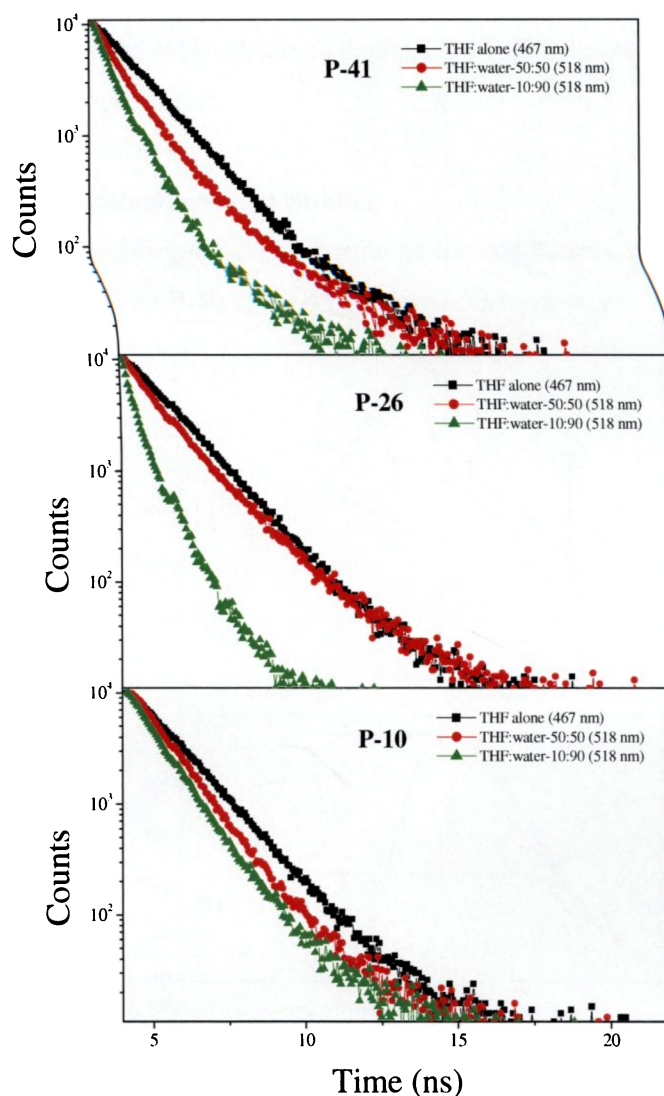

*Figure-4.15: Time resolved Fluorescence life time spectra of **P-10**, **P-26** and **P-41** in THF, THF: water-50:50 and THF: water-10:90. The excitation wavelength is 401 nm.*

In THF alone, τ_1 is in the range of 1.52 ns for **P-10** but the incorporation of more **OPV** units decrease its life time: for example 1.51 ns for **P-26** and 1.48 ns for **P-41**. With the addition of water the first and the second decay life times were found to decrease. For instance in THF: water-50:50, the decay life time of **P-10** are 1.85 ns where as for **P-26** it is 1.5 ns which further decreases to 1.25 ns for **P-41**.[56] In the case

of THF: water-10:90 solvent combinations the values were found to decrease from 1.15 ns for **P-10**, 0.73 ns for **P-26** and 0.66 ns for **P-41**. The time resolved FL measurements confirmed the presence of strong aggregates in THF + water solution via π-stacking and also the enhancement of aggregation with increase in **OPV** content in the random block copolymers.

4.3.9. Solid State Photoluminescence Studies

The solid state photophysical properties of the copolymers were studied and the representative plots for **P-10** and **P-41** are shown in figure-4.16.
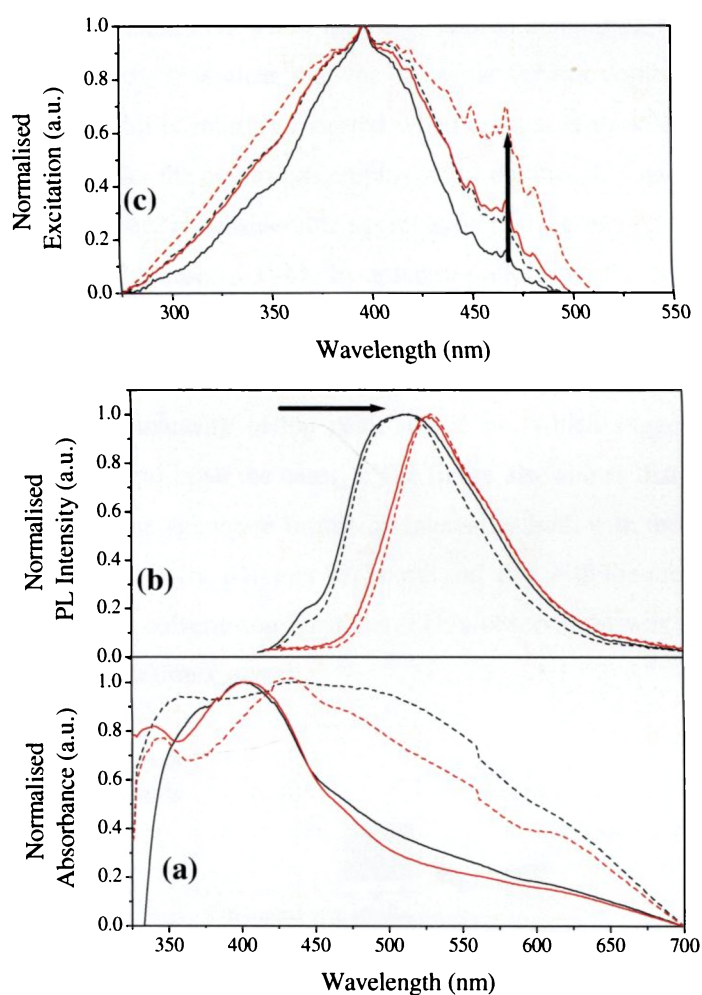

Figure-4.16: Normalised Absorbance (a), normalised PL spectra (b) and normalised excitation spectra of P-10 (black) and P-41 (red) in THF (—) and THF: water-90:10 (---) of the films. Emission spectra were obtained at peak maxima.

The polymer solution in THF or THF: water solvent combinations were drop cast on a glass slide and allowed to evaporate under ambient conditions to obtain polymer films (same conditions applied for SEM analysis). The solid state absorbance spectra of the polymers are shown in figure-4.16a. The absorption spectra of the polymers in solid state (from THF solution) were much broader compared to their solution spectra with a peak maximum at around 401 nm and a shoulder at 465 nm. For the films prepared in THF: water-90:10, there is a red shift in the peak maximum from 401 nm to 432 nm and a considerable broad tailing of the spectra which suggests greater tendency for aggregation through π-π stacking.[57-59] The normalized emission spectra of these films excited at the peak maximum are shown in figure-4.16b. On comparing figure-4.16b with figure-4.13b (or 4.13d), it is clear that for the same solvent combination, the emission maxima in the film is more red shifted when compared to solution (table-4.3). This suggests that under the conditions employed for the morphological study in the present investigation, there is considerable aggregation in the copolymers, and this is found to be greater in the case of **P-41**. In order to understand the nature of the emissive species, the excitation spectra of the solid polymer films were monitored at 518 nm (figure-4.16c). The excitation spectra were identical for all the polymers except for an increase in intensity of the peak at 465 nm which suggests that the emissive species are identical in all the cases.[42] The figure also shows that the peak at 465 nm corresponding to the aggregate formation intensifies both with the increase in the amount of OPV content in the polymer backbone and also with the increase in the volume % of water in the solvent combinations. (This observation was comparable with the solution state excitation spectra).
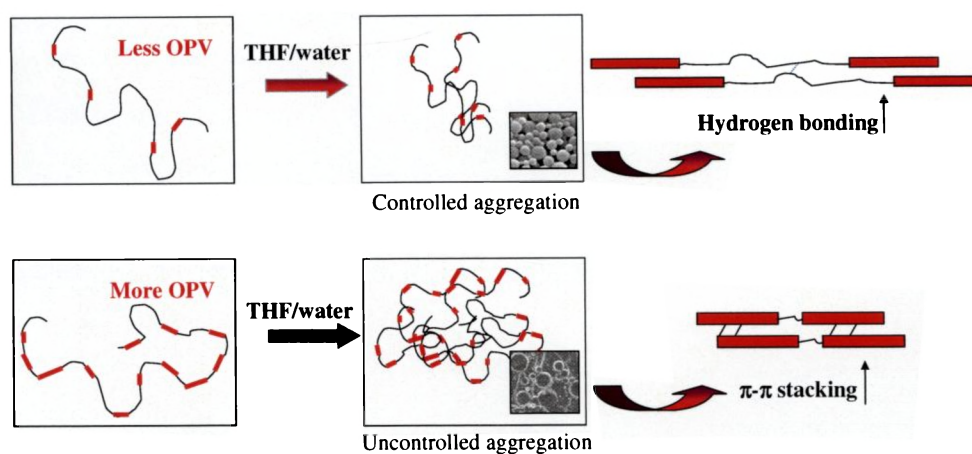
Scheme-4.7: Aggregation in polyurethane-oligophenylene vinylene block copolymers

All these studies revealed that solvent induced self-organization takes place in copolymers but the extent to which it undergoes is determined by the solvent combination as well as on the mol % of OPV in the copolymer backbone. The aggregation can be driven by two forces, viz. hydrogen bonding or π-π stacking (scheme-4.7). For **P-10** having less amount of OPV in the copolymer backbone, the addition of water into polymer solution in THF results in controlled aggregation which could be mostly favoured through hydrogen bonding interaction. In the case of **P-41** with higher OPV content the major driving force for aggregation could be π-π stacking resulting in uncontrolled aggregation with the addition of water.

4.4. Conclusion

The above studies provides a clear insight into the solvent induced self-organization in polyurethane-OPV random copolymer for various morphologies and sizes ranging from micron to nano-meter sized pores, hexagons, vesicles and solid luminescent spheres. The polyurethane-OPV random block copolymers were synthesized by the melt transurethane route and the polymers possess high thermal stability and solubility in common solvents to study the self-organization process. The approaches demonstrated here as well the resultant nano-materials has many advantages: (i) polyurethane-OPV random block copolymers were synthesised with various amounts of π-conjugated segments to trace the solvent induced self-organization process, (ii) various polymeric architectures such as micropores, vesicles, hexagons and micron to nano-sized spheres luminescent under shining light were produced for the first time in the literature, (iii) SEM, TEM and fluorescent microscopic techniques were employed to confirm the formation of various types of morphologies, (iv) T_g values and solution FTIR studies revealed that the increase in the OPV content in the copolymer resulted in a decrease in the extent of hydrogen bonding (v) the absorption and emission studies of the polymers uncovered that π-stacking is strongly favoured in polymers with higher OPV content, and (vi) the time resolved fluorescent techniques confirmed the formation of molecular chain aggregates. The present investigation showed that polyurethane copolymers containing OPV units are very interesting classes of polymers, which are soluble, thermally stable and also have tendency to form self-organized structures through solvent evaporation process. The mechanistic aspects of the self-organization process were studied by many experimental techniques in solid as well as solution state to trace the factors which control the morphology of the polyurethane-OPV systems. The approach demonstrated here may be adopted to produce variety of thermoplastic-conducting polymeric micron to nano structures, which may be very promising candidates in opto-electronics and sensor applications.

4.5. References

1. Lee, M.; Cho, B-K.; Zin, W-C. *Chem. Rev.*, **2001**, *101*, 3869.

2. Govor, L. V.; Bashmakov, I. A.; Kiebooms, R.; Dyakonov, V.; Parisi, J. *Adv. Mater.* **2001**, *13*, 588.

3. Bolognesi, A.; Mercogliano, C.; Yunus, S.; Civardi, M.; Comoretto, D.; Turturro, A. *Langmuir* **2005**, *21*, 3480.

4. You, C-C.; Wurthner, F. *J. Am. Chem. Soc.* **2003**, *125*, 9716.

5. Brunsveld, L.; Folmer, B. J. B.; Meijer, E. W.; Sijbesma, R. P. *Chem. Rev.* **2001**, *101*, 4071.

6. Zhang, Y.; Jiang, M.; Zhao, J.; Wang, Z.; Dou, H.; Chen, D. *Langmuir* **2005**, *21*, 1531.

7. Lehn, J-M. Supramolecular Chemistry; VCH: Weinheim, **1995**.

8. Moniruzzaman, M.; Sundararajan, P. R. *J. Phys. Chem. B* **2005**, *109*, 1192.

9. Sijbesma, R. P.; Meijer, E. W. *Chem. Commun.* **2003**, 5.

10. Lee. S-H.; Balasubramanian, S.; Kim, D. Y.; Viswanathan, N. K.; Bian, S.; Kumar, J.; Tripathy, S. K. *Macromolecules* **2000**, *33*, 6534.

11. Tien, J.; Terfort, A.; Whitesides, G. M. *Langmuir* **1997**, *13*, 5349.

12. Wurthner, F. *Chem. Commun.* **2004**, 1564.

13. Samori, P.; Francke, V.; Mullen, K.; Rabe, J. P. *Chem. Eur. J.* **1999**, *5*, 2312.

14. Sun, S-S.; Silva, A. S.; Brinn, I. M. Lees, A. J. *Inorg. Chem.* **2000**, *39*, 1344.

15. Leininger, S.; Olenyuk, B.; Stang, P. J. *Chem. Rev.* **2000**, *100*, 853.

16. Scudiero, L.; Barlow, D. E.; Hipps, K. W. *J. Phys. Chem. B* **2000**, *104*, 11899.

17. (a) Ghosh, S.; Ramakrishnan, S. *Angew. Chem. Int. Ed.*, **2004**, *43*, 3264. (b) Ghosh, S.; Ramakrishnan, S. *Angew. Chem.*, **2004**, *116*, 3326. (c) Ghosh, S.; Ramakrishnan, S. *Macromolecules* **2005**, *38*, 676.

18. Wurthner, F.; Thalacker, C.; Sautter, A. *Adv. Mater.* **1999**, *11*, 754.

19. (a) Bunz, U. H. F. *Adv. Mater.* **2006**, *18*, 973. (b) Ishchenko, A. *Polym. Adv. Technol.* **2002**, *13*, 744. (c) de Boer, B.; Stalmach, U.; van Hutten, P. F.; Melzer, C.; Krasnikov, V. V.; Hadziioannou, G. *Polymer* **2001**, *42*, 9097.

20. Schenning, A. P. H. J.; Jonkheijm, P.; Peeters, E.; Meijer, E. W. *J. Am. Chem. Soc.* **2001**, *123*, 409.

21. Stenzel, M. H.; Davis, T. P.; Fane, A. G. *J. Mater. Chem.* **2003**, *13*, 2090.

22. Xie, D.; Bai, W.; Xu, K.; Bai, R.; Zhang, G. *J. Phys. Chem. B* **2007**, *111*, 8034.

23. Bang, J.; Jain, S.; Li, Z.; Timothy P. Lodge, T. P.; Pedersen, J. S.; Kesselman, E.; Talmon, Y. *Macromolecules* **2006**, *39*, 1199.

24. Suzuki, A.; Nagai, D.; Ochiai, B.; Endo, T. *Macromolecules* **2004**, *37*, 8823.

25. Zhang, Y. J.; Jin, M.; Lu, R.; Song, Y.; Jiang, L.; Zhao, Y.; Li, T. J. *J. Phys. Chem. B* **2002**, *106*, 1960.

26. Tzanetos, N. P.; Dracopoulos, V.; Kallitsis, J. K.; Deimede, V. A. *Langmuir* **2005**, *21*, 9339.

27. Jenekhe, S. A.; Chen, X. L. *Science* **1999**, *283*, 372.

28. Widawski, G.; Rawiso, M.; Francois, B. *Nature* **1994**, *369*, 387.

29. a) Li, W.; Wang, H.; Yu, L.; Morkved, T. L.; Jaeger, H. M. *Macromolecules* **1999**, *32*, 3034. b) Wang, H.; Wang, H. H.; Urban, V. S.; Littrell, K. C.; Thiyagarajan, P.; Yu, L. *J. Am. Chem. Soc.* **2000**, *122*, 6855.

30. Tung, P-H.; Kuo, S-W.; Jeong, K-U.; Cheng, S. Z. D.; Huang, C-F.; Chang, F-C. *Macromol. Rapid Commun.* **2007**, *28*, 271.

31. Auweter, H.; Haberkorn, H.; Heckmann, W.; Horn, D.; Luddecke, E.; Rieger, J.; Weiss, H. *Angew. Chem. Int. Ed.* **1999**, *38*, 2188.

32. a) Tew, G. N.; Li, L.; Stupp, S. I. *J. Am. Chem. Soc.* **1998**, *120*, 5601. b) Tew, G. N.; Pralle, M. U.; Stupp, S. I. *J. Am. Chem. Soc.* **1999**, *121*, 9852.

33. Cheng, C. X.; Tian, Y.; Shi, Y. Q.; Tang, R. P.; Xi, F. *Langmuir* **2005**, *21*, 6576.

34. Ni, H.; Kawaguchi, H. *J. Polym. Sci. Part A: Polym. Chem.* **2004**, *42*, 2833.

35. (a) Park, M. S.; Kim, J. K. *Langmuir* **2005**, *21*, 11404. (b) Park, M. S.; Joo, W.; Kim, J. K. *Langmuir* **2006**, *22*, 4594.

36. de Boer, B.; Stalmach, U.; Nijland, H.; Hadziioannou, G. *Adv. Mater.* **2000**, *12*, 1581.

37. Kuo, C-H.; Peng, K-C.; Kuo, L-C.; Yang, K-H.; Lee, J-H.; Leung, M-K.; Hsieh, K-H. *Chem. Mater.* **2006**, *18*, 4121.

38. Lin, K-R.; Kuo, C-H.; Kuo, L-C.; Yang, K-H.; Leung, M-k.; Hsieh, K-H. *Eur. Polym. J.* **2007**, *43*, 4279.

39. Crenshaw, B. R.; Weder, C. *Macromolecules* **2006**, *39*, 9581.

40. (a) Wang, H-L.; Fu, C-M.; Gopalan, A.; Wen, T-C. *Thin Solid Films* **2004**, *466*, 197. (b) Wang, H-L.; Wen, T-C. *Mater. Chem. Phys.* **2003**, *82*, 341. (c) Wang, H-L.; Gopalan, A.; Wen, T-C. *Mater. Chem. Phys.* **2003**, *82*, 793.

41. Amrutha, S. R.; Jayakannan, M. *J. Phys. Chem. B* **2006**, *110*, 4083.

42. Amrutha, S. R.; Jayakannan, M. *Macromolecules* **2007**, *40*, 2380.

43. Karthaus, O.; Maruyama, N.; Cieren, X.; Shimomura, M.; Hasegawa, H.; Hashimoto, T. *Langmuir* **2000**, *16*, 6071.

44. Wang, Y.; Liu, Z.; Huang, Y.; Han, B.; Yang, G. *Langmuir* **2006**, *22*, 1928.

45. Thandavamoorthy, S.; Gopinath, N.; Ramkumar, S. S. *J. Appl. Polym. Sci.* **2006**, *101*, 3121.

46. Soo, P. L.; Eisenberg, E. *J. Polym. Sci. Part B Polym. Phys.* **2004**, *42*, 923-938.

47. Huang, W. ; Luo, C. ; Zhang, J. ; Yu, K. ; Han, Y. *Macromolecules* **2007**, *40*, 8022.

48. Mu, M. ; Ning, F.; Jiang, M.; Chen, D. *Langmuir* **2003**, *19*, 9994.

49. Deepak, V. D.; Asha, S. K. *J. Phys. Chem. B* **2006**, *110*, 21450.

50. Lutz, J-F.; Pfeifer, S.; Chanana, M.; Thunemann, A. F.; Bienert, R. *Langmuir* **2006**, *22*, 7411.

51. Syamakumari, A.; Schenning, A. P. H. J.; Meijer, E. W. *Chem. Eur. J.* **2002**, *8*, 3353.

52. Winkler, B.; Dai, L.; Mau, A. W. H. *Chem. Mater.* **1999**, *11*, 704.

53. Huo, H.; Li, K.; Wang, Q.; Wu, C. *Macromolecules* **2007**, *40*, 6692.

54. Jancy, B.; Asha, S. K. *J. Phys. Chem. B* **2006**, *110*, 20937.

55. Lim, S-J.; An, B-K.; Jung, S. D.; Chung, M-A.; Park, S. Y. *Angew. Chem. Int. Ed.* **2004**, *43*, 6346.

56. van Hutten, P. F.; Krasnikov, V. V.; Hadziioannou, G. *Acc. Chem. Res.* **1999**, *32*, 257.

57. Hoeben, F. J. M.; Wolffs, M.; Zhang, J.; De Feyter, S.; Leclere, P.; Schenning, A. P. H. J.; Meijer, E. W. *J. Am. Chem. Soc.* **2007**, *129*, 9819.

58. Lee, K. ; Kim, H-J. ; Cho, J. C.; Kim, J. *Macromolecules* **2007**, *40*, 6457.

59. Chen, Z-K.; Meng, H.; Lai, Y-H.; Huang, W. *Macromolecules* **1999**, *32*, 4351.

Chapter-5

Conclusions

Conclusions

A novel melt transurethane polycondensation route for polyurethanes under solvent free and non-isocyanate condition was developed for soluble and thermally stable aliphatic or aromatic polyurethanes. In the process, a di-urethane monomer was polycondensed with equimolar amounts of diol in presence of $Ti(OBu)_4$ as catalyst under melt to produce polyurethanes followed by the removal of low boiling alcohol from equilibrium. The new transurethane process was investigated for A+ B, A-A + B and A-A + B-B (A-urethane and B-hydroxyl) type condensation reactions and also monomers bearing primary and secondary urethane or hydroxyl functionalities. The transurethane process was confirmed by ^1H and ^{13}C-NMR and molecular weight of the polymers were obtained as $M_n = 10 -15 \times 10^3$ and $M_w = 15- 45 \times 10^3$ g/mol with the polydispersity in the range of 1.5 – 3.0. The number average degree of polymerization (n = 25-50) indicated that the transurethane reaction proceeded up to 95-98 % conversion during the polycondensation. The mechanistic aspects of the melt transurethane process and role of the catalyst were investigated using model reactions, ^1H-NMR and MALDI-TOF MS. The detailed model reactions and the NMR and HR-MS analysis data collected for the aliquots confirmed that almost 97 % reaction occurred in the presence of catalyst whereas less than 2 % reaction alone was possible in the absence of catalyst. The polymer samples were subjected to end group analysis using MALDI-TOF mass spectrometry. The mass spectrum confirmed the presence of three types of end groups in the polymer chains: chain-AA, chain-BB and chain-AB and the mass spectrum was completely devoid of any isocyanate groups and isocyanate cross-linked compounds. All these reactions proved the Ti-catalyst mediated non-isocyanate pathway for the melt transurethane process. Almost all the polyurethanes were stable up to 280 °C and thermal properties particularly T_g of the polyurethanes were easily fine-tuned from -30 to 120 °C by using appropriate diols in the melt transurethane process.

A new class of fully and partially cycloaliphatic polyurethanes synthesized by expending the melt transurethane reaction were subjected to solvent induced self-organization under atmospheric conditions. The strategy employed resulted in the formation of micro-porous polyurethane templates of various pore sizes (0.5 to 1 μM), and also micron and nano-meter sized polymeric hexagons (1 μM to 50 nm) and spheres (1μM to 200 nm), for the first time, via the solvent induced self-organization

process. The various morphologies obtained depended on factors such as structural backbone of the polyurethane, solvent combinations and the concentration of the polymer solutions employed. Only fully cycloaliphatic structures produced micro-porous templates, which further seeds for higher ordered hexagons and spheres in large amount of water content in the solvent combination. Concentration dependant solution FT-IR and ^{1}H-NMR titration studies revealed that the fully cycloaliphatic rings have strong hydrogen bonding interactions and hence higher hydrogen-bonding association constants (K) compared to their partially cyclic counterparts. It was found that fully cycloaliphatic structures have three times stronger hydrogen bonding compared to partially cyclic systems and supports the solvent induced self-organization mechanism. This was further supported by the T_g analysis of the polymers. AM1 calculations for the polymeric repeating units provided a conclusive remark on the orientation of hydrogen bonding vectors and its influence on the self-organization. All these investigations proved that hydrogen bonding operated as the main driving force for the phase separation process for producing various morphologies such as pores, hexagons and spheres.

Finally, based on the observations of the above chapter, a new series of polyurethane- oligo(phenylenevinylene) random block copolymers were synthesized and their solvent induced self-organization into nano-materials such as pores, vesicles, hexagons and luminescent spheres were studied. The polymers were synthesized by polycondensing a hydroxyl functionalized oligo(phenylenevinylene) (OPV) with diurethane monomer and diol under melt transurethane conditions. The amount of OPV was varied up to 50 mol % in the feed to incorporate various amounts of π-conjugated segments into the polyurethane backbone. The structures of the polymers were confirmed by NMR, FT-IR and the molecular weights were determined by GPC. The π-conjugated segmented polymers were subjected to solvent induced self-organization in THF or THF+water to produce variety of morphologies ranging from pores (500 nm-1 µm) to spheres (100 nm-2 µm) which were analyzed using various microscopic techniques such as SEM, TEM and FL-microscopes. Upon shining 370 nm light, the dark solid nano-spheres of the copolymers were transformed into blue luminescent nano-balls under fluorescence microscope. The mechanistic aspects of the self-organization process were studied using solution FT-IR and photophysical techniques such as absorption, emission, and excitation to trace the factors which

control the morphology of the polyurethane-OPV systems. FT-IR studies revealed that the hydrogen bonding plays a significant role in the copolymers with lower amount of OPV units. The rapid decrease of solution quantum yield and large red-shift absorbance spectra indicated the increasing tendency for π-stack induced molecular aggregation in OPV segments. Time resolved fluorescent decay measurements of copolymers showed a single exponential decay in THF (no aggregation) whereas the samples showed a bi-exponential decay in THF+ water (also in higher OPV containing polymers) corresponding to the presence of molecular aggregation. The studies revealed that molecular aggregation via π-conjugated segments play a major role for both the samples in THF+water and also with higher OPV content in the random block copolymers.

The synthesis of polyurethanes using a solvent free and isocyanate free green chemical route has great potential, especially in the industry. Though the polymerization route is in its infancy, utilizing custom made polymerization reactors will help in achieving polymers with high molecular weights for many practical purposes. Also, the self-organization approach demonstrated in this thesis provides a novel technique for the formation of several types as well as sizes of thermoplastic polymeric morphologies which will find use as delivery vehicles, templates and in the field of opto-electronics and sensor applications.

List of Publications

Chapter-2 has appeared as a cover page

List of Publications:

1. **Deepa, P.**; Jayakannan, M. Solvent Free and Non-isocyanate Melt Transurethane Reaction for Aliphatic Polyurethanes and Mechanistic Aspects. *J. Polym. Sci. Polym. Chem.* **2008,** *46* (in press).

2. **Deepa, P.**; Jayakannan, M. Melt-transurethane Process for the preparation of Polyurethanes. *USPTO* **2007/0117950 A1**, May 24, **2007.**

3. **Deepa, P.**; Jayakannan, M. Solvent Induced Self-organization Approach for Polymeric Architectures of Micropores, Hexagons and Spheres based on Polyurethanes Prepared via Novel Melt Transurethane Methodology. *J. Polym. Sci. Polym. Chem.* **2007,** *45*, 2351-2366. (This article has appeared as a cover page in the Journal, issue-12, 2007).

4. **Deepa, P.**; Jayakannan, M. Micro-Porous Polyurethanes: Synthesis and Investigation of the Mechanism of the Pore Formation. *J. Polym. Sci. Polym. Phys.* **2006,** 44, 1296-1308.

5. **Deepa, P.**; Sona, C.; Jayakannan, M. Synthesis and Investigation of the Effect of Nematic Phases on the Glass Transition Behavior of Novel Cycloaliphatic Liquid Crystalline Poly(ester-amide)s. *J. Polym. Sci. Polym. Chem.* **2006,** *44*, 5557-5571.

6. **Deepa, P.**; Divya, K.; Jayakannan, M. Synthesis and Liquid Crystalline Properties of New Amide Modified Poly(cyclohexanedimethylene terephthalate). *J. Polym. Sci. Polym. Chem.* **2006,** *44*, 42-52.

7. **Deepa, P.**; Jayakannan, M. Polyurethane-Oligophenylenevinylene Random Block Copolymers: An Approach for π-conjugated Porous Templates, Vesicles and Nano-spheres via Solvent Induced Self-organization. Manuscript submitted for publication

Papers Published in Conferences

8. **Deepa, P.**; Jayakannan, M. Novel Melt Transurethane Process for Polyurethanes and Hydrogen-bond Induced Self-organization into Micro and Nano-Materials. *MACRO* 2006, Pune, India, Dec 17-20, **2006. Best Poster Award**

9. **Deepa, P.**; Jayakannan, M. A Robust Molecular Design for Micro-Porous Polymeric Materials- A Closer Look into the Mechanism of Pore Formation. *EMSI* 2006, Thiruvananthapuram, India, April **2006**.

10. **Deepa, P.**; Jayakannan, M. A Facile Approach for Thermotropic Liquid Crystalline Cycloaliphatic Polyesters. *IP 2005*, Goa, India, October, **2005**.

11. **Deepa, P.**; Jayakannan, M. New cycloaliphatic polyurethanes: synthesis and structure-property relationship. *MACRO 2004*, Thiruvananthapuram, India, Dec. 15-17, **2004**.